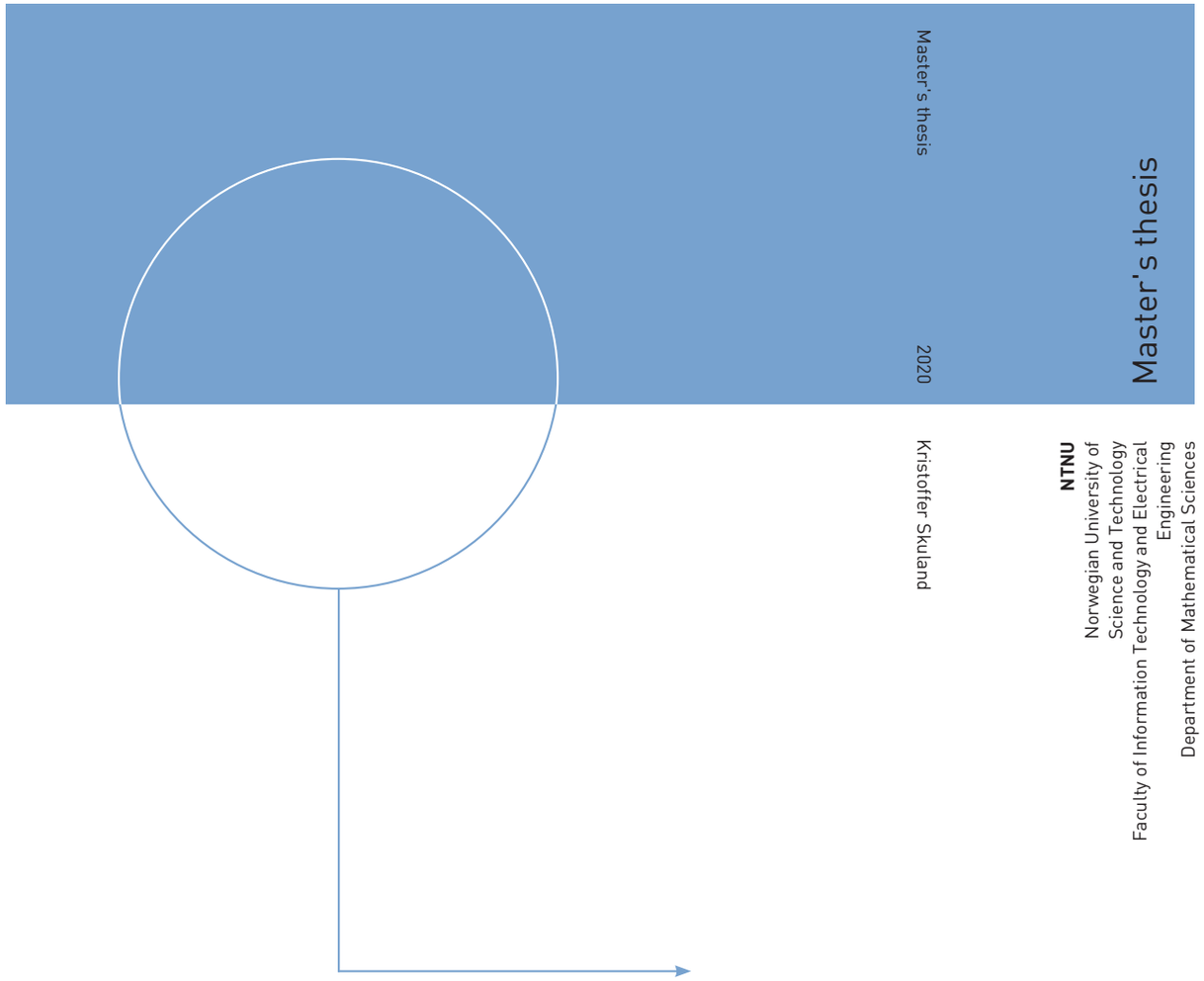

Master's thesis

2020

Kristoffer Skuland

NTNU
Norwegian University of
Science and Technology
Faculty of Information Technology and Electrical
Engineering
Department of Mathematical Sciences

Kristoffer Skuland

Lévy processes in term structure and market risk models

June 2020

NTNU
Norwegian University of
Science and Technology

NTNU
Norwegian University of
Science and Technology

NTNU
Norwegian University of
Science and Technology

Lévy processes in term structure and market risk models

Kristoffer Skuland

Applied Physics and Mathematics
Submission date: June 2020
Supervisor: Jacob Kooter Laading

Norwegian University of Science and Technology
Department of Mathematical Sciences

Abstract

We model fixed-income markets with Lévy term structure models generated by normal–inverse Gaussian (NIG) distributions and generalised hyperbolic skew Student's (GSS) t-distributions. We compare the models against a classical Gaussian Heath–Jarrow–Morton model in out-of-sample backtests of one-day value-at-risk and expected shortfall on interest rate derivatives. The NIG and GSS models provide the best approximations of the studied risk measures, and we conclude that we cannot accurately assess the market risks of interest rate derivatives without taking into account jump dynamics, semi-heavy tails, and possible skewness in the return distributions. The GSS models admit the best overall description of one-day expected shortfall. During the financial crises from 2008 to 2009 and spring 2020, the Gaussian models consistently underestimate the tail risks. During the recent crisis from February to April 2020, the highly skewed and heavy-tailed market behaviour is incompatible with a Gaussian generating distribution, while the NIG and GSS models, though too conservative in the lower tail of the return distributions, provide reasonable approximations of the risks corresponding to falling interest rates.

Sammendrag

Vi modellerer rentemarkeder med Lévy-terminstrukturmodeller generert av normal–inverse gaussiske (NIG) fordelinger og generaliserte hyperboliske skjeve Students (GSS) t-fordelinger. Vi sammenlikner modellene med en klassisk gaussisk Heath–Jarrow–Morton-modell i backtester av endags value-at-risk og expected shortfall på rentederivater. NIG- og GSS-modellene gir de beste tilnærmingene av de undersøkte risikomålene, og vi konkluderer med at vi ikke kan vurdere markedsrisikoen til rentederivater nøyaktig uten å ta hensyn til diskontinuerlige hopp, halvtunge haler og potensiell skjevhet i avkastningsfordelingene. GSS-modellene gir den beste beskrivelsen av endags expected shortfall. Under finanskrisene fra 2008 til 2009 og våren 2020 undervurderer de gaussiske modellene konsekvent halerisikoen. Under den nylige krisen fra februar til april 2020 er den ekstremt skjeve og haletunge markedsatferden uforenlig med en gaussisk genererende fordeling, mens NIG- og GSS-modellene, selv om de er for konservative i den nedre halen av avkastningsfordelingen, gir en rimelig tilnærming av risikoen tilsvarende fallende renter.

Preface

This thesis concludes my Master of Science in Industrial Mathematics at the Norwegian University of Science and Technology (NTNU). I would like to direct huge thanks to my supervisor Jacob Laading for productive discussions and constructive feedback throughout the semester. I would also like to thank DNB for supplying the primary interest rate data investigated in this thesis.

Kristoffer Skuland
Trondheim, June 2020

Contents

Chapter 1

Introduction

A curious situation arises when we examine a model: Things that are assumed to happen, do. The significant losses banks incurred during, for example, the dot-com bubble, the 2007–2009 global financial crisis, and the recent market movements during the spring of 2020, highlights the need for stricter regulatory capital requirements and better estimates of financial risks. To be fair, some model breakdowns are due to the onset of extreme and unprecedented events, structural changes, or black swans. However, innumerable breakdowns are due to ill-conceived model assumptions and negligence of well-known market features. An infamous example is the issue of negative interest rates, which historically was undesired in interest rate models. The frequent observation of negative interest rates during the last decade, however, puts this supposition to rest.

At the end of 2019, the outstanding notional amount in the over-the-counter derivatives market totalled 558 trillion USD, where interest rate derivatives encompass nearly 80 % of the market (Bank for International Settlements, 2020). In comparison, the total capitalisation of listed equities totalled a mere 43 trillion USD (The World Bank, 2020). Interest rate derivatives additionally represent unique modelling challenges. In equity markets, there is a single security to be modelled. In interest rate markets, the problem is theoretically infinite-dimensional, and we need to model a whole family of securities indexed by the time of maturity. In order to prudently assess the risks inherent in interest rate derivatives both during normal and highly stressed market conditions, a realistic description of the future dynamics and mechanics of interest rates are needed.

The classical approach to model fixed-income markets are short-rates models, which exogenously specify the dynamics of the short-rate. The idea was pioneered by Vasicek (1977), who model the instantaneous short-rate dynamics under the real-world measure as an Ornstein–Uhlenbeck process, and later models include Dothan (1978) and Cox, Ingersoll Jr, and Ross (1985).

While short-rate models are analytically tractable, their main drawbacks are that *one* explanatory variable describes the evolution of the entire market and that no time-independent short-rate model can reproduce the observed market yield curve (see, e.g., Björk, 2004). Hull and White (1990) and subsequent papers later addressed the poor fitting of initial yield curves by including time-varying parameters in the Vasicek model, where the functional dependence is carefully chosen to make model prices exactly replicate market prices. There is, however, no reason to expect that these models will provide reasonable market prices and volatilities as they evolve

since “yield curve fitting” is famously inconsistent (Wilmott, 2006).

An alternative to short-rate models was proposed by Ho and Lee (1986), who model the evolution of the entire term structure of interest rates in a binomial-tree setting. This intuition is translated into continuous-time by Heath, Jarrow, and Morton (1992), who model the stochastic evolution of the entire term structure of interest rates through instantaneous forward rates. In a Heath–Jarrow–Morton (henceforth HJM) model, the arbitrage-free framework is fully specified through the forward rates' instantaneous volatility structure, and virtually any (exogenous term-structure) interest rate model, including the aforementioned short-rate models, can be derived within such a framework. Similar models of forward LIBOR and swap rates were developed in a series of papers by Miltersen, Sandmann, and Sondermann (1997), Brace, Gÿatarek, and Musiela (1997), Jamshidian (1997), and Musiela and Rutkowski (1997). These models are especially well-liked by practitioners, since they allow for perfect calibration to cap, floor, and swaption quotes, thus reproducing well-established market formulae.

HJM models are well-studied in financial literature, but they build on the classical assumption that interest rates follow a diffusion process generated by a Gaussian distribution. Indeed, Brownian motions have emerged as a crucial constituent of financial mathematics following the pioneering introduction of geometric Brownian motions as driving processes in stock price models by Samuelson (1965) and later by Black and Scholes (1973). It is, however, well-established that normal distributions provide inadequate descriptions of empirically observed financial return distributions.

Two essential properties of Brownian motions are continuity of sample paths and scale invariance. Equity and bond prices, however, admit discontinuities in their price trajectories (so-called jumps), and these discontinuities become more evident at shorter time scales. While a normal distribution reasonably represents the monthly log-returns of stock prices, the distributional deviation becomes significant for prices on a daily or intra-daily time scale (Eberlein, Keller, et al., 1995; Eberlein & Özkan, 2003; Feinstone, 1987; Jarrow & Rosenfeld, 1984). Similarly, the empirical distributions of interest rates and interest rate derivatives exhibit kurtosis, skewness, higher moments, and volatility smiles which are inconsistent with a Gaussian distributional assumption (Eberlein, 2001; Eberlein & Raible, 1999; Raible, 2000; Das, 2002).

Price jumps are abrupt price movements over very short time intervals that are very large compared to the current market situation, and they cannot be connected to a noisy Gaussian distribution. Price jumps have been recognised as a significant part of volatility since Merton (1975), and some early contributions on option pricing theory with jump risk includes Naik and Lee (1990), Bates (1991), Ahn (1992), and Amin (1993). The proposed primary reasons of the sources of jumps are, firstly, that price jumps can reflect the markets' reactions to unexpected information (Lahaye, Laurent, & Neely, 2011; Lee, 2012; Piazzesi, 2005; Johannes, 2004), and, secondly, that jumps can be caused by a local lack of liquidity in the market (Joulin, Lefevre, Grunberg, & Bouchaud, 2008).

The principal motivation for studying jump processes is that the presence of jumps significantly affects instrument pricing and financial risk management. Broadie and Jain (2008) find that the effect of jumps is significant in swap pricing and that

the corresponding risk cannot be accurately priced without taking into account the presence of jumps. Glasserman and Kou (2003) note the presence of a positive jump risk premium, and Arshanapalli, Fabozzi, and Nelson (2013) document a need for jump components in risk measures to estimate the proper risk–return relationship accurately. Johannes (2004) finds that jumps may not necessarily have a massive impact on the cross-section of bond prices, but that they have a significant impact on derivative contracts such as bond options, caps, or floors, whose prices depend heavily on the tails of the conditional distribution of interest rate increments. Johannes further notes that the presence of jumps generates more than half the conditional variance of interest rate movements.

Consequently, to accurately capture the risk inherent in fixed-income markets, interest rate models need to incorporate the observed stylised features. Early jump–diffusion short-rate models include Ahn and Thompson (1988), Babbs and Webber (1994), and El-Jahel, Lindberg, Perraudin, et al. (1996). Shirakawa (1991) extends the HJM model by incorporating pure jump components with a constant jump intensity in the forward rate dynamics, while Björk (1995) and Jarrow and Madan (1995) consider interest rate models generated by Wiener processes and a finite number of counting processes with stochastic jump intensities generated by exogenous processes. At the high end of generality is the jump–diffusion interest rate models generated by general semimartingales presented in Björk, Di Masi, Kabanov, and Rungaldier (1997).

The general model presented by Björk et al. (1997) is not very tractable. A special case of the model is introduced in Eberlein and Raible (1999), who develop a general HJM-type term structure model generated by Lévy processes. Lévy processes admit discontinuous paths with independent and identically distributed increments that can incorporate jumps, dense tails, skewness, and kurtosis, and the term structure models are fairly tractable. A generalisation to term structure models generated by time-inhomogeneous Lévy processes, which are processes with weaker assumptions about the stationarity of increments, is given by Eberlein, Jacod, and Raible (2005) and Kluge (2005). No-arbitrage conditions in these models exist under certain conditions and are provided by Eberlein et al. (2005) and Filipovi and Tappe (2008).

In this thesis, we consider the Lévy term structure model developed by Eberlein et al. (2005) and Kluge (2005). More specifically, we will consider Lévy processes generated by the normal–inverse Gaussian (NIG) distribution and the generalised hyperbolic skew Student's (GSS) t-distribution. The NIG distribution is frequently used for modelling financial data, as the conditional distribution of a GARCH model (e.g. Jensen and Lunde, 2001; Forsberg and Bollerslev, 2002; Chen, Härdle, and Jeong, 2008) or as an unconditional returns distribution (e.g. Prause, 1997; Raible, 2000; Kassberger, 2009). The GSS distribution is briefly mentioned in Prause et al. (1999); Barndorff-Nielsen and Shephard (2002); Mencía and Sentana (2005) and applied in a univariate setting in Aas and Haff (2006), but it has not obtained much attention in the financial literature compared to the NIG distribution. We present a theoretical justification for the choice of model and explore the key properties of the generating distributions. Methods for calibrating the term structure models are based on the calibration framework by Eberlein and Kluge (2007) and the EM

algorithm (Dempster, Laird, & Rubin, 1977).

Using NIBOR and swap rates from 2009 to 2019, we calibrate term structure models generated by univariate Gaussian, NIG, and GSS distributions. To assess if the increased flexibility of driving Lévy processes is justified, the term structure models are compared in an out-of-sample historical backtest of one-day value-at-risk and one-day expected shortfall on portfolios consisting of zero-coupon bonds and interest rate derivatives such as swaps and caps. For one-day expected shortfall, the NIG and GSS models are significantly better than the Gaussian models both in-sample and out-of-sample for all securities but shorter-maturity bonds, where all (time-homogeneous, univariate) term structure models provide a poor fit. Time-inhomogeneous models appear to provide a superior in-sample fit on shorter-maturity bonds compared to their time-homogeneous counterparts, but their out-of-sample predictions of one-day expected shortfall are only sporadically significantly better at the 2.5 and 97.5 % quantiles. For the more complex derivative portfolios, the NIG and GSS models are additionally better than the Gaussian models at predicting one-day value-at-risk. The GSS models are found to be significantly better than the NIG models at predicting one-day expected shortfall.

Lastly, we study if the different term structure models are suited to describe the highly stressed market data observed during the global financial crisis and the coronavirus crisis. Whereas the traditional HJM model cannot capture skewed and heavy-tailed return distributions, the NIG and GSS term structure models can. For the global financial crisis, the NIG and GSS models fit the observed bond return data reasonably well, while the Gaussian models consistently underestimate the observed market risks due to the models' inability to encompass skewness and semi-heavy tails. Compared to the global financial crisis, the market crash during March to April 2020 is much less well-behaved: The crisis admits remarkably skewed return distributions with one heavy and one lighter tail. The NIG and GSS models are generally too conservative in the lighter tail, as they do not adequately manage to capture the skewed market situation, but the models do fit the heavier tail reasonably well. The Gaussian models are entirely inept at describing the observed market behaviour.

The remainder of the thesis is organised as follows: In Chapter 2, we present the basic theory of derivative pricing for continuous-time models. Following the introduction of the market structure, the HJM model is presented as a model for the evolution of the term structure of interest rates in Chapter 3. The term structure model is extended to driving Lévy processes in Chapter 4. First, we present the qualitative argument for jump–diffusion processes and the theoretical properties of the driving motion. Secondly, we present the term structure model and derive arbitrage-free conditions. Lastly, we present the NIG and GSS distributions as tractable generating distributions, and we present a calibration scheme to zero-coupon bond quotes. In Chapter 5, we present the notion of market risks and some standard market risk measures.

In Chapter 6, we present two data sets of Norwegian rates to motivate the application of more general term structure models. In Chapter 7, we give a calibration example to market data, and we perform an out-of-sample backtest of one-day value-at-risk and expected shortfall on a series of interest rate derivatives. At last, in

Chapter 8, we qualitatively study the flexibility of the different term structure models during highly stressed market scenarios. The results of this thesis are discussed in Chapter 9 and concluded in Chapter 10.

Chapter 2

Derivative Pricing Theory

Fixed-income markets are financial markets wherein market participants trade securities which pay fixed interest and dividends payments at prescribed dates. The fundamental problem is how to value these contracts and how to measure the associated risks. In this chapter, we present the theory of derivative pricing for continuous-time models applied in subsequent chapters. We first present the model market structure and the concept of equivalent martingale measures and arbitrage pricing. We lastly present some common financial instruments and interest rate derivatives. For a more thorough introduction to interest rate theory, we refer to Brigo and Mercurio (2007) and Björk (2004).

2.1 The Market Structure

We consider a frictionless and competitive continuous-time financial market with a finite trading window $[0, T^*]$, for a fixed maximum finite time horizon $T^* > 0$. All trading occurs at times $t \in [0, T^*)$, and the outcomes of all trades are realised at time T^*. By frictionless, we mean that there are no transaction costs or taxes, that shares are infinitely divisible, and that there are no trading constraints, e.g. short sales restrictions, borrowing limits, or margin requirements. By competitive, we mean that traders act as price-takers.

The uncertainty in the market is represented by filtered complete probability space $(\Omega, \mathscr{F}, (\mathscr{F}_t)_{0\leq t\leq T^*}, \mathbb{P})$, for a state space Ω, a σ-algebra of measurable events $\mathscr{F}$, a filtration $(\mathscr{F}_t)_{0\leq t\leq T^*}$, and a probability measure $\mathbb{P}$. The filtration satisfies $\mathscr{F} = \mathscr{F}_{T^*}$, and we always assume that the *usual hypothesis* holds.

Definition 2.1. *A filtered complete probability space* $(\Omega, \mathscr{F}, (\mathscr{F}_t)_{0\leq t\leq T^*}, \mathbb{P})$ *satisfies the* usual hypothesis *if*

(i) $\mathscr{F}_0$ *contains* $\{F \in \mathscr{F} | \mathbb{P}(F) = 0\}$ *and*

(ii) $\mathscr{F}_t = \cap_{u>t}\mathscr{F}_u$ *for all* $0 \leq t < \infty$.

The first requirement in Definition 2.1 assures that the filtration is complete, and the second requirement assures that the filtration is right-continuous, which implies that the information at time t^+ is known at time t (Medvegyev, 2007).

Traded in the market are the money-market account, with an associated spot interest rate with time-t value $r(t)$, and n risky assets. Let

$$B(t) = \exp\left(\int_0^t r(s)\mathrm{d}s\right) \tag{2.1}$$

denote the money-market account at time t, such that $B(0) \equiv 1$, where the spot rate, which is adapted to $\mathscr{F}_t$, satisfies $\int_0^t |r(s)|\mathrm{d}s < \infty$. Let $S(t) = (S_1(t), \ldots, S_n(t))'$ denote the n risky asset prices at time t, which are strictly positive semimartingales with respect to $\mathscr{F}_t$. We assume that there are no dividends over $[0, T^*)$.

2.2 Arbitrage Pricing Theory

The *efficient-market hypothesis* states that all previous history is fully reflected in the present instrument price, which does not hold any further information, and that markets respond immediately to any new information about an instrument. A direct implication of the efficient-market hypothesis is that it is impossible to consistently beat the market and that the only way to earn returns greater than the market, is by assuming greater risks (Wilmott, Howson, Howison, Dewynne, et al., 1995).

Related to the efficient-market hypothesis is the concept of *arbitrage* and *arbitrage opportunities*. Bluntly stated, an arbitrage opportunity is a possibility of undertaking a financial operation without any net investment, which almost surely admits a profit without any risk of loss. In the real world, arbitrage opportunities do exist, though their life spans are short-lived. Financial markets are assumed to be efficient, such that as soon as arbitrage opportunities arise, market prices immediately move to eliminate them as a result of the actions of investors who succeed in exploiting such opportunities. This dynamic of efficient markets is often informally stated as "there is no such thing as free lunch."

From a theoretical perspective, it is apparent that any reasonable market model must avoid lasting arbitrage opportunities. Indeed, the no-arbitrage principle has become one of the leading criteria in financial derivative pricing. To develop arbitrage-free markets, however, we first need to introduce the concept of equivalent martingale measures.

Definition 2.2. *An* equivalent martingale measure $\mathbb{Q}$ *with numéraire* Y *is a probability measure on* $(\Omega, \mathscr{F}, \mathbb{P})$ *if* $\mathbb{Q}$ *is equivalent to* $\mathbb{P}$ *and the* Y*-discounted price processes are* $\mathbb{Q}$*-martingales; that is,*

$$\frac{S(t)}{Y(t)} = \mathbb{E}_{\mathbb{Q}}\left(\frac{S(T)}{Y(T)}\Big|\mathscr{F}_t\right), \tag{2.2}$$

for every $0 \le t \le T$*, where* $\mathbb{E}_{\mathbb{Q}}$ *denotes the expectation with respect to* $\mathbb{Q}$*.*

If we choose numéraire $Y = B$ in Definition 2.2, $\mathbb{Q}$ defines the *risk-neutral measure*, which assigns to each risky asset the price a risk-neutral investor assigns to the said asset. That is, the current risk-neutral price is equal to the discounted expected future profit.

The risk-neutral measure is heavily used in the pricing of financial derivatives due to the fundamental theorems of asset pricing, which provide sufficient conditions

for the investigated market to be arbitrage-free and complete. For proofs of the following theorems, and a precise definition of arbitrage, see, e.g., Jarrow (2018) or Pascucci (2011).

Theorem 2.3 (First Fundamental Theorem)**.** *A financial market is arbitrage-free if and only if there exists at least one equivalent martingale measure.*

In an incomplete market which is arbitrage-free, there exist infinitely many risk-neutral probabilities. While there exist infinitely many risk-neutral prices, it is not, generally, possible to define the arbitrage price (Pascucci, 2011).

Theorem 2.4 (Second Fundamental Theorem)**.** *An arbitrage-free market* (B, S) *is complete if and only if there exists a unique equivalent martingale measure with numéraire* B*.*

Hence, in a complete arbitrage-free market, the arbitrage prices and the risk-neutral prices coincide. The risk-neutral pricing formula (2.2) yields the arbitrage price.

2.3 Zero-Coupon Bonds and Interest Rates

Zero-coupon bonds are fundamental auxiliary quantities from which all interest rates can be recovered. Financial markets, however, usually quote interest rates, whereas zero-coupon bonds are theoretical instruments that are not directly observable.

Definition 2.5. *Fix a maturity* $T \leq T^*$*. A* zero-coupon bond *is a financial security which pays one unit of currency to its holder at maturity. Its value at time* $t \leq T$ *is denoted by* $p(t, T)$*, with* $p(T, T) = 1$ *for all* T*.*

We assume that there exists a zero-coupon bond traded in the market for each maturity $T \in [0, T^*]$. We further assume that all bonds are risk-free, meaning that the issuer will not default on his obligation. This is the case for government bonds of financially stable countries.

A natural question regards the relationship between the zero-coupon bond price and the money-market account. The two quantities are, respectively, the "value of a contract" and an "equivalent amount of currency." The money-market account is the future value of one unit of currency invested today, whereas the discount factor $1/B(T)$ is today's value of one unit of currency at time T. If the spot-rate is deterministic, the money-market account is deterministic and necessarily $p(t, T)/B(t) = 1/B(T)$ for all $t \leq T$. Spot-rates are, however, stochastic, such that the money-market account is a random quantity which depends on the future path of interest rates. Contrarily, the zero-coupon bond price is "traded" and known at time t. From an arbitrage perspective, it is apparent that $p(t, T)/B(t)$ is the expectation of $1/B(T)$ under the risk-neutral measure.

Interest rates are the cost of borrowing capital, reflecting the risk-free cost of capital, expected inflation, risk premiums, and transaction costs. That is, the interest rate is the amount charged by the lender to the borrower to cover the opportunity cost incurred to the lender by not investing the capital in another alternative.

The interest rate seen from time t for borrowing or lending cash over a future time interval $[T, U]$ is known as the *forward rate*, and it is denoted by $F(t, T, U)$. From a simple arbitrage argument, a deposit of one unit of currency made at time T which earns the interest F during the period $[T, U]$ must equal $p(t, T)/p(t, U)$, the income accumulated by investing one unit of currency at time T in a zero-coupon bond which matures at time U. Hence,

$$F(t, T, U) = -\frac{\log p(t, U) - \log p(t, T)}{U - T}. \tag{2.3}$$

A more theoretically convenient concept is *instantaneous forward rates*, which emerge as the limit of forward rates for infinitesimal-length accrual periods. They are purely mathematical concepts and are not directly observed in the market.

Definition 2.6. *The* instantaneous (continuously compounded) forward rate*, denoted by $f(t, T)$ for $t \leq T$, is the interest rate one can commit at time t, which is applicable on an infinitesimal-length risk-less loan that initiates at time T. Formally,*

$$f(t, T) = -\frac{\partial}{\partial T} \log p(t, T), \tag{2.4}$$

where $f(t, t) =: r(t)$ is the spot-rate *or the* short-rate*.*

Equivalently, the price of a zero-coupon bond given the present forward rate curve is

$$p(t, T) = e^{-\int_t^T f(t,u)\mathrm{d}u} \quad \text{for all} \quad 0 \leq t \leq T \leq T^*. \tag{2.5}$$

We herein assume that forward rates are continuously compounded. The simple compounded versions of forward rates, which are directly observed in the market, are called LIBOR (London Interbank Offered Rate) and are denoted by $L(t, T, U)$. For any $t \leq T \leq U$, the forward LIBOR is defined by

$$L(t, T, U) = \frac{1}{U - T} \left(\frac{p(t, T)}{p(t, U)} - 1 \right). \tag{2.6}$$

2.4 Interest Rate Derivatives

We conclude this chapter by introducing two important derivative products of the fixed-income market, namely swaps and caps.

Definition 2.7. *A* vanilla interest rate swap *is a financial agreement between two parties to exchange n interest payments between two differently indexed legs. At every instant T_i in a prespecified set of dates $0 < T_1 < \ldots < T_n \leq T^*$, with $\tau_i = T_i - T_{i-1}$ for $1 \leq i \leq n$, the fixed leg pays an accrual amount corresponding to a fixed interest rate r_s over τ_i, whereas the floating leg pays an accrual amount corresponding to the observed interest rate over τ_i.*

When the fixed leg is paid, and the floating leg is received, the interest rate swap is termed a payer interest rate swap, whereas the opposite case is named a receiver interest rate swap.

Usually, the floating leg is based on the LIBOR, but we will, for simplicity, express it through the continuously compounded spot-rate. Let the swap be initialised at $T_0 = 0$. The time-t value of a payer interest rate swap is

$$\begin{aligned} V_{\text{swap}}(t) &= \mathbb{E}_{\mathbb{Q}}\left(\sum_{i=1}^{n}\left(\frac{B(T_i)}{B(T_{i-1})} - e^{r_s\tau_i}\right)\frac{1}{B(T_i)}\middle|\mathscr{F}_t\right) \\ &= \frac{1}{B(t)}\sum_{i=1}^{n}\left(p(t,T_{i-1}) - e^{r_s\tau_i}p(t,T_i)\right), \end{aligned} \tag{2.7}$$

where the second equality holds in a market where the discounted bond price processes are $\mathbb{Q}$-martingales.

Definition 2.8. *A* caplet *is a call option on a floating rate with strike rate κ, which is initialised at T and matures at U. An* interest rate cap *is a series of n subsequent caplets for a set of start and end dates $0 = T_0 < T_1 < \ldots < T_n \leq T^*$, with $\tau_i = T_i - T_{i-1}$ for $1 \leq i \leq n$. Its time-t value is*

$$V_{\text{cap}}(t) = \mathbb{E}_{\mathbb{Q}}\left(\sum_{i=1}^{n}\frac{1}{B(t_i)}\left(\frac{B(t_i)}{B(t_{i-1})} - e^{\kappa\tau_i}\right)^{+}\middle|\mathscr{F}_t\right). \tag{2.8}$$

A cap can be viewed as a payer interest rate swap where each exchange is only executed if the exchange has a positive value. Analogously, a *floorlet* is a put option on a floating rate, and an *interest rate floor* is a series of n subsequent floorlets with time-t value

$$V_{\text{floor}}(t) = \mathbb{E}_{\mathbb{Q}}\left(\sum_{i=1}^{n}\frac{1}{B(t_i)}\left(e^{\kappa\tau_i} - \frac{B(t_i)}{B(t_{i-1})}\right)^{+}\middle|\mathscr{F}_t\right). \tag{2.9}$$

Caps and floors are predominantly used to hedge against adverse interest rate fluctuations. For instance, an investor who is paying the LIBOR may protect his position against rising interest rates by buying a cap at, e.g., 3 %. The investor's effective maximum interest payment is then 3 %.

Chapter 3

The Heath–Jarrow–Morton Model

The classical approach to model fixed-income markets are short-rates models, which exogenously specify the dynamics of the short-rate. While the models are analytically tractable, their main drawbacks are that the short-rate alone cannot describe the evolution of the entire fixed-income market, and short-rate models cannot consistently replicate market prices of interest rate derivatives. An alternative to short-rate models was introduced in Heath et al. (1992), who model the stochastic evolution of the entire term structure of interest rates through instantaneous forward rates in an arbitrage-free framework fully specified through the forward rates' instantaneous volatility structure.

In this chapter, we present the Heath–Jarrow–Morton (HJM) model introduced in Heath et al. (1992), and we suggest a feasible simulation scheme therefrom. The chapter is outlined as follows: Sections 3.1 and 3.2 outline the market structure and the postulated forward-rate dynamics, and Section 3.3 presents sufficient conditions for the market to be arbitrage-free and complete. Lastly, Section 3.4 presents a feasible simulation scheme from the HJM model. We do not dive deep into the underlying mathematics of measure theory, but excellent references thereof include Jacod and Protter (2012), Pascucci (2011), and Protter (2005).

3.1 The Market Structure

We consider a non-normalised, frictionless, and competitive continuous-time financial market (B, S) equipped with a complete filtered probability space $(\Omega, \mathscr{F}, (\mathscr{F}_t)_{0\leq t\leq T^*}, \mathbb{P})$ and an instantaneous risk-free spot interest rate with time-t value $r(t)$. The market has a finite trading window $[0, T^*]$, for $T^* > 0$, where all trading occurs at times $t \in [0, T^*)$, and the outcomes of all trades are realised at time T^*. The filtration satisfies $\mathscr{F} = \mathscr{F}_{T^*}$ and the usual hypothesis.

We let the risky assets $S(t) = (S_1(t), \ldots, S_n(t))'$ correspond to the term structure of default-free zero-coupon bonds of all available maturities. Denote the bond prices at time t with maturity T by $p(t, T)$, and scale all principal payments to one, $p(T, T) = 1$. To exclude trivial arbitrage opportunities from the market, we assume that all bond prices are strictly positive, $p(t, T) > 0$ (Jarrow, 2018).

3.2 Term Structure Evolution

We assume the market structure presented in Section 3.1. Following the analysis in Heath et al. (1992), we postulate the following forward rate process:

Definition 3.1 (Heath et al., 1992)**.** *For a fixed, non-random initial forward rate curve* $\{f(0,T) : 0 \leq T \leq T^*\}$*, the dynamics of the instantaneous forward rates* $f(t,T)$ *are given by an Itô process of the form*

$$f(t,T) = f(0,T) + \int_0^t \mu(s,T)\mathrm{d}s + \sum_{i=1}^{D} \int_0^t \sigma_i(s,T)\mathrm{d}W_i(s), \tag{3.1}$$

for any $0 \leq t \leq T \leq T^*$*, where* $W_i(t)$ *for* $i = 1, \ldots, D$ *are independent* $\mathbb{P}$*-standard Brownian motions that generate the filtration* $\mathscr{F}_t$*, and* $\mu(t,T)$ *and* $\sigma_i(t,T)$ *are* $\mathscr{F}_t$*-measurable and satisfy the regularity conditions*

(i) $\int_0^T |\mu(t,T)|\mathrm{d}t < \infty$ $\mathbb{P}$*-a.s. and*

(ii) $\int_0^T \sigma_i^2(t,T)\mathrm{d}t < \infty$ $\mathbb{P}$*-a.s. for* $i = 1, \ldots, D$*.*

The only substantial economic restrictions we impose on the forward rate process is that it has continuous sample paths and is generated by a finite number of random shocks (Heath et al., 1992). The assumption of continuous sample paths may be relaxed, see Chapter 4. Forward rates may too turn negative and are unbounded below; this may be avoided by imposing additional restrictions on the forward rate dynamics (see, e.g., the LIBOR and swap market models introduced in Miltersen et al., 1997; Brace et al., 1997; Jamshidian, 1997; Musiela and Rutkowski, 1997).

Under the postulated forward rate process, the evolution of the spot rate is found by inserting maturity $T = t$ into (3.1),

$$r(t) = f(0,t) + \int_0^t \mu(v,t)\mathrm{d}v + \sum_{i=1}^{D} \int_0^t \sigma_i(v,t)\mathrm{d}W_i(v). \tag{3.2}$$

To derive the corresponding evolution of zero-coupon bond prices, we insert the postulated forward rate curve evolution (3.1) into the bond-pricing equation (2.5),

$$p(t,T) = e^{\int_t^T f(0,u)\mathrm{d}u - \int_t^T \left(\int_0^t \mu(s,u)\mathrm{d}s\right)\mathrm{d}u - \sum_{i=1}^{D} \int_t^T \left(\int_0^t \sigma(s,u)\mathrm{d}W_i(s)\right)\mathrm{d}u}. \tag{3.3}$$

To fully determine the dynamics of the bond price processes, and later derive conditions for the absence of arbitrage, we need to impose additional regularity conditions on the drift term, the volatility terms, and the initial forward rate curve:

Condition 3.2 (Heath et al., 1992)**.** *To ensure that the money-market account is well-behaved,* $0 < B(t) < \infty$ $\mathbb{P}$*-a.s. for all* $0 \leq t \leq T^*$*, we require that*

(i) $\int_0^{T^*} |f(0,v)|\mathrm{d}v < \infty$ $\mathbb{P}$*-a.s. and*

(ii) $\int_0^{T^*} \left(\int_0^t |\mu(v,t)| \mathrm{d}v \right) \mathrm{d}t < \infty$ $\mathbb{P}$-*a.s.*

Condition 3.3 (Heath et al., 1992)**.** *To ensure that the bond price process is well-behaved, we require that, for all* $0 \leq t \leq T \leq T^*$ *and* $i = 1, \ldots, n$*,*

(i) $\int_0^t \left(\int_v^t \sigma_i(v,y) \mathrm{d}y \right)^2 \mathrm{d}v < \infty$ $\mathbb{P}$-*a.s.;*

(ii) $\int_0^t \left(\int_t^T \sigma_i(v,y) \mathrm{d}y \right)^2 \mathrm{d}v < \infty$ $\mathbb{P}$-*a.s.; and*

(iii) $t \to \int_t^T \left(\int_0^t \sigma_i(v,y) \mathrm{d}W_i(v) \right) \mathrm{d}y$ *is continuous* $\mathbb{P}$-*a.s..*

Under the regularity conditions posted in Conditions 3.2 and 3.3, we may apply a general Fubini's theorem for stochastic variables (see Heath et al., 1992, pp. 98–100) and switch the order of integration in (3.3). If we further insert the evolution of the spot interest rate (3.2), we find that

$$p(t,T) = p(0,T) e^{\int_0^t (r(s) + b(s,T)) \mathrm{d}s - \frac{1}{2} \sum_{i=1}^D \int_0^t a_i(s,T)^2 \mathrm{d}s + \sum_{i=1}^D \int_0^t a_i(s,T) \mathrm{d}W_i(s)}$$

$\mathbb{P}$-a.s. for

$$a_i(t,T) = -\int_t^T \sigma_i(t,u) \mathrm{d}u \quad \text{and} \quad b(t,T) = -\int_t^T \mu(t,u) \mathrm{d}u + \frac{1}{2} \sum_{i=1}^D a_i(t,T)^2.$$

Employing Itô's lemma (e.g. Protter, 2005, Theorem II.32), the evolution of zero-coupon bond prices is given as an Itô process on the form

$$\frac{\mathrm{d}p(t,T)}{p(t,T)} = (r(t) + b(t,T)) \mathrm{d}t + \sum_{i=1}^D a_i(t,T) \mathrm{d}W_i(t). \tag{3.4}$$

That is, the bond price processes advance according to a drift term and D random shocks generated by a Gaussian distribution. The function $b(t,T)$ may be interpreted as the risk premium on T-maturity zero-coupon bonds in excess of the default-free spot rate, and $(a_1(t,T), \ldots, a_D(t,T))$ are the bonds' volatilities.

3.3 Arbitrage-Free Conditions

The dynamics in (3.1) and (3.4) do not guarantee the absence of arbitrage. Heath et al. (1992) proved that there exists an equivalent martingale measure and thus no arbitrage opportunities in the market if we choose the drift function in a particular form. Our proof closely follows that of Jarrow (2018).

Theorem 3.4. *A martingale measure $\mathbb{Q} \sim \mathbb{P}$ such that $p(t,T)/B(t)$ are $\mathbb{Q}$-martingales for all $0 \le t \le T \le T^*$, exists if and only if there exist risk premium processes $\phi_i(t)$ for $i = 1, \dots, D$ which are $\mathscr{F}_t$-measurable with $\int_0^{T^*} \phi_i(t)^2 \mathrm{d}t < \infty$ a.s. for all i, where*

(i) $\mathbb{E}\left(e^{\sum_{i=1}^D \int_0^T (a_i(s,T)+\phi_i(s))\mathrm{d}W_i(s) - \frac{1}{2}\sum_{i=1}^D \int_0^T (a_i(s,T)+\phi_i(s))^2 \mathrm{d}s}\right) = 1$ *and*

(ii) $\mu(t,T) = -\sum_{i=1}^D \sigma_i(t,T)\left(\phi_i(t) - \int_t^T \sigma_i(t,v)\mathrm{d}v\right)$

for all $0 \le t \le T \le T^*$.

Proof. Since $\mathbb{Q} \sim \mathbb{P}$, there exists a unique strictly positive Radon–Nikodym derivative $Y_T = \mathrm{d}\mathbb{Q}/\mathrm{d}\mathbb{P}$ which defines $\mathbb{Q}$, where (Protter, 2005, Corollary IV.43.4)

$$Y_t = \exp\left(\sum_{i=1}^D \int_0^t \phi_i(s)\mathrm{d}W_i(s) - \frac{1}{2}\sum_{i=1}^D \int_0^t \phi_i(s)^2 \mathrm{d}s\right) \quad \text{for} \quad 0 \le t \le T.$$

From Girsanov's Theorem (e.g. Pascucci, 2011, Theorem 10.5), $\mathrm{d}W_i^{\mathbb{Q}}(t) = \mathrm{d}W_i(t) - \phi_i(t)\mathrm{d}t$ are independent $\mathbb{Q}$-standard Brownian motions. Using integration-by-parts (e.g. Protter, 2005, Corollary II.22.2),

$$\frac{\mathrm{d}p(t,T)}{p(t,T)} - r_t \mathrm{d}t = \frac{\mathrm{d}\left(\frac{p(t,T)}{B(t)}\right)}{\frac{p(t,T)}{B(t)}},$$

and combined with the $\mathbb{Q}$-Brownian motions,

$$\frac{\mathrm{d}\left(p(t,T)/B(t)\right)}{p(t,T)/B(t)} = \sum_{i=1}^D a_i(t,T)\mathrm{d}W_i^{\mathbb{Q}}(t) + \left(b(t,T) + \sum_{i=1}^D \phi_i(t)a_i(t,T)\right)\mathrm{d}t.$$

As a necessary condition for $p(t,T)/B(t)$ to be a $\mathbb{Q}$-martingale, we choose the risk premiums in such a way that the drift terms of the discounted bond price processes vanish. That is,

$$b(t,T) + \sum_{i=1}^D \phi_i(t)a_i(t,T) = 0. \tag{3.5}$$

If we differentiate (3.5) with respect to T, we arrive at the drift condition (ii). We now need to prove that $p(t,T)/B(t)$ is a $\mathbb{Q}$-martingale. From (3.2), we observe that

$$\frac{p(T,T)/B(T)}{p(0,T)/B(0)} = e^{\int_0^T (b(s,T)+\sum_{i=1}^D \phi(s)a_i(s,T))\mathrm{d}s - \frac{1}{2}\sum_{i=1}^D \int_0^T a_i(s,T)^2 \mathrm{d}s} \times e^{\sum_{i=1}^D \int_0^T a_i(s,T)\mathrm{d}W_i^{\mathbb{Q}}(s)},$$

where the drift condition states that $b(s,T) + \sum_{i=1}^{D} \phi(s) a_i(s,T) = 0$ for all $s \leq T$. A process $(M_t)_{0 \leq t \leq T}$ is a $\mathbb{Q}$-martingale if and only if $(M_t Y_t)_{0 \leq t \leq T}$ is a $\mathbb{P}$-martingale (e.g. Pascucci, 2011, Lemma 10.3). That is, we require

$$\mathbb{E}\left(\frac{p(T,T)}{B(T)} Y_T\right) \frac{1}{p(0,T)/B(0)} = 1.$$

Replacing the $\mathbb{Q}$-Brownian motions and algebra gives condition (i). □

We have proven that an equivalent martingale measure exists, but we have not proven that it is unique. To obtain uniqueness, we impose the following condition:

Condition 3.5 (Heath et al., 1992)**.** *To ensure that the equivalent martingale measure is unique, we require that, for fixed* $T_1, \ldots, T_D \in [0, T^*]$ *such that* $0 < T_1 < T_2 < \ldots < T_D \leq T^*$*, the volatility matrix*

$$\begin{bmatrix} a_1(t,T_1) & \ldots & a_D(t,T_1) \\ \vdots & & \vdots \\ a_1(t,T_D) & \ldots & a_D(t,T_D) \end{bmatrix}$$

is nonsingular $\mathbb{Q} \times \lambda$*-a.s, where* λ *is the Lebesgue measure.*

The following proposition states that Condition 3.5 is a necessary and sufficient condition for the uniqueness of the equivalent martingale measure, and equivalently by Theorem 2.4 for market completeness.

Proposition 3.6 (Heath et al., 1992)**.** *Fix* $T_1, \ldots, T_D \in [0, T^*]$ *such that* $0 < T_1 < T_2 < \ldots < T_D \leq T^*$*. Given a vector of forward rate drifts* $\{\mu(\cdot, T_1), \ldots, \alpha(\cdot, T_D)\}$ *and volatilities* $\{\sigma_i(\cdot, T_1), \ldots, \sigma_i(\cdot, T_D)\}$ *for* $i = 1, \ldots, D$ *satisfying the regularity conditions posted in Definition 3.1 and Conditions 3.2 and 3.3, then Condition 3.5 holds if and only if the equivalent martingale measure is unique.*

Modelling under a risk-neutral measure $\mathbb{Q}$ implies a particular choice of risk premiums, namely $\phi_i(t) \equiv 0$. The evolution of the forward rates under the risk-neutral measure is

$$\mathrm{d}f(t,T) = \sum_{i=1}^{D} \int_0^t \left(\sigma_i(s,T) \int_s^T \sigma_i(s,u)\mathrm{d}u\right) \mathrm{d}s + \sum_{i=1}^{D} \int_0^t \sigma_i(s,T)\mathrm{d}W_i^{\mathbb{Q}}(s). \quad (3.6)$$

The HJM model is, therefore, fully specified by the volatility structure $\{\sigma(t,T) : 0 \leq t \leq T \leq T^*\}$ and the initial forward curve $\{f(0,T) : 0 \leq T \leq T^*\}$ observed in the market.

3.4 Discretisation of the HJM Model

An exact simulation from (3.6) is infeasible for general volatility factors. Following the analysis in Glasserman (2013), we thus introduce discrete approximations to attain simulations from the HJM framework.

Let $\hat{f}(t_i, t_j)$ denote the discrete estimation of the forward rate at time t_i with maturity t_j. Both t_i and t_j need to be discretised, and for simplicity, they are fixed to the same time grid $0 = t_0 < t_1 < \ldots < t_M = T^*$. The discrete approximation of the price of a zero-coupon bond is

$$\hat{p}(t_i, t_j) = \exp\left(-\sum_{l=1}^{j-1} \hat{f}(t_i, t_l)(t_{l+1} - t_l)\right), \tag{3.7}$$

and we initialise the discretised bond prices to those observed in the market, $\hat{p}(0, t_j) = p(0, t_j)$, for $j = 0, \ldots, M$. Imposing this restriction and comparing the approximated bond prices with the bond pricing equation (2.5), the estimated instantaneous forward rates are given by

$$\hat{f}(0, t_l) = \frac{1}{t_{l+1} - t_l} \log \frac{p(0, t_l)}{p(0, t_{l+1})}, \tag{3.8}$$

for $l = 0, \ldots, M - 1$. For these initial conditions, a generic approximative simulation of (3.6) takes the form

$$\hat{f}(t_i, t_j) = \hat{f}(t_{i-1}, t_j) + \hat{\mu}(t_{i-1}, t_j)(t_i - t_{i-1}) + \sqrt{t_i - t_{i-1}}\hat{\sigma}(t_{i-1}, t_j)' Z_i, \tag{3.9}$$

for $j = i, \ldots, M$, where $\hat{\sigma}(t_{i-1}, t_j) = (\hat{\sigma}_1(t_{i-1}, t_j), \ldots, \hat{\sigma}_D(t_{i-1}, t_j))'$ and Z_i are independent standard normally distributed random vectors of length D. Requiring that the discretised discounted bond prices are martingales, the combined drift is given by

$$\hat{\mu}(t_{i-1}, t_j) = \sum_{k=1}^{D} \hat{\mu}_k(t_{i-1}, t_j), \tag{3.10}$$

where

$$\begin{aligned} \hat{\mu}_k(t_{i-1}, t_j)(t_{j+1} - t_j) =& \frac{1}{2}\left(\sum_{l=i}^{j} \hat{\sigma}_k(t_{i-1}, t_l)(t_{l+1} - t_l)\right)^2 \\ & - \frac{1}{2}\left(\sum_{l=i}^{j-1} \hat{\sigma}_k(t_{i-1}, t_l)(t_{l+1} - t_l)\right)^2, \end{aligned} \tag{3.11}$$

for $k = 1, \ldots, D$. In order to select a volatility structure which mirrors that observed in the market, the discrete volatility factors $\hat{\sigma}_k(t_i, t_j)$ are usually found by performing

a *principal component analysis* on the historical instantaneous forward rates (see, e.g., Litterman and Scheinkman, 1991; Lekkos, 2000).

A principal component analysis is used to summarise a possibly highly correlated data set by transforming the data into a new set of uncorrelated variables referred to as principal components (James, Witten, Hastie, & Tibshirani, 2013). A principal component analysis by Litterman and Scheinkman (1991) shows that the first three components capture approximately 95 % of the variability in the yield curve for US treasury bonds: The first component explains the average level and the parallel movement of the curve. The second component explains the development of the slope. The third component explains the development of the curvature.

This behaviour is, however, seldom equally pronounced for the forward rate curve. While the movement of forward rates reflects that of simple rates, the decay of eigenvalues is considerably slower, and Kletskin et al. (2004) find that three factors only explain 73.8 % of the variability in US forward rates during the period 1982–2003. Exactly how many volatility factors to use in a model is inevitably a question of model simplicity versus goodness of fit.

Chapter 4

The Lévy Term Structure Model

The HJM model presented in Chapter 3 is well-studied in financial literature, but the model builds on the classical assumption that interest rates follow a diffusion process generated by a Gaussian distribution. It is well-established that normal distributions provide inadequate descriptions of empirically observed financial return distributions. The price trajectories of interest rate derivatives admit jump discontinuities, and empirical distributions of interest rates and interest rate derivatives exhibit kurtosis, skewness, higher moments, and volatility smiles which are inconsistent with a Gaussian distributional assumption.

Inspired by the HJM model, a more general jump–diffusion model was introduced in Björk et al. (1997), where the forward rate curve is modelled by a finite number of Wiener processes and a random jump measure. A more restrictive model where the driving force is a Lévy process was introduced in Eberlein and Raible (1999) and extended to time-inhomogeneous Lévy processes in Eberlein et al. (2005). In this chapter, we present the time-inhomogeneous Lévy term structure model introduced in Eberlein et al. (2005) and Kluge (2005) and derive HJM-like conditions which ensure the existence of an equivalent martingale measure. Lastly, we present a calibration scheme to zero-coupon quotes when a generalised hyperbolic distribution generates the Lévy process.

4.1 Probabilistic Structure of Lévy Processes

A Lévy process $X = (X_t)_{t\geq 0}$ is a process with stationary and independent increments adapted to a filtered probability space $(\Omega, \mathscr{F}, (\mathscr{F}_t)_{t\geq 0}, \mathbb{P})$. For any Lévy process, there exists a unique modification which is both càdlàg (i.e., $\mathbb{P}$-almost surely right-continuous with left limits) and a Lévy process (see Protter, 2005, Theorem 30). In the remainder, we always assume that we study the càdlàg modification of X. For convenience, we assume $X_0 = 0$ $\mathbb{P}$-almost surely.

Lévy processes are semimartingales, but some semimartingale components, like the continuous martingale part, the compensator of the random measure of jumps, and the drift part, are considerably simplified. Lévy processes still, however, constitute a broad class of stochastic processes generated by infinitely divisible distributions in the same way Brownian motions are generated by Gaussian distributions. We should emphasise that Brownian motions are Lévy processes. However, whereas Brownian motions admit continuous sample paths, all other proper Lévy motions admit discontinuous paths. Two Lévy processes (with equal variances) are illustrated

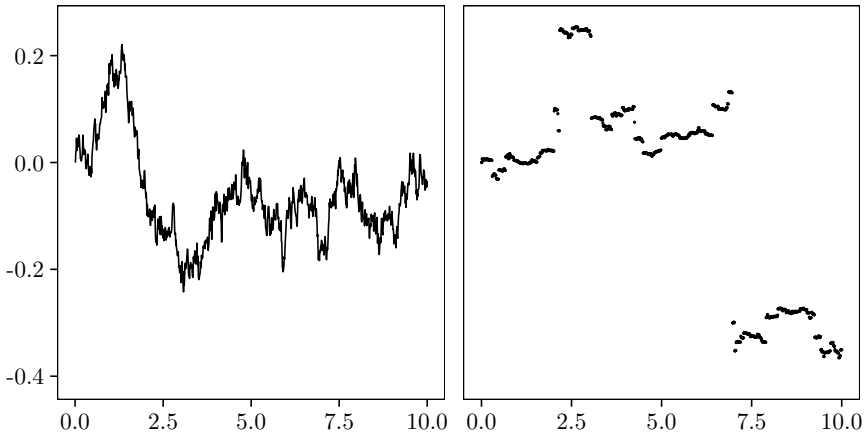

Figure 4.1: Sample path of (left) $\sqrt{0.02}$ times a standard Brownian motion initialised at zero and (right) a NIG($\alpha = 0.2, \beta = 0, \delta = 0.04, \mu = 0$) Lévy process initialised at zero. Hence, the two processes have equal variances.

in Figure 4.1: a Brownian motion and a Lévy process generated by a normal–inverse Gaussian distribution.

A one-dimensional Lévy process X can be represented by (see Protter, 2005, Theorem 42)

$$X_t = bt + \sqrt{c}W_t + Z_t + \sum_{0<s\leq t} \Delta X_s \mathbb{1}_{\{|\Delta X_s|>1\}}, \tag{4.1}$$

where $b \in \mathbb{R}$, $c \in \mathbb{R}_{\geq 0}$, $(W_t)_{t\geq 0}$ is a one-dimensional $\mathbb{P}$-standard Brownian motion, and $(Z_t)_{t\geq 0}$ is a purely discontinuous martingale which is independent of W. $\Delta X_s = X_s - X_{s-}$ denotes the jump of X at time s, and the sum in (4.1) is the sum over the jumps of X with absolute jump size larger than 1.

Since a Lévy process has càdlàg paths, any path only admits a finite number of jumps with absolute size larger than ε, for $\varepsilon>0$, over a finite interval. Consequently, the sum of all jumps with absolute size larger than 1 during $[0, t]$ in (4.1) is finite for all paths. In contrast, the sum of small jumps, $\sum_{s\leq t} \Delta X_s \mathbb{1}_{\{|\Delta X_s|\leq 1\}}$, does not in general converge.

We may, however, force the sum of small jumps to converge by subtracting its average increase during $[0, t]$. The average may be expressed by the intensity $F(\mathrm{d}x) := \mathbb{E}(\sum_{0<s\leq t} \mathbb{1}_{\mathrm{d}x}(\Delta X_s))$ with which the jumps arrive. Then the following limit exists in the sense of convergence in probability:

$$\lim_{\varepsilon\to 0} \left(\sum_{s\leq t} \Delta X_s \mathbb{1}_{\{\varepsilon\leq|\Delta X_s|\leq 1\}} - t \int x \mathbb{1}_{\{\varepsilon\leq|x|\leq 1\}} F(\mathrm{d}x) \right). \tag{4.2}$$

To simplify notation, we introduce the random measure of jumps of X, which we denote by μ^X. The measure is defined by

$$\mu^X(\omega; \mathrm{d}t, \mathrm{d}x) \coloneqq \sum_{s>0} \mathbb{1}_{\{\Delta X_s \neq 0\}} \varepsilon_{(s, \Delta X_s(\omega))}(\mathrm{d}t, \mathrm{d}x). \tag{4.3}$$

That is, if a path ω admits a jump of size $\Delta X_s(\omega) = x$ at time s, the random measure $\mu^X(\omega; \cdot, \cdot)$ places a unit mass $\varepsilon_{(s,x)}$ at $(s, x) \in \mathbb{R}_+ \times \mathbb{R}$. Hence, for a time interval $[0, t]$ and a set $A \subset \mathbb{R}$, the measure $\mu^X(\omega; [0, t] \times A)$ counts how many jumps of sizes within A occur in the given path and time interval,

$$\mu^X(\omega; [0, t] \times A) = |\{(s, x) \in [0, t] \times A | \Delta X_s(\omega) = x\}|.$$

The expected number of jumps may be expressed by the intensity measure $F(A)$,

$$\mathbb{E}\left(\mu^X(\cdot; [0, t] \times A)\right) = tF(A). \tag{4.4}$$

Then, the sum of jumps with absolute size larger than 1 may be articulated as

$$\int_0^t \int_{\mathbb{R}} x \mathbb{1}_{\{|x|>1\}} \mu^X(\mathrm{d}s, \mathrm{d}x), \tag{4.5}$$

and the martingale of compensated jumps with absolute size smaller than 1, $(Z_t)_{t\geq 0}$ in (4.1), is

$$\int_0^t \int_{\mathbb{R}} x \mathbb{1}_{\{|x|\leq 1\}} \left(\mu^X(\mathrm{d}s, \mathrm{d}x) - \mathrm{d}sF(\mathrm{d}x)\right), \tag{4.6}$$

where we for notational simplicity suppress the dependence on ω.

We note that $\mu^X(\omega, \mathrm{d}s, \mathrm{d}x)$ is a random measure which depends on ω, while $\mathrm{d}sF(\mathrm{d}x)$ is a product measure on $\mathbb{R}_+ \times \mathbb{R}$ which does not depend on ω. Moreover, we can, in general, not separate μ^X and F unless the sum of small jumps converges for almost every path; i.e., if $\int_{\{|x|\leq 1\}} |x| F(\mathrm{d}x) < \infty$. For a complete discussion of Lévy processes, we refer to Protter (2005).

Intuitively, a model generated by a Lévy process consists of two parts. The first part is a classical drift–diffusion term generated by a Gaussian distribution. The second part is a jump process, which we can interpret as a model for the arrival of unexpected news and how market prices move discontinuously in reaction. The jump process admits a finite amount of jumps larger than some threshold and an infinite amount of jumps smaller than some threshold.

In comparison, Piazzesi (2005) specified a term structure model that embed jump processes triggered by macroeconomic news announcements from the Federal Reserve. The problem with this approach is that there are a large number of different announcements (or sources) that generate jumps, and it is intractable to model more than a few announcements. In a Lévy term structure model, we do not specify what types of announcements that trigger jumps; we calibrate the generating process to observed market data, such that any simulated path admits jumps from some calibrated jump size density and intensity caused by a series of unspecified jump sources.

4.2 The Driving Process

It is convenient to consider a driving process which is not necessarily a Lévy process, but a process with *independent increments and absolutely continuous characteristics* (PIAAC), which is commonly called a *time-inhomogeneous Lévy process*. Precisely, we relax the assumption of stationarity of increments in order to adequately capture the term structure of implied volatilities (see Eberlein and Kluge, 2006, Figure 1).

We assume a complete stochastic basis $(\Omega, \mathscr{F}, (\mathscr{F}_t)_{0\le t\le T^*}, \mathbb{P})$ for a finite time horizon $T^* > 0$, where $\mathscr{F} = \mathscr{F}_{T^*}$ and the filtration satisfies the usual hypothesis. For convenience, we work with the following definition of a time-inhomogeneous Lévy process:

Definition 4.1. *An adapted, càdlàg stochastic process $L = (L_t)_{0\le t\le T^*}$ taking values in $\mathbb{R}^d$ with $L_0 = 0$ $\mathbb{P}$-a.s., is a d-dimensional* time-inhomogeneous Lévy process *if*

(i) $L_t - L_s$ is independent of $\mathscr{F}_s$ for $0 \le s \le t \le T^*$ and

(ii) for every $0 \le t \le T^*$, the law of L_t is described by the characteristic function

$$\mathbb{E}(e^{i\langle u, L_t\rangle}) = e^{\int_0^t \left(i\langle u, b_s\rangle - \frac{1}{2}\langle u, c_s u\rangle + \int_{\mathbb{R}^d}(e^{i\langle u,x\rangle} - 1 - i\langle u,x\rangle \mathbb{1}_{\{|x|\le 1\}})F_s(\mathrm{d}x)\right)\mathrm{d}s}, \quad (4.7)$$

where $u \in \mathbb{R}^d$, $b_s \in \mathbb{R}^d$, c_s is a symmetric nonnegative-definite $d \times d$ matrix, and the Lévy measure F_s is a measure on $\mathbb{R}^d$ with $F_s(\{0\}) = 0$ and $\int_{\mathbb{R}^d}(|x|^2 \wedge 1)F_s(\mathrm{d}x) < \infty$. Lastly, Condition 4.2 holds.

We call $(b, c, F) := (b_s, c_s, F_s)_{0\le s\le T^*}$ the local characteristics *of L.*

Condition 4.2. *The Lévy triplets $(b_s, c_s, F_s)_{0\le s\le T^*}$ satisfy*

$$\int_0^{T^*} \left(|b_s| + \|c_s\| + \int_{\mathbb{R}^d}(|x|^2 \wedge 1)F_s(\mathrm{d}x)\right)\mathrm{d}s < \infty.$$

Under Condition 4.2, the characteristic function of a time-inhomogeneous Lévy process L has a finite variation over finite intervals. By Jacod and Shiryaev (2003, Theorem II.4.14), L is then a semimartingale with respect to $(\Omega, \mathscr{F}, (\mathscr{F}_t)_{0\le t\le T^*}, \mathbb{P})$.

In the term structure models which we will consider, the underlying processes are exponentials of stochastic integrals with respect to the driving processes. To allow for derivative pricing, we require that the underlying processes are martingales under the risk-neutral measure, and they must then admit finite expectations. We will, therefore, impose the following condition:

Condition 4.3. *There exist constants $M, \epsilon > 0$ such that*

$$\int_0^{T^*} \int_{\{|x|>1\}} \exp\langle u, x\rangle F_s(\mathrm{d}x)\mathrm{d}s < \infty \quad \textit{for all} \quad u \in [-(1+\epsilon)M, (1+\epsilon)M]^d.$$

Without loss of generality, $\int_{\{|x|>1\}} \exp\langle u, x\rangle F_s(\mathrm{d}x)$ is assumed to be finite for all s.

Condition 4.3 holds if and only if $\mathbb{E}(\exp\langle u, L_t\rangle) < \infty$ for all $0 \le t \le T^*$ and u as given above (Kluge, 2005, Lemma 1.6). Consequently, L_t has a finite expectation on the studied time horizon. We may then remove the truncation function from the law of L, and (4.7) simplifies to

$$\mathbb{E}(e^{i\langle u, L_t\rangle}) = e^{\int_0^t \left(i\langle u, \tilde{b}_s\rangle - \frac{1}{2}\langle u, c_s u\rangle + \int_{\mathbb{R}^d}(e^{i\langle u,x\rangle} - 1 - i\langle u,x\rangle)F_s(\mathrm{d}x)\right)\mathrm{d}s}, \tag{4.8}$$

where $\int_0^t(\tilde{b}_s - b_s)\mathrm{d}s = (x - x\mathbb{1}_{\{|x|\le 1\}}) * \nu$. In the remaining, we will always consider the local characteristics $(\tilde{b}_s, c_s, F_s)$, and we write b_s in lieu of $\tilde{b}_s$.

Proposition 4.4. *Under Condition 4.3, L is a* special semimartingale *(Kluge, 2005, Lemma 1.7), and it admits the canonical representation (Jacod and Shiryaev, 2003, II.2.38)*

$$L_t = \int_0^t b_s \mathrm{d}s + \int_0^t \sqrt{c_s}\mathrm{d}W_s + \int_0^t \int_{\mathbb{R}^d} x(\mu - \nu)(\mathrm{d}s, \mathrm{d}x), \tag{4.9}$$

where $\sqrt{c}$ is a measurable version of the square root of c, $(W_t)_{0\le t\le T^*}$ is a d-dimensional $\mathbb{P}$-standard Brownian motion, and μ is the random measure of jumps with $\mathbb{P}$-compensator $\nu(\mathrm{d}s, \mathrm{d}x) = F_s(\mathrm{d}x)\mathrm{d}s$.

We let θ_s denote the cumulant associated with the L as given in (4.9) with local characteristics (b_s, c_s, F_s); that is,

$$\theta_s(z) \coloneqq \langle z, b_s\rangle + \frac{1}{2}\langle z, c_s z\rangle + \int_{\mathbb{R}^d}(e^{\langle z,x\rangle} - 1 - \langle z, x\rangle)F_s(\mathrm{d}x),$$

for $M, \epsilon > 0$, a fixed $t \in [0, T^*]$, and $z \in \mathbb{C}^d$ with $\Re(z) \in [-(1+\epsilon)M, (1+\epsilon)M]^d$.

We will need the next proposition to derive an equivalent martingale measure in subsequent sections. See, e.g., Kluge (2005, Proposition 1.9) for proof.

Proposition 4.5. *Suppose that $f : \mathbb{R}_+ \to \mathbb{C}^d$ is a continuous function such that $|\Re(f^i(x))| \le M$ for all $i \in \{1, \dots, d\}$ and $x \in \mathbb{R}_+$, then*

$$\mathbb{E}\left(\exp\left(\int_t^T f(s)\mathrm{d}L_s\right)\right) = \exp\left(\int_t^T \theta_s(f(s))\mathrm{d}s\right).$$

4.3 The Lévy Term Structure Model

Assume a fixed time horizon $T^* > 0$ and that there exists a zero-coupon bond for every maturity $T \in [0, T^*]$ traded in the market. The model is driven by a d-dimensional time-inhomogeneous Lévy process $L = (L_t)_{0\le t\le T^*}$ with local characteristics $(b_s, c_s, F_s)_{0\le s\le T^*}$ on the probability space $(\Omega, \mathscr{F}, \mathbb{P})$ equipped with the canonical filtration $(\mathscr{F}_t)_{0\le t\le T^*}$. As in Eberlein et al. (2005), we assume the following forward rate process:

Definition 4.6. *We assume that the dynamics of the instantaneous forward rate curve are given by a stochastic process of the form*

$$f(t,T) = f(0,T) + \int_0^t \alpha(s,T)\mathrm{d}s - \int_0^t \sigma(s,T)\mathrm{d}L_s, \tag{4.10}$$

for all $0 \le t \le T \le T^*$*, where* $\{f(0,T) : 0 \le T \le T^*\}$ *is deterministic and bounded and measurable in* T*, and* α *and* σ *are respectively* $\mathbb{R}$*- and* $\mathbb{R}^d$*-valued stochastic processes on* $\Omega \times [0,T^*] \times [0,T^*]$ *that satisfy (where* $\mathcal{P}$ *denotes the predictable* σ*-field on* $\Omega \times [0,T^*]$*)*

(i) $(\omega,s,T) \mapsto \alpha(\omega,s,T)$ *and* $(\omega,s,T) \mapsto \sigma(\omega,s,T)$ *are* $\mathcal{P} \otimes \mathcal{B}([0,T^*])$*-measurable;*

(ii) for $s > T$*,* $\alpha(\omega,s,T) = 0$ *and* $\sigma(\omega,s,T) = 0$*; and*

(iii) $\sup_{s,T \le T^*}(|\alpha(\omega,s,T)| + |\sigma(\omega,s,T)|) < \infty$*.*

From the postulated forward rate process, we may derive an equivalent expression for the zero-coupon bond price process using the same approach as in Björk et al. (1997, Proposition 5.2):

Proposition 4.7. *The dynamics of the zero-coupon bond price process* $p(t,T)$ *for* $0 \le t \le T \le T^*$ *is given by*

$$p(t,T) = p(0,T)\exp\left(\int_0^t (r(s) - A(s,T))\mathrm{d}s + \int_0^t \Sigma(s,T)\mathrm{d}L_s\right), \tag{4.11}$$

where

$$A(s,T) \coloneqq \int_{s\wedge T}^T \alpha(s,u)\mathrm{d}u \quad \text{and} \quad \Sigma(s,T) \coloneqq \int_{s\wedge T}^T \sigma(s,u)\mathrm{d}u. \tag{4.12}$$

Proof. We insert the forward rate process (4.10) into the bond-pricing equation (2.5) and use the stochastic version of Fubini's theorem (see, e.g., Björk et al., 1997) to change the order of integration:

$$\begin{aligned}
p(t,T) &= \exp\left(-\int_t^T f(0,u)\mathrm{d}u - \int_t^T \int_0^t \alpha(s,u)\mathrm{d}s\mathrm{d}u + \int_t^T \int_0^t \sigma(s,u)\mathrm{d}L_s\mathrm{d}u\right) \\
&= \exp\left(-\int_t^T f(0,u)\mathrm{d}u - \int_0^t \int_t^T \alpha(s,u)\mathrm{d}u\mathrm{d}s + \int_0^t \int_t^T \sigma(s,u)\mathrm{d}u\mathrm{d}L_s\right) \\
&= \exp\left(-\int_0^T f(0,u)\mathrm{d}u - \int_0^t \int_s^T \alpha(s,u)\mathrm{d}u\mathrm{d}s + \int_0^t \int_s^T \sigma(s,u)\mathrm{d}u\mathrm{d}L_s\right. \\
&\qquad \left. + \int_0^t f(0,u)\mathrm{d}u + \int_0^t \int_s^t \alpha(s,u)\mathrm{d}u\mathrm{d}s - \int_0^t \int_s^t \sigma(s,u)\mathrm{d}u\mathrm{d}L_s\right).
\end{aligned}$$

We want to insert an expression for the spot rate. We recognise that, using (4.10) with maturity $T = t$,

$$\begin{aligned}\int_0^t f(0,u)\mathrm{d}u &= \int_0^t r(u)\mathrm{d}u - \int_0^t \int_0^u \alpha(s,u)\mathrm{d}s\mathrm{d}u + \int_0^t \int_0^u \sigma(s,u)\mathrm{d}L_s\mathrm{d}u \\ &= \int_0^t r(u)\mathrm{d}u - \int_0^t \int_s^t \alpha(s,u)\mathrm{d}u\mathrm{d}s + \int_0^t \int_s^t \sigma(s,u)\mathrm{d}u\mathrm{d}L_s,\end{aligned}$$

again using Fubini's theorem. If we insert this expression into the expanded bond-pricing equation,

$$\begin{aligned}\log p(t,T) = &- \int_0^T f(0,u)\mathrm{d}u - \int_0^t \int_s^T \alpha(s,u)\mathrm{d}u\mathrm{d}s + \int_0^t \int_s^T \sigma(s,u)\mathrm{d}u\mathrm{d}L_s \\ &+ \int_0^t r(u)\mathrm{d}u + \int_0^t \int_s^t \alpha(s,u)\mathrm{d}u\mathrm{d}s - \int_0^t \int_s^t \sigma(s,u)\mathrm{d}u\mathrm{d}L_s \\ &- \int_0^t \int_s^t \alpha(s,u)\mathrm{d}u\mathrm{d}s + \int_0^t \int_s^t \sigma(s,u)\mathrm{d}u\mathrm{d}L_s.\end{aligned}$$

Algebra completes the proof. □

Using $A(s,t,T) := A(s,T) - A(s,t)$ and $\Sigma(s,t,T) := \Sigma(s,T) - \Sigma(s,t)$, we obtain a useful representation of the zero-coupon bond price process,

$$p(t,T) = \frac{p(0,T)}{p(0,t)} \exp\left(-\int_0^t A(s,t,T)\mathrm{d}s + \int_0^t \Sigma(s,t,T)\mathrm{d}L_s\right). \tag{4.13}$$

Combining the alternative representation (4.13) with the zero-coupon bond price process (4.11), we obtain an expression for the money-market account,

$$B(t) = \frac{1}{p(0,t)} \exp\left(\int_0^t A(s,t)\mathrm{d}s - \int_0^t \Sigma(s,t)\mathrm{d}L_s\right). \tag{4.14}$$

We consider only deterministic volatility structures. In addition to assuming Condition 4.3, we require that the driving process satisfies:

Condition 4.8. *The volatility structure σ is deterministic and bounded. For $0 \le s \le T \le T^*$ we have*

$$0 \le \Sigma^i(s,T) \le M \quad \textit{for all} \quad i = 0,\dots,d,$$

where Σ is given by (4.12) and M is the constant from Condition 4.3. Note that $\Sigma(s,s) = 0$.

We now wish to find a necessary condition for which the discounted bond price processes are martingales. For simplicity, we assume that $d = 1$. Define the process $Y(t,T) \coloneqq -\int_0^t A(s,T)\mathrm{d}s + \int_0^t \Sigma(s,T)\mathrm{d}L_s$. Using the canonical representation of a Lévy process with triplet (b_s, c_s, F_s), the canonical representation of Y is

$$\begin{aligned} Y(t,T) = &-\int_0^t A(s,T)\mathrm{d}s + \int_0^t \Sigma(s,T)b_s\mathrm{d}s + \int_0^t \Sigma(s,T)\sqrt{c_s}\mathrm{d}W_s \\ &+ \int_0^t \int_{\mathbb{R}} \Sigma(s,T)x(\mu-\nu)(\mathrm{d}s,\mathrm{d}x). \end{aligned}$$

We define a function $f(Y_t) \coloneqq p(0,T)\exp Y(t,T)$ which is twice continuously differentiable. Itô's lemma for general Lévy processes (see, e.g., Kyprianou, 2006, Chapter 4) then states

$$\begin{aligned} f(Y_t) =& f(Y_0) + \int_0^t f'(Y_{s-})\mathrm{d}Y_s + \frac{1}{2}\int_0^t c_s\Sigma(s,T)^2 f''(Y_{s-})\mathrm{d}s \\ &+ \int_0^t \int_{\mathbb{R}} (f(Y_{s-}+\Sigma(s,T)x) - f(Y_{s-}) - \Sigma(s,T)xf'(Y_{s-}))F_s(\mathrm{d}x)\mathrm{d}s \\ =& f(Y_0) + \int_0^t f(Y_{s-})(-A(s,T)\mathrm{d}s + \Sigma(s,T)b_s\mathrm{d}s + \Sigma(s,T)\sqrt{c_s}\mathrm{d}W_s) \\ &+ \frac{1}{2}\int_0^t c_s\Sigma(s,T)^2 f(Y_{s-})\mathrm{d}s + \int_0^t \int_{\mathbb{R}} f(Y_{s-})\Sigma(s,T)x(\mu-\nu)(\mathrm{d}s,\mathrm{d}x) \\ &+ \int_0^t \int_{\mathbb{R}} (f(Y_{s-}+\Sigma(s,T)x) - f(Y_{s-}) - \Sigma(s,T)xf'(Y_{s-}))F_s(\mathrm{d}x)\mathrm{d}s. \end{aligned}$$

As a necessary condition for the function f to be a martingale, we require that the deterministic drift term is zero. That is, for all $0 \le s \le T$,

$$\begin{aligned} A(s,T) &= \Sigma(s,T)b_s + \frac{1}{2}c_s\Sigma(s,T)^2 + \int_{\mathbb{R}} (e^{\Sigma(s,T)x} - 1 - \Sigma(s,T)x)F_s(\mathrm{d}x) \\ &= \theta_s(\Sigma(s,T)). \end{aligned}$$

4.4 Arbitrage-Free Conditions

Equivalent to Theorem 3.4, we wish to give sufficient conditions for the existence of an equivalent martingale measure under which the discounted bond price processes are martingales. The ensuing theorem proposes a HJM-like drift condition which ensures that the discounted bond price processes are martingales and, consequently, that the market is arbitrage-free.

Theorem 4.9. *Let $A(s,T) = \theta_s(\Sigma(s,T))$. Then, for all $0 \le s \le T \le T^*$, the discounted bond price process $\tilde{p}(t,T) = p(t,T)/B(t)$ is a martingale.*

Proof. By construction, the studied Lévy process is càdlàg, adapted, and admits a finite expectation on the studied time horizon. To prove that the discounted bond price process is a martingale, we only need to prove that its conditional expectation with respect to previous observations equals the most recent observation.

We use Proposition 4.5 with $f(s) \coloneqq \Sigma(s,T)$ for a fixed $0 \leq T \leq T^*$, such that

$$\mathbb{E}\left(\exp\left(\int_0^t \Sigma(s,T)\mathrm{d}L_s\right)\right) = \exp\left(\int_0^t \theta_s(\Sigma(s,T))\mathrm{d}s\right).$$

Let $A(s,T) = \theta_s(\Sigma(s,T))$ and $X_t \coloneqq \int_0^t \Sigma(s,T)\mathrm{d}L_s$. Using the previous equation,

$$\mathbb{E}(\exp X_t) = \exp\left(\int_0^t A(s,T)\mathrm{d}s\right).$$

The discounted bond price process may then be expressed as

$$\tilde{p}(t,T) = \frac{1}{B(t)}p(t,T) = p(0,T)\frac{\exp X_t}{\mathbb{E}(\exp X_t)}.$$

Lastly, since X is a Lévy process, it has independent increments. Thus,

$$\mathbb{E}(\exp(X_t)|\mathscr{F}_s) = \mathbb{E}\left(\exp(X_t - X_s)\exp(X_s)|\mathscr{F}_s\right) = \frac{\mathbb{E}(\exp(X_t))}{\mathbb{E}(\exp(X_s))}\exp(X_s).$$

Consequently, $\mathbb{E}(\tilde{p}(t,T)|\mathscr{F}_s) = \tilde{p}(s,T)$, and the discounted bond price process is a martingale. □

We have only proved the existence of an equivalent martingale measure. Eberlein et al. (2005) showed that the equivalent martingale measure is unique for $d = 1$, but that this property does not hold in general for $d \geq 2$.

4.5 Generalised Hyperbolic Distributions

Before we can calibrate the term structure model to market data, we need to specify the generating distribution of the driving Lévy process in (4.10). If we let L_s equal a Brownian motion, such that $\theta(u) = u^2/2$, we arrive at the Gaussian HJM forward rate model (3.1). In this thesis, we will, however, consider Lévy processes generated by generalised hyperbolic (GH) distributions.

Barndorff-Nielsen and Halgreen (1977) showed that generalised hyperbolic distributions are infinitely divisible, and hence (e.g., Protter, 2005, Chapter I.4) every member of this family of distributions generates a Lévy process $(X_t)_{t\geq 0}$. That is, it generates a process with stationary and independent increments such that $X_0 = 0$ and $\mathcal{L}(X_1)$, the law of X_1, equals $\mathrm{GH}(\lambda, \alpha, \beta, \delta, \mu)$. We might then choose a càdlàg version of this process, and we call this the generalised hyperbolic Lévy motion. The (univariate) distribution is characterised by its characteristic function

$$\Psi_{\mathrm{GH}}(u) = e^{i\mu u}\left(\frac{\alpha^2-\beta^2}{\alpha^2-(\beta+iu)^2}\right)^{\lambda/2}\frac{K_\lambda(\delta\sqrt{\alpha^2-(\beta+iu)^2})}{K_\lambda(\delta\sqrt{\alpha^2-\beta^2})}, \tag{4.15}$$

and it admits the density function

$$f_{\mathrm{GH}}(x) = \frac{(\alpha^2-\beta^2)^{\lambda/2}K_{\lambda-1/2}\left(\alpha\sqrt{\delta^2+(x-\mu)^2}\right)\exp(\beta(x-\mu))}{\sqrt{2\pi}\alpha^{\lambda-1/2}\delta^\lambda K_\lambda\left(\delta\sqrt{\alpha^2-\beta^2}\right)\left(\sqrt{\delta^2+(x-\mu)^2}\right)^{1/2-\lambda}}, \tag{4.16}$$

where K_λ is the modified Bessel function of the third kind and $x \in \mathbb{R}$. The domain of variation of the parameters is $\mu \in \mathbb{R}$ and

$$\begin{aligned}
&\delta \geq 0,\ |\beta| < \alpha \quad \text{if} \quad \lambda > 0,\\
&\delta > 0,\ |\beta| < \alpha \quad \text{if} \quad \lambda = 0,\\
&\delta > 0,\ |\beta| \leq \alpha \quad \text{if} \quad \lambda < 0.
\end{aligned}$$

Generally, α determines the shape of the distribution, β determines the skewness, μ determines the location, and δ is a scaling parameter. The index parameter λ characterises specific subclasses and changing λ roughly affects the heaviness of the tails.

While several subclasses of the GH distribution are frequently used in financial applications, the GH distribution itself is rarely directly used. The distribution is not particularly analytical tractable, and even for large sample sizes, it is difficult to distinguish between different values of λ due to the flatness of the GH likelihood function in this parameter (Prause et al., 1999).

4.5.1 Normal–Inverse Gaussian Distributions

One frequently used distribution for modelling financial data is the normal–inverse Gaussian (NIG) distribution (Barndorff-Nielsen, 1997). It is repeatably used as the conditional distribution of a GARCH model (Andersson, 2001; Jensen & Lunde, 2001; Forsberg & Bollerslev, 2002; Chen et al., 2008) or as an unconditional returns distribution (Rydberg, 1997; Prause, 1997; Bølviken & Benth, 2000; Raible, 2000; Kassberger, 2009; Kassberger & Kiesel, 2006; Fergusson & Platen, 2006). The NIG distribution possesses several attractive analytical properties, including skewness, semi-heavy tails, and analytical tractability.

The NIG distribution is a special case of the generalised hyperbolic distribution when $\lambda = -1/2$, such the characteristic function simplifies to

$$\Psi_{\mathrm{NIG}}(u) = e^{iu\mu}\frac{\exp(\delta\sqrt{\alpha^2-\beta^2})}{\exp(\delta\sqrt{\alpha^2-(\beta+iu)^2})}, \tag{4.17}$$

and the density function simplifies to

$$f_{\text{NIG}}(x) = \frac{\delta\alpha \exp(\delta\sqrt{\alpha^2-\beta^2}) K_1\left(\alpha\sqrt{\delta^2+(x-\mu)^2}\right) \exp(\beta(x-\mu))}{\pi\sqrt{\delta^2+(x-\mu)^2}}, \tag{4.18}$$

where $\delta > 0$ and $0 < |\beta| < \alpha$. In general, for GH distributions, none of the increments of length different from 1 admits a density from the same class. However, the NIG distributions admit the densities $\mathcal{L}(X_t) = \text{NIG}(\alpha, \beta, t\delta, t\mu)$. Moreover, NIG is the only subclass with the convolution property

$$\text{NIG}(\alpha, \beta, \delta_1, \mu_1) * \text{NIG}(\alpha, \beta, \delta_2, \mu_2) = \text{NIG}(\alpha, \beta, \delta_1 + \delta_2, \mu_1 + \mu_2).$$

The NIG distribution has two semi-heavy tails. Using the properties of the modified Bessel function (Abramowitz, Stegun, & Romer, 1988)

$$K_\nu(x) \sim \sqrt{\frac{\pi}{2x}} \exp(-x) \quad \text{for } x \to \pm\infty, \tag{4.19}$$

it can be shown that the tails of the NIG distribution are

$$f_{\text{NIG}}(x) \sim \text{const}|x|^{-3/2} \exp(-\alpha|x| + \beta x) \quad \text{as } x \to \pm\infty.$$

Thus, the heaviest tail decays as

$$f_{\text{NIG}}(x) \sim \text{const}|x|^{-3/2} \exp(-\alpha|x| + \beta|x|) \quad \text{when } \begin{cases} \beta < 0 \text{ and } x \to -\infty, \\ \beta > 0 \text{ and } x \to +\infty, \end{cases}$$

and the lightest tail decays as

$$f_{\text{NIG}}(x) \sim \text{const}|x|^{-3/2} \exp(-\alpha|x| - \beta|x|) \quad \text{when } \begin{cases} \beta < 0 \text{ and } x \to +\infty, \\ \beta > 0 \text{ and } x \to -\infty. \end{cases}$$

4.5.2 Generalised Hyperbolic Skew Student's t-Distributions

An alternative set of distributions for modelling skewed and heavy-tailed financial data is the generalised hyperbolic skew Student's (GSS) t-distribution, briefly mentioned in Prause et al. (1999); Barndorff-Nielsen and Shephard (2002); Mencía and Sentana (2005) and applied in a univariate setting in Aas and Haff (2006). It is too a subclass of the generalised hyperbolic distribution, and it is the only subclass of this family of distributions with one tail determined by a polynomial behaviour and the other by an exponential behaviour.

The GSS distribution follows from the limit of the generalised hyperbolic distribution when $\alpha \to |\beta|$ and $\lambda = -\nu/2$ for $\nu > 0$. Using the following properties of the modified Bessel function (Abramowitz et al., 1988),

$$K_\nu(x) = K_{-\nu}(x) \quad \text{and} \quad K_\nu(x) \sim \Gamma(\nu)2^{\nu-1}x^{-\nu} \quad \text{for} \quad x \to 0,\ \nu > 0, \tag{4.20}$$

the density of the GSS distribution is given by (Aas & Haff, 2006)

$$f_{\mathrm{GSS}}(x) = \frac{2^{\frac{1-\nu}{2}}\delta^\nu|\beta|^{\frac{\nu+1}{2}}K_{\frac{\nu+1}{2}}\left(\sqrt{\beta^2(\delta^2+(x-\mu)^2)}\right)\exp(\beta(x-\mu))}{\Gamma(\frac{\nu}{2})\sqrt{\pi}\left(\sqrt{\delta^2+(x-\mu)^2}\right)^{\frac{\nu+1}{2}}}, \tag{4.21}$$

for $\beta \neq 0$, and its characteristic function is given by

$$\Psi_{\mathrm{GSS}}(u) = e^{i\mu u}\frac{(u^2-2i\beta u)^{\nu/4}\delta^{\nu/2}}{\Gamma\left(\frac{\nu}{2}\right)2^{\nu/2-1}}K_{\nu/2}\left(\delta\sqrt{u^2-2i\beta u}\right). \tag{4.22}$$

Again using the properties of the modified Bessel function (4.19), the tails of the GSS distribution are given by

$$f_{\mathrm{GSS}}(x) \sim \mathrm{const}|x|^{-\nu/2-1}\exp(-|\beta||x|+\beta x) \quad \text{as } x \to \pm\infty.$$

Hence, the heaviest tail decays as a polynomial,

$$f_{\mathrm{GSS}}(x) \sim \mathrm{const}|x|^{-\nu/2-1} \quad \text{when} \begin{cases} \beta < 0 \text{ and } x \to -\infty, \\ \beta > 0 \text{ and } x \to +\infty, \end{cases}$$

and the lightest tail decays exponentially,

$$f_{\mathrm{GSS}}(x) \sim \mathrm{const}|x|^{-\nu/2-1}\exp(-2|\beta||x|) \quad \text{when} \begin{cases} \beta < 0 \text{ and } x \to +\infty, \\ \beta > 0 \text{ and } x \to -\infty. \end{cases}$$

4.6 Calibration of Lévy Term Structure Models

In this section, we present a calibration scheme for the (one-dimensional, time-homogeneous) Lévy term structure models using zero-coupon bond quotes of M maturities observed over D consecutive trading days.

Two possible calibration strategies involve estimating the parameters of the driving process under the real-world measure or the risk-neutral measure. Under the risk-neutral measure, we attempt to calibrate the model by minimising the differences between market prices and risk-neutral model prices simultaneously across all available maturities (e.g. Kluge, 2005). Under the real-world measure, we attempt to estimate the empirical increments of the driving process and then maximise the likelihood of the driving process conditional on these increments (e.g. Eberlein and Kluge, 2007).

The market quotes contain a maximum of information, and a direct fit to market prices may provide more reliable calibration results – at least if we want to use the model to price complex instruments. In this thesis, we are, however, more interested in the movements of interest rates and their generating distributions. A real-world calibration provides a more smoothed-out fit to market data, possibly avoiding overfitting, with a more explicit focus on the generating return distribution. In this thesis, we thus concentrate on real-world calibration.

Assume a discretisation of tenor dates $0 = t_0 < t_1 < \ldots < t_M$. We consider a Lévy process with a one-dimensional time-homogeneous driving process L. That is, L has stationary increments. Precisely, we model the increments of length 1 to follow a normal–inverse Gaussian distribution, $L_1 \sim \mathrm{NIG}(\alpha, \beta, \delta, \mu)$, or equivalently a generalised hyperbolic skew Student's t-distribution, $L_1 \sim \mathrm{GSS}(\nu, \beta, \delta, \mu)$.

We consider the (stationary) Ho–Lee volatility structure $\Sigma(s,T) = \hat{\sigma}(T-s)$. Without loss of generality, one can set $\hat{\sigma} \equiv 1$ as this parameter may be included in the specification of the Lévy process. To see this, define $\tilde{L} = \hat{\sigma}L$ and $\tilde{\Sigma}(s,T) = \Sigma(s,T)/\hat{\sigma}$. Then (e.g. Eberlein, 2001) $\mathcal{L}(\tilde{L}_1) = \mathrm{NIG}(\alpha/|\hat{\sigma}|, \beta|\hat{\sigma}|, \delta|\hat{\sigma}|, \mu\hat{\sigma})$, and $\int_0^t \tilde{\Sigma}(s,T)\mathrm{d}\tilde{L}_s = \int_0^t \Sigma(s,T)\mathrm{d}L_s$.

Following the framework in Eberlein and Kluge (2007), we consider the daily log-returns, which are given by the ratio of bond prices and their forward price on the previous day,

$$LR(t,T) \coloneqq \log \frac{p(t+1,t+T)}{p(t,t+1,t+T)},$$

where the forward price of $p(t+1,t+T)$ at time t is defined by

$$p(t,t+1,t+T) \coloneqq \frac{p(t,t+T)}{p(t,t+1)}.$$

Using the bond-price process (4.13), we express the daily log-returns by

$$LR(t,T) = -\int_t^{t+1} A(s,t+1,t+T)\mathrm{d}s + \int_t^{t+1} \Sigma(s,t+1,t+T)\mathrm{d}L_s. \tag{4.23}$$

In the risk-neutral measure defined by Theorem 4.9, stationarity of the drift term follows from the stationarity of the volatility structure. That is, $A(s,T) = A(0,T-s)$ for $s \leq T$, and

$$\begin{aligned} d(T) &\coloneqq -\int_t^{t+1} A(s,t+1,t+T)\mathrm{d}s = \int_0^1 (A(s,1) - A(s,T))\mathrm{d}s \\ &= \int_0^1 (\theta(\Sigma(s,1)) - \theta(\Sigma(s,T)))\mathrm{d}s, \end{aligned} \tag{4.24}$$

which is deterministic and independent of t. (Since L is stationary, we may omit the time index of the cumulant, and $\theta(z) = \log \Psi(-iu)$.) Moreover, the expectation of the stochastic integral in (4.23) is

$$\mathbb{E}\left(\int_t^{t+1} \Sigma(s, t+1, t+T)\mathrm{d}L_s\right) = (T-1)\mathbb{E}(L_{t+1} - L_t) = 0,$$

since $Y_{t+1} \coloneqq (L_{t+1} - L_t)$ admits the law $\mathcal{L}(Y_{t+1}) = \mathcal{L}(L_1)$ and $\mathbb{E}(L_1) = 0$. Thus $\mathbb{E}(LR(t,T)) = d(T)$ with the estimator

$$\bar{x}_T \coloneqq \frac{1}{D-1}\sum_{t=0}^{D-2} LR(t,T),$$

and $LR(t,T) - \mathbb{E}(LR(t,T)) = (T-1)Y_{t+1}$.

We now need to determine the observed daily log-returns. That is, for $k = 0, \ldots, D-2$ and $T = t_1, \ldots, t_M$, we find

$$LR(k,T) = \log p(k+1, k+T) + \log\frac{p(k,k+1)}{p(k,k+T)}.$$

Here we can only retrieve $p(k, k+T)$ (and possibly $p(k,k+1)$) directly from the data. To estimate $p(k+1, k+T)$ and $p(k,k+1)$, we apply the method of Raible (2000, Section 5.3) and interpolate the negative of the log-bond prices with a cubic spline separately for each day in the data set.

We find an estimate for y_{k+1} by

$$\arg\min_{y_{k+1}} \sum_{T=t_1}^{t_M} (LR(k,T) - \bar{x}_T - (T-1)y_{k+1})^2. \tag{4.25}$$

If we repeat this process for each k, we retrieve estimates $y_1, \ldots, y_{D-1}$. The parameters of $\mathcal{L}(L_1)$ may then be estimated by maximising the likelihood of the generating distribution. This may be performed using the EM-algorithm, see Appendix A.

The in-sample distribution fit to log-bond returns of one or more maturities may be improved by considering fewer maturities in the estimation of the empirical increments in (4.25). That is, we assume that the dynamics of the driving process is dependent on the time to maturity. In the following, we will refer to these models as (piecewise) time-inhomogeneous Lévy processes.

We may similarly extend the calibration scheme to multivariate distributions. While it is not obvious how we can include correlations between risk factors generated by different piecewise time-inhomogeneous Lévy processes, multivariate GH distributions naturally exhibit non-linear dependence. The tail behaviour of multivariate models mirrors the fact that extreme market movements usually co-occur for several risk factors. An EM algorithm for multivariate GH distributions is presented in, e.g., Protassov (2004); McNeil, Frey, and Embrechts (2005); Hu (2005).

Chapter 5

Market Risk

Market risk is the risk of losses on financial investments arising from adverse movements in market prices, including equity and commodity prices, currencies, credit spreads, and interest rates. In order to ensure the safety of financial institutions and their liability holders, banks are required to maintain a minimum amount of capital to safeguard against market risks. The significant losses banks incurred during the 2007–2009 global financial crisis as a result of failures to prudently measure market and credit risks, however, highlighted the need for stricter regulatory capital requirements and better estimates of market risks. As a result, the Basel Committee's revised frameworks include improvements of capital charges of market risks and market risks under stressed market conditions. In this chapter, we present the notion of coherent risk measures and two standard measures of market risk. We lastly present backtesting frameworks for the considered risk measures.

5.1 Coherent Risk Measures

There are several ways in which risk can be defined and measured. To clarify the notion of risks, Artzner, Delbaen, Eber, and Heath (1999) articulate a unified framework for the analysis, construction, and implementation of measures of risk to provide a sound basis for developing capital adequacy tests. Artzner et al. describe four properties that risk measures should possess. A risk measure which satisfies all four properties is called *coherent*.

Definition 5.1. *Let $\mathscr{G}$ be the set of all risky positions. A measure of risk ρ is a mapping from $\mathscr{G}$ to $\mathbb{R}$, and it is called a* coherent risk measure *if it satisfies the following properties:*

(i) (Translation invariance) For all $X \in \mathscr{G}$ and a deterministic portfolio Y with a certain real return α, then $\rho(X + Y) = \rho(X) - \alpha$. That is, the addition of a sure amount of capital to a position will decrease the risk by that amount.

(ii) (Subadditivity) For all $X_1, X_2 \in \mathscr{G}$, then $\rho(X_1 + X_2) \leq \rho(X_1) + \rho(X_2)$. That is, a merger between two portfolios does not add additional risk, cf. diversification.

(iii) (Positive homogeneity) For all $\lambda \geq 0$ and all $X \in \mathscr{G}$, then $\rho(\lambda X) = \lambda \rho(X)$. That is, increasing the position by a factor increases the risk proportionally.

(iv) (Monotonicity) For all $X_1, X_2 \in \mathscr{G}$ with $X_1 \leq X_2$, then $\rho(X_2) \leq \rho(X_1)$. That is, if the returns in position X_1 are consistently lower than in X_2, the risk is greater in X_1.

5.2 Market Risk Measures

5.2.1 Value-at-Risk

The most prominent capital adequacy tests used by the banking sector are based on the value-at-risk (VaR) measure.

Definition 5.2. *Given a portfolio return distribution X, a probability measure $\mathbb{P}$, and a level $\alpha \in (0,1)$, the* value-at-risk *at confidence level $1-\alpha$ is the negative of the α-quantile of X; that is,*

$$VaR_X(\alpha) \coloneqq -\inf\{x \in \mathbb{R} : \mathbb{P}(X \leq x) \geq \alpha\}.$$

The market risk capital charge defined in the Basel Accords is based on the value-at-risk at a future ten-day time horizon and a one-tailed, 99 percentile confidence level (Basel Committee on Banking Supervision, 2013). It is usually required that the model is calibrated using at least one previous year of trading data. The measure represents the maximum portfolio loss at a 99 per cent probability, and it is often interpreted as the degree of risk inherent in a position.

From a theoretical perspective, VaR performs poorly in meeting regulatory objectives due to two prominent deficiencies: VaR is not a coherent risk measure as it can be shown that it is non-subadditive for non-elliptical portfolios (see Artzner et al., 1999), and VaR possesses a structural blindness of the "far tail" of a position (e.g. Acerbi, Nordio, and Sirtori, 2001; Longin, 2001). Herein, the far tail refers to the tail beyond the quantile implied by the VaR level.

The lack of subadditivity implies that VaR measures may, contrary to classical economic theory, discourage diversification. The structural blindness implies that capital requirements based on VaR may incentivise excessive and uncontrolled risk-taking in the far tail since VaR does not consider what occurs beyond the specified threshold. The tail blindness is particularly problematic if the loss distribution is heavy-tailed.

We consider the following simplified example: Consider an investment in a coin-flip. For a \$100 bet on tails, the 99 % VaR is \$100, as the investor will lose the bet 50 per cent of the time. Instead, consider a bet where the investor offers 128 to 1 odds on \$100 that heads will not come up seven times in a row. The investor wins 99.2 per cent of the time, and consequently, the 99 % VaR is zero. For a capital charge solely based on 99 % VaR, the investor would not have to put up any capital to cover the bet, even though he is exposed to a possible \$12,800 loss (Einhorn & Brown, 2008).

Despite its deficiencies, VaR remains the most widely used risk measure due to its conceptual simplicity, historical precedence, broad applicability, and computational

simplicity, which may be perceived to outweigh its theoretical shortcomings (Danielsson, Jorgensen, Samorodnitsky, Sarma, & de Vries, 2013). Nevertheless, following the criticisms of VaR, the revised standards for minimum capital requirements for market risk (Basel Committee on Banking Supervision, 2013, 2016) include a shift from VaR to expected shortfall (ES) as the preferred risk measure for market risks and risks under periods of significant financial market stress.

5.2.2 Expected Shortfall

Expected shortfall (Acerbi and Tasche, 2002b, 2002a) is a coherent risk measure which assesses the riskiness of a position in a more comprehensive manner, by considering both the magnitude and the likelihood of losses above a specified confidence level.

Definition 5.3. *For a portfolio return distribution X and a level $\alpha \in (0,1)$, the* expected shortfall *at confidence level $1-\alpha$ is the measure of risk defined by*

$$ES_X(\alpha) \coloneqq \frac{1}{\alpha}\int_0^\alpha VaR_X(\gamma)\mathrm{d}\gamma.$$

That is, the expected shortfall is the average weight of all portfolio losses beyond the value-at-risk threshold.

The market risk capital charge based on expected shortfall is calculated for a future ten-day time horizon at a one-tailed, 97.5 percentile confidence level (Basel Committee on Banking Supervision, 2013). The 97.5 % ES will approximately equal the 99 % VaR for Gaussian distributions and penalise heavier tails.

A critique of ES is the way it accounts for extreme tail losses: Averages are generally poor indicators of risk. While the primary objective of financial regulation is traditionally to ensure the safety of financial institutions and protect the institutions' liability holders, the aforementioned averaging process does not offer fundamentally better control of what liability holders stand to lose in case of extreme market movements. Secondly, a VaR test may be perceived as less "deceiving" than an ES test as it does not purport to carry any information about the risks in the far tail. An ES test which inadequately captures tail risk may, however, lull regulators into a false sense of security (Koch-Medina & Munari, 2016). While this critique does not diminish the merits of ES as a risk measure, it provides an argument against an indiscriminate use.

5.3 Backtesting Frameworks

5.3.1 Backtesting Value-at-Risk

The standard approach to assess the accuracy of VaR forecast is to backtest using VaR coverage tests, which inherently amounts to counting the number of VaR threshold exceedances during the backtesting interval. This approach leads to the Traffic Light approach to backtesting VaR first proposed in Basel Committee on

Banking Supervision (1996). A more general approach is the test of Kupiec (1995), which we describe below.

For every day $t = 1, \ldots, T$, let X_t denote a realised return generated by the real return distribution F_t, which is forecasted by a model distribution P_t conditional on previous information. The random variables $X = (X_t)_{1 \leq t \leq T}$ are assumed to be independent but not identically distributed. We define an indicator function of α-level exceedances

$$I_t = \begin{cases} 1 & \text{if } X_t < -VaR_t(\alpha), \\ 0 & \text{otherwise,} \end{cases} \tag{5.1}$$

where $VaR_t(\alpha)$ is the VaR forecast for time t at probability level α issued at time $t-1$. VaR_t is $\mathscr{F}_{t-1}$-measurable, and according to Christoffersen (1998), the indicator sequence should then satify

$$\mathbb{E}(I_t | \mathscr{F}_{t-1}) = \alpha \quad \text{for all } t. \tag{5.2}$$

Christoffersen (2012) states that a proper VaR model should satisfy two conditions: The number of exceedances should be as close as possible to the number implied by the VaR quantile and randomly distributed across the sample. The unconditional coverage test by Kupiec (1995) may test the first condition, and both conditions may be tested by the conditional coverage tests by, e.g., Christoffersen (1998) or Engle and Manganelli (2004). In this thesis, we assume that the independence of tail event arrivals is tested separately, typically by visual inspection, as this provides better insight than the aforementioned tests.

Testing the unconditional coverage $\mathbb{E}(I_t) = \alpha$ amounts to testing if the sequence $(I_t)_{1 \leq t \leq T}$ is independent and identically Bernoulli-distributed with parameter α. Kupiec (1995) proposes a likelihood ratio test to reveal whether a VaR model provides desirable unconditional coverage. Hence, an indicator sequence of length n with n_1 exceedances admits the likelihood function

$$L(\alpha; I_t, I_{t-1}, \ldots) = \alpha^{n_1}(1-\alpha)^{n-n_1},$$

with the maximum likelihood estimate $\hat{\alpha} = n_1/n$. Under the null hypothesis $\mathbb{E}(I_t) = \alpha$ for all t, the test statistic is

$$K = -2 \log \frac{L(\alpha; I_t, I_{t-1}, \ldots)}{L(\hat{\alpha}; I_t, I_{t-1}, \ldots)}, \tag{5.3}$$

which is asymptotically χ^2-distributed with one degree of freedom. Unlike the Basel VaR test, which is only interested in testing risk underestimation, the Kupiec test simultaneously tests both risk under- and overestimation.

5.3.2 Backtesting Expected Shortfall

Unlike the case of VaR, there is no well-established ES backtesting framework; the current Basel proposal to backtest ES at the 97.5 quantile is to backtest VaR at the

97.5 and 99 quantiles. However, some proposed backtesting frameworks include, but is not limited to, McNeil and Frey (2000); Embrechts, Kaufmann, and Patie (2005); Wong (2008); Acerbi and Szekely (2014); Costanzino and Curran (2015, 2018); Du and Escanciano (2017). A study of the empirical performance of several expected shortfall backtests is presented in Clift, Costanzino, and Curran (2016).

Acerbi and Szekely (2014) propose three non-parametric methods to backtest the unconditional coverage of the expected shortfall measure analogous to the standard VaR setting proposed by the Basel Committee. We again assume that we test the independence of tail event arrivals separately. Their second test, which tests ES directly by jointly evaluating the frequency and magnitude of α-tail events, follows from the unconditional expectation $ES_t(\alpha) = -\mathbb{E}(X_t I_t/\alpha)$, which suggests the test statistic

$$Z(X) = \sum_{t=1}^{T} \frac{X_t I_t}{T\alpha ES_t(\alpha)} + 1. \tag{5.4}$$

We let $ES_t^F(\alpha)$ denote the expected shortfall measure when $X_t \sim F_t$, and $P_t^{[\alpha]}(x) := \min(1, P_t(x)/\alpha)$ is the distribution tail for $x < -VaR_t(\alpha)$. Appropriate hypotheses for the unconditional coverage test are

$$\begin{aligned} H_0 &: P_t^{[\alpha]} = F_t^{[\alpha]}, && \text{for all } t, \\ H_1 &: ES_t^F(\alpha) \geq ES_t(\alpha), && \text{for all } t \text{ and } > \text{ for some } t, \\ & \quad VaR_t^F(\alpha) \geq VaR_t(\alpha), && \text{for all } t. \end{aligned} \tag{5.5}$$

Here, $\mathbb{E}_{H_0}(Z) = 0$ and $\mathbb{E}_{H_1}(Z) < 0$ (Acerbi and Szekely, 2014, Proposition A.3). We choose the alternative hypothesis in the direction of risk underestimation in line with the Basel VaR test, which is only meant to detect an excess of VaR violations. This test does not require the independence of $(X_t)_{1 \leq t \leq T}$.

To estimate the p-value from hypothesis test (5.5), we simulate $X_t^i \sim P_t$ for all $t = 1, \ldots, T$ and $i = 1, \ldots, M$, for a suitably large M. The p-value is estimated by

$$p = \frac{1}{M} \sum_{i=1}^{M} I(Z(X^i) < Z(x)), \tag{5.6}$$

for true observations x (Acerbi & Szekely, 2014).

An alternative backtest proposed by Embrechts et al. (2005) considers the test score $V = (|V_1| + |V_2|)/2$, where

$$V_1 = \frac{\sum_{t=1}^{T} (X_t - (-ES_t(\alpha))) \mathbb{1}_{\{X_t < -VaR_t(\alpha)\}}}{\sum_{t=1}^{T} \mathbb{1}_{\{X_t < -VaR_t(\alpha)\}}}$$

is a standard backtesting measure of ES that reports the average excess below the expected shortfall for times when a VaR violation occurs. Its weakness is, similar to the backtests proposed by Acerbi and Szekely (2014), its dependence of VaR estimates without adequately reflecting the quality of these estimates. Only values

which fall beyond the VaR threshold are considered. To correct for this, Embrechts et al. introduce a penalty that measures the excess below the predicted expected shortfall for the α-quantile of observed returns. Let $r_t \coloneqq X_t - (-ES_t(\alpha))$ for all t, and let $r(\alpha)$ be the α-quantile of $(r_t)_{1 \leq t \leq T}$. Then, we let

$$V_2 = \frac{\sum_{t=1}^{T} r_t \mathbb{1}_{\{r_t < r(\alpha)\}}}{\sum_{t=1}^{T} \mathbb{1}_{\{r_t < r(\alpha)\}}}.$$

A good estimate of ES leads to a low value of V.

To test the significance of score differences between two competing methods in the Embrechts et al. framework, we can apply a permutation test based on resampling (Good, 2013; Möller, Lenkoski, & Thorarinsdottir, 2013). Two competing predictive distributions $\hat{F}_1$ and $\hat{F}_2$ are compared under the scoring rule $V(F, \cdot)$ using the statistic

$$s \coloneqq S(\hat{F}_1, y) - S(\hat{F}_2, y), \tag{5.7}$$

for a set of observations $y = (y_1, \ldots, y_T)$. The permutation test is then based on resampling copies of s with the predictions of $\hat{F}_1$ and $\hat{F}_2$ swapped for a random number of observations.

Chapter 6

Preliminary Data Analysis

In this thesis, we calibrate term structure models generated by generalised hyperbolic distributions. The motivation behind this generalisation arises from the need for more flexible return distributions for interest rates derivatives. The daily log-returns of interest rate derivatives are heavy-tailed, possibly skewed, and dominated by discontinuous jumps, which makes it challenging to accurately describe the returns by a Gaussian distribution. We herein present two data sets, one which captures a "normal" market situation and one which captures two highly stressed market situations, to motivate the application of more general term structure models.

6.1 Primary Interest Rate Data

The primary data set used in this thesis is provided by DNB and consists of daily Norwegian Inter-Bank Offered Rates (NIBOR) and Norwegian swap rates of differing maturities. The first recorded date is 6 July 2009, and the last recorded date is 11 March 2019. The relevant rates are the one-day and one-year NIBOR rates, as well as two- to ten-year daily swap rates. Descriptive statistics of the entire data set are given in Table 6.1, and a selection of the simple rates is visualised in Figure 6.1.

Table 6.1: Descriptive statistics of the daily NIBOR and swap rates from 6 July 2009 to 11 March 2019.

Maturity	**Mean (%)**	**SD (%)**	**Mean log-changes (%)**	**SD log-changes (%)**
NIBOR 1d	1.2876	0.6301	−0.0003	0.0825
NIBOR 1Y	1.7114	0.7154	−0.0001	0.0127
Swap 2Y	1.9434	0.9085	−0.0002	0.0148
Swap 3Y	2.0838	0.9735	−0.0003	0.0155
Swap 4Y	2.2277	1.0080	−0.0003	0.0156
Swap 5Y	2.3670	1.0266	−0.0003	0.0156
Swap 6Y	2.4939	1.0370	−0.0003	0.0152
Swap 7Y	2.6068	1.0423	−0.0003	0.0147
Swap 8Y	2.7053	1.0450	−0.0004	0.0142
Swap 9Y	2.7903	1.0472	−0.0004	0.0138
Swap 10Y	2.8626	1.0504	−0.0004	0.0136

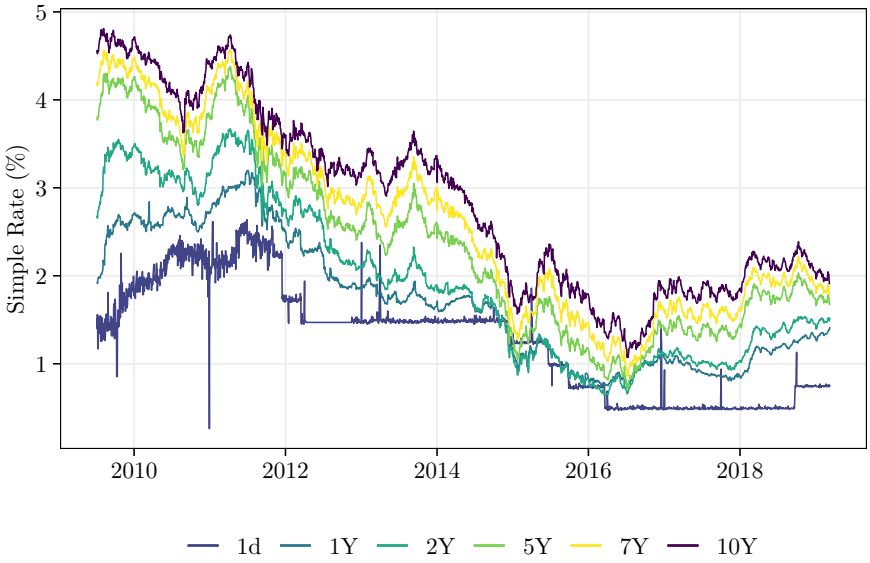

Figure 6.1: A selection of simple historical rates for different maturities from 6 July 2009 to 11 March 2019. The one-day and one-year rates are simple NIBOR rates, while the remaining rates are simple swap rates.

As one would expect, the average yields increase with maturity; since binding up capital for a longer period increases exposure and sensitivity to inflation and interest rate risk, investors demand compensation for doing so. The average yield curve is, therefore, upward sloping, which typically indicates that the market expects interest rates to remain stable or potentially grow. As expected, the spot rate is the most volatile. However, seemingly contrary to classical economic intuition, the volatility of one- and two-year rates are slightly smaller or equal to that of intermediate- and long-term rates.

Since the global financial crisis of 2007–2009, fixed-income markets have mostly witnessed an upward sloping yield curve. The Norwegian rates, however, fell to an all-time low in 2016, succeeding reductions in Norges Bank's policy rate first initiated in December 2011 due to turbulence in financial markets and weakened expected growth (Norges Bank, 2011). Weakened growth prospects and a sharp fall in oil prices broadly caused a gradual decrease in the term spread during 2011–2016 (Norges Bank, 2015), and during 2015–2017 the yield curve was withal inverted at the short end. (This decline of yields at relatively short horizons usually captures the market expectation of a near-term monetary policy easing (Gürkaynak, Sack, & Wright, 2007).) In 2017, however, the rates and the term spread started to slowly grow in reaction to better economic prospects and an anticipated increase in the policy rate, which occurred in September 2018.

While Norges Bank's commitment to a low-interest rate policy for any foreseeable

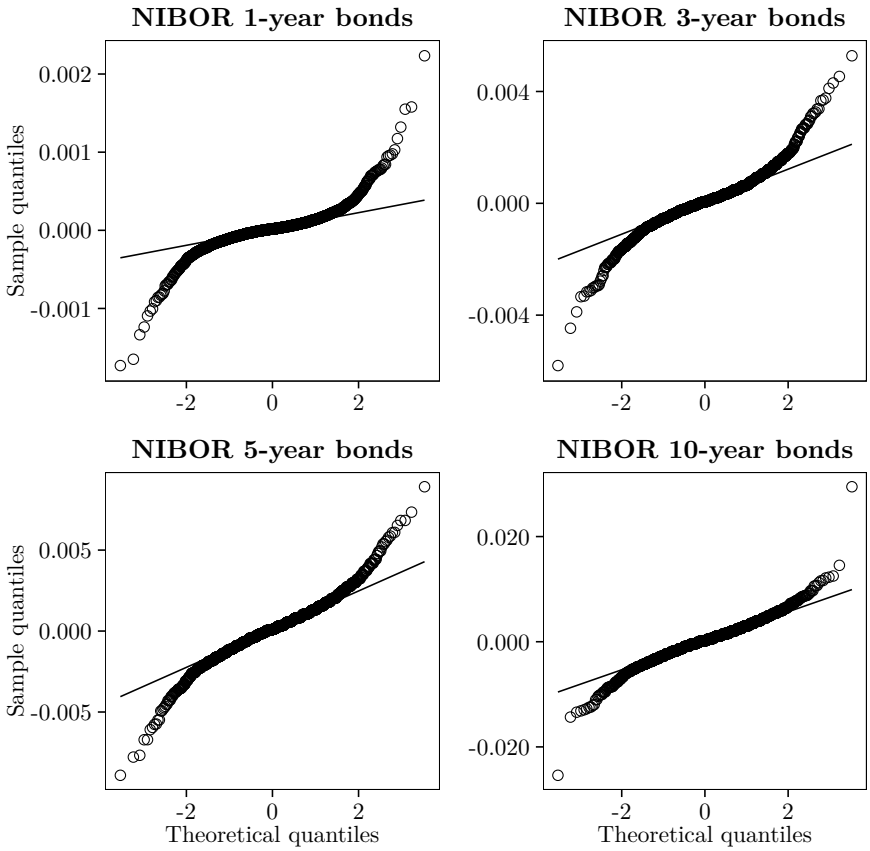

Figure 6.2: Gaussian QQ-plots for centred daily log-returns on 1-year, 3-year, 5-year, and 10-year zero-coupon bonds from 6 July 2009 to 11 March 2019.

future might have rendered the short-term rate less responsive to macroeconomic events (see, e.g., Xia, 2014), intermediate- and long-term rates are still responsive – and have historically moved significantly in response to unexpected components in macroeconomic data releases and monetary policy announcements (Gürkaynak, Sack, & Swanson, 2005). This behaviour is consistent with a market wherein investors' views of long-run inflation are not firmly anchored. One explanation for the relatively larger-than-expected volatility on long-term interest rates is that the long-term rates are less constrained in the prevailing monetary setting, letting the rates and their embedded risk premiums react aggressively and elusively to the aforementioned period of financial uncertainty.

Figure 6.2 presents Gaussian QQ-plots for the daily log-returns on 1-year, 3-year, 5-year, and 10-year zero-coupon bonds derived from the yields presented in Table 6.1. All bonds admit denser tails than consistent with a Gaussian distributional

assumption, and the tails grow heavier for shorter maturities. None of the distributions appears to be distinctly skewed with profoundly asymmetrical or different tail behaviours.

6.2 Stressed Interest Rate Data

A second (uncleaned) data set used in this thesis is downloaded directly from Bloomberg and consists of NIBOR and swap rates of differing maturities. The relevant rates are the daily three-month and one-year NIBOR rates as well as two- to ten-year daily swap rates. We are interested in market movements during two stressed periods: 2008–2009 and 2019–2020. Descriptive statistics of the two periods are given in Table 6.2, and a selection of the simple rates is visualised in Figures 6.3 and 6.4. The daily log-returns on 1-year, 5-year, and 10-year zero-coupon bonds during the two stressed periods, as well as during "normal" reference period from 19 April 2018 to 19 November 2019, are visualised in Figure 6.5.

Table 6.2: Descriptive statistics of the daily simple NIBOR and swap rates from (a) 16 May 2008 to 12 August 2009 and (b) 15 November 2019 to 16 April 2020.

Maturity	**Mean (%)**	**SD (%)**	**Mean log-changes (%)**	**SD log-changes (%)**
NIBOR 3m	4.4998	1.9202	−0.0041	0.0257
NIBOR 1Y	4.0876	1.9674	−0.0033	0.0223
Swap 2Y	4.0647	1.6877	−0.0021	0.0211
Swap 3Y	4.2452	1.3604	−0.0014	0.0175
Swap 5Y	4.5292	0.9270	−0.0008	0.0135
Swap 7Y	4.7448	0.6794	−0.0006	0.0124
Swap 10Y	4.9496	0.4916	−0.0004	0.0131

(a) 16 May 2008 to 12 August 2009

Maturity	**Mean (%)**	**SD (%)**	**Mean log-changes (%)**	**SD log-changes (%)**
NIBOR 3m	1.6082	0.3452	−0.0085	0.0383
NIBOR 1Y	1.5961	0.4626	−0.0103	0.0374
Swap 2Y	1.5214	0.4921	−0.0114	0.0387
Swap 3Y	1.5608	0.4865	−0.0104	0.0365
Swap 5Y	1.5641	0.4447	−0.0094	0.0351
Swap 7Y	1.6007	0.4034	−0.0083	0.0341
Swap 10Y	1.6665	0.3583	−0.0067	0.0298

(b) 15 November 2019 to 16 April 2020

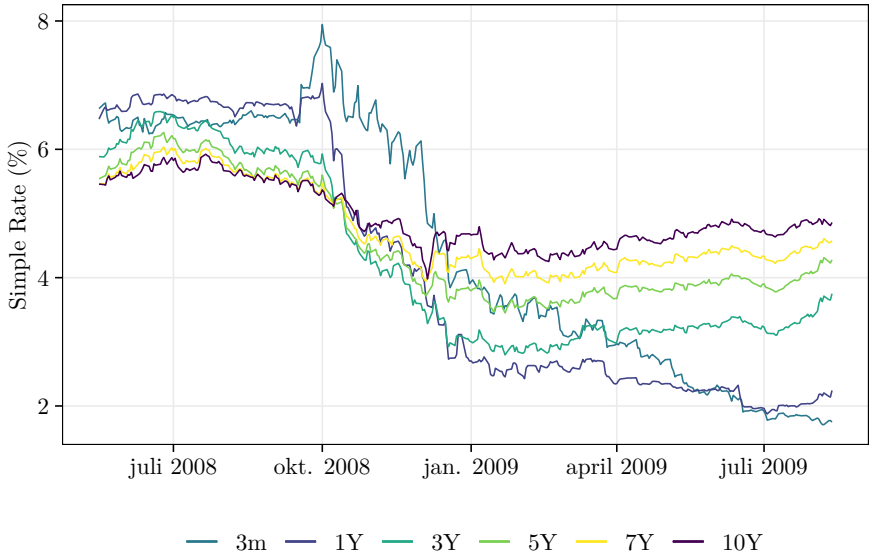

Figure 6.3: A selection of simple historical rates for different maturities from 16 May 2008 to 12 August 2009.

The first period lasts from 16 May 2008 to 12 August 2009 and includes the main stretch of the global financial crisis. The crisis began with a depreciation in the American subprime mortgage market before developing into an international banking crisis following the collapse of the investment bank Lehman Brothers on 15 September 2008. The nadir of the crisis occurred around March 2009, and Norges Bank's policy rate was further lower by 0.25 % to 1.25 % at 17 June 2009 to combat falling economic activity and a rising unemployment rate (Norges Bank, 2009).

The second period lasts from 15 November 2019 to 16 April 2020. The period ends during the financial crash that occurred as a result of, firstly, a massive fall in oil prices after the Opec collaboration collapsed as Russia refused to agree to further production cuts and announced an increased production, while Saudi Arabia announced that they would sell oil for a discount. Secondly and more predominantly, the crash occurred as a result of the coronavirus pandemic with ensuing world-wide government and business shutdowns. To halt the falling economic activity Norges Bank's policy rate was lowered from 1.5 % to 1.0 % at 13 March 2020, to 0.25 % at 20 March 2020, and later to 0 % at 7 May 2020. Norges Bank cites an abnormally large uncertainty about future developments, a fall in oil prices, and an ensuing weak Norwegian krone, and Norges Bank states that they hope the expansionary monetary policy will cushion the economic setback and avoid an increase in equilibrium unemployment (Norges Bank, 2020).

Figures 6.6 and 6.7 present Gaussian QQ-plots for the daily log-returns on 1-year, 3-year, 5-year, and 10-year zero-coupon bonds during the global financial crisis and

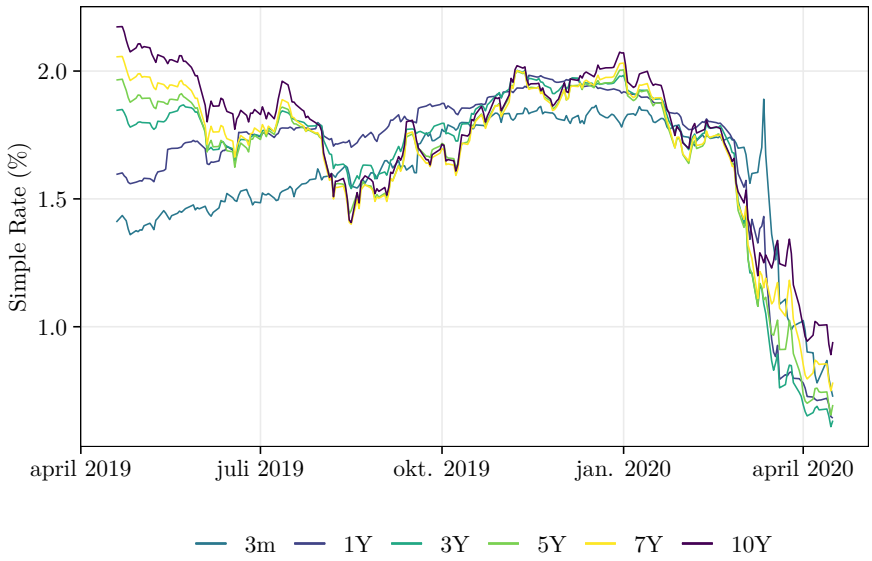

Figure 6.4: A selection of simple historical rates for different maturities from 19 April 2019 to 16 April 2020.

the coronavirus crisis, respectively. The log-returns during the coronavirus crisis are highly skewed for all maturities. The upper tails are exceptionally dense, while the lower-tails – though heavier than consistent with a Gaussian distribution – are more well-behaved.

Compared to the coronavirus crisis, the log-returns during the financial crisis are greater but less skewed and more "conventional": The one-year and three-year bonds admit fat-tailed and somewhat skewed return distributions, while the five-year and ten-year bonds, though possessing heavy tails, appear to be reasonably well-represented by a Gaussian distribution except in the distant tails.

The previous remarks are too evident in Figure 6.5. We must be careful as to not be too assertive in a comparison between the two periods; we observe the 2008–2009 data over an extended period which includes the main stretch of the crisis, while the 2019–2020 data consists of fewer data points and only includes the start of the crisis. That said, we again note that the 2008–2009 return distribution is symmetric, but it is far wider and fatter-tailed than the reference period. In comparison, the return distribution during the coronavirus crisis is much more peaked and with a far lighter lower tail. The upper tail, however, is equally dense to that of the 2008–2009 situation.

That is, during 2008–2009, we observed relatively equal market movements in both directions. A fall one day was usually followed by a positive correction of equal magnitude. During March–April 2020, the markets have, to an even greater extent, plummeted. As a result of market pessimism and the quick response of Norges

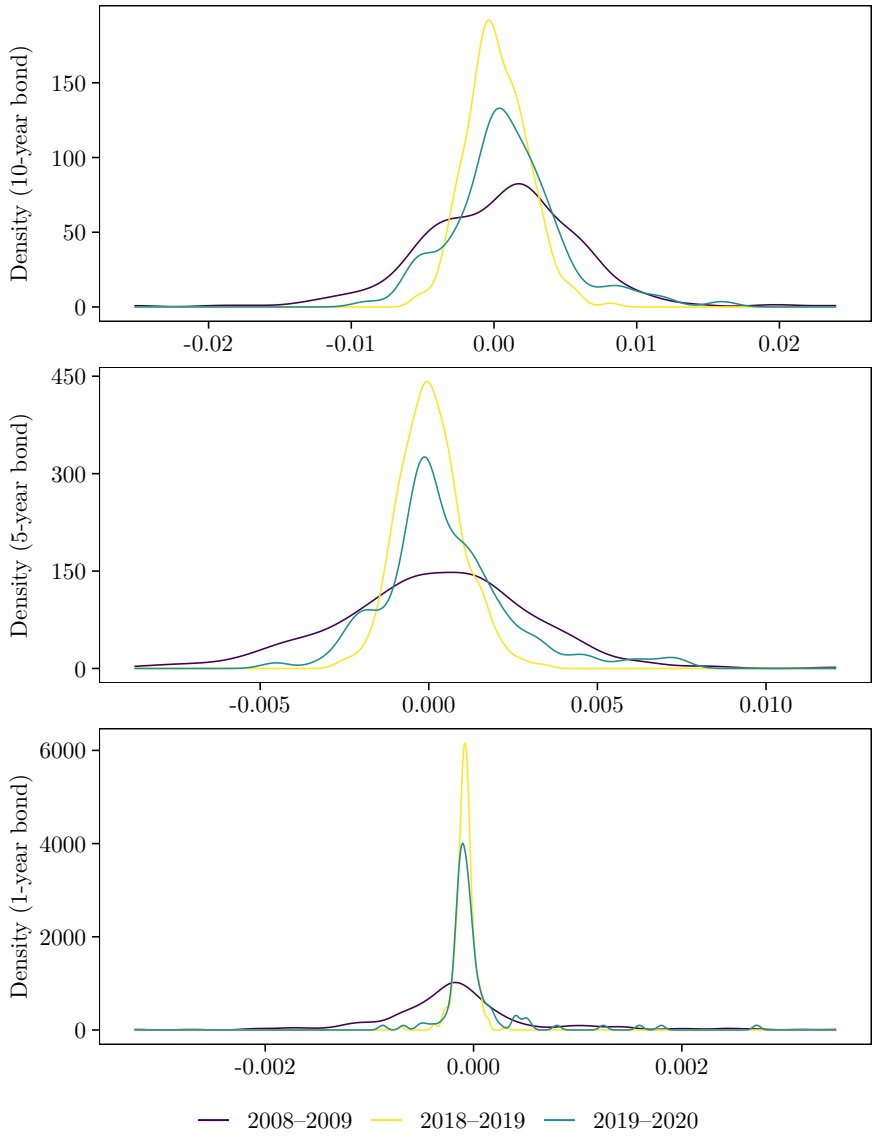

Figure 6.5: Density of daily log-returns on (top) 10-year, (middle) 5-year, and (bottom) 1-year zero-coupon bonds from 16 May 2008 to 12 August 2009, 19 April 2018 to 19 November 2019, and 15 November 2019 to 16 April 2020.

Bank, interest rates have quickly dropped, and the market has priced in fewer and smaller positive corrections. Per observation, this self-reinforcing market behaviour generates a profoundly skewed and heavy-tailed return distribution.

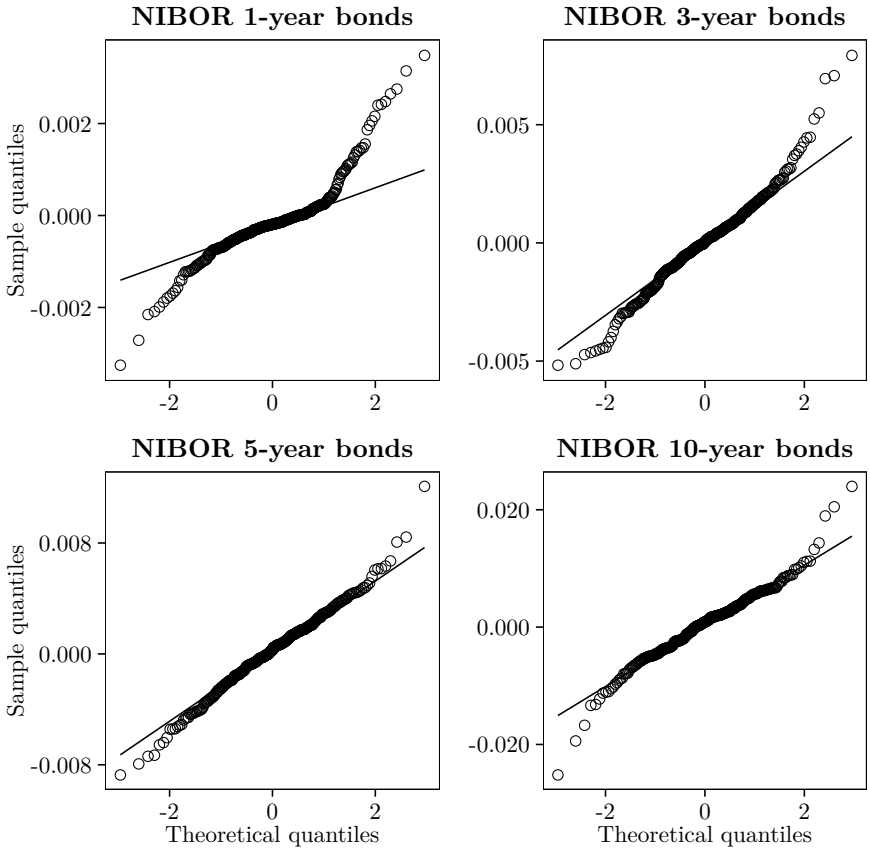

Figure 6.6: Gaussian QQ-plots for centred daily log-returns on 1-year, 3-year, 5-year, and 10-year zero-coupon bonds from 16 May 2008 to 12 August 2009.

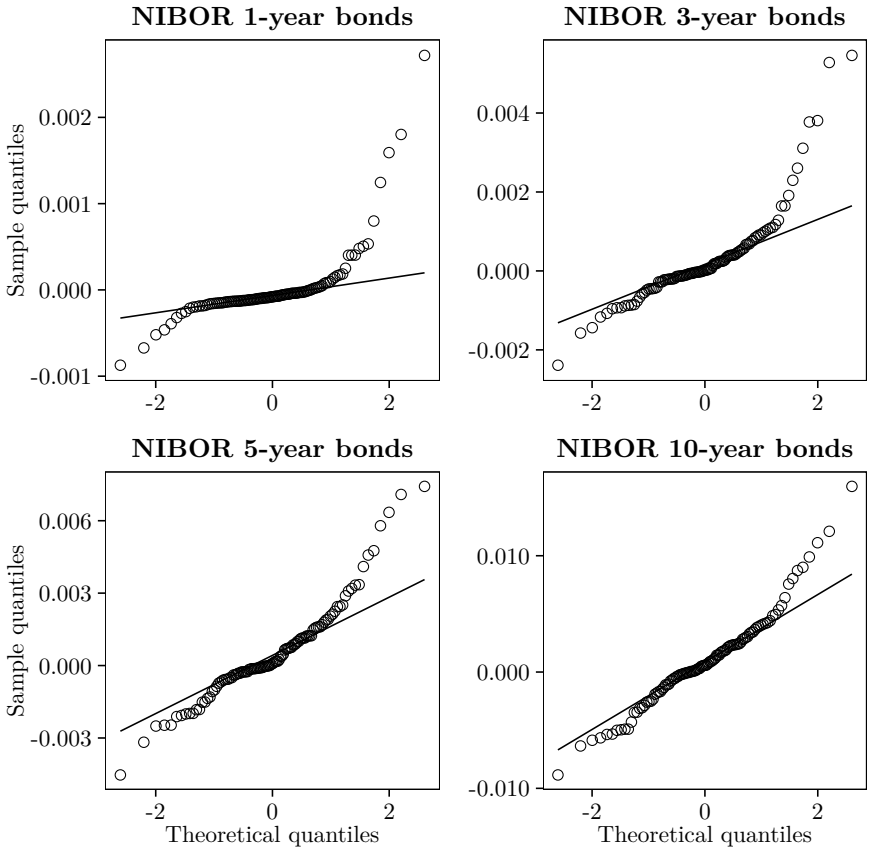

Figure 6.7: Gaussian QQ-plots for centred daily log-returns on 1-year, 3-year, 5-year, and 10-year zero-coupon bonds from 15 November 2019 to 16 April 2020.

Chapter 7

Results

Having established methods for parameter estimation in the Lévy term structure models, we apply these to the NIBOR data described in Chapter 6. We first give a preliminary calibration example in Section 7.1, and we qualitatively study the in-sample fit of time-homogeneous and time-inhomogeneous term structure models generated by Gaussian, normal–inverse Gaussian, and generalised hyperbolic skew Student's t-distributions. In Section 7.2, we perform an out-of-sample backtest of one-day value-at-risk and expected shortfall on zero-coupon bonds using the backtesting frameworks described in Chapter 5. The out-of-sample backtests are extended to portfolios consisting of swaps and caps in Section 7.3.

7.1 Calibration to Zero-Coupon Bond Quotes

We first give a preliminary calibration example of the considered term structure models to financial data. Using the calibration scheme outlined in Section 4.6, we calibrate time-homogeneous (hereafter TH) and time-inhomogeneous (hereafter TIH) term structure models generated by univariate Gaussian, NIG and GSS distributions to one- to ten-year zero-coupon bond quotes from 24 June 2011 to 19 June 2013 (500 trading days). The parameter estimates for the TH driving Gaussian process are

$$\hat{\sigma} = 1.54 \cdot 10^{-6} \quad \text{and} \quad \hat{\mu} = -7.68 \cdot 10^{-24},$$

the parameter estimates for the TH driving NIG process are

$$\hat{\alpha} = 972968.4, \quad \hat{\beta} = -80936.62, \quad \hat{\delta} = 2.30 \cdot 10^{-6}, \quad \text{and} \quad \hat{\mu} = 1.91 \cdot 10^{-7},$$

and the parameter estimates for the TH driving GSS process are

$$\hat{\nu} = 7.64, \quad \hat{\beta} = -80177.95, \quad \hat{\delta} = 3.66 \cdot 10^{-6}, \quad \text{and} \quad \hat{\mu} = 1.90 \cdot 10^{-7}.$$

The parameter estimates for the TIH driving Gaussian, NIG, and GSS processes are given in Tables B.1 to B.3 in Appendix B, respectively. For the TIH processes, we have fitted one process to each M-maturity bond, for $M = 1, \ldots, 10$ years.

The empirical density of estimated increments of the TH driving process and the density of the fitted TH generating Gaussian, NIG, and GSS distributions

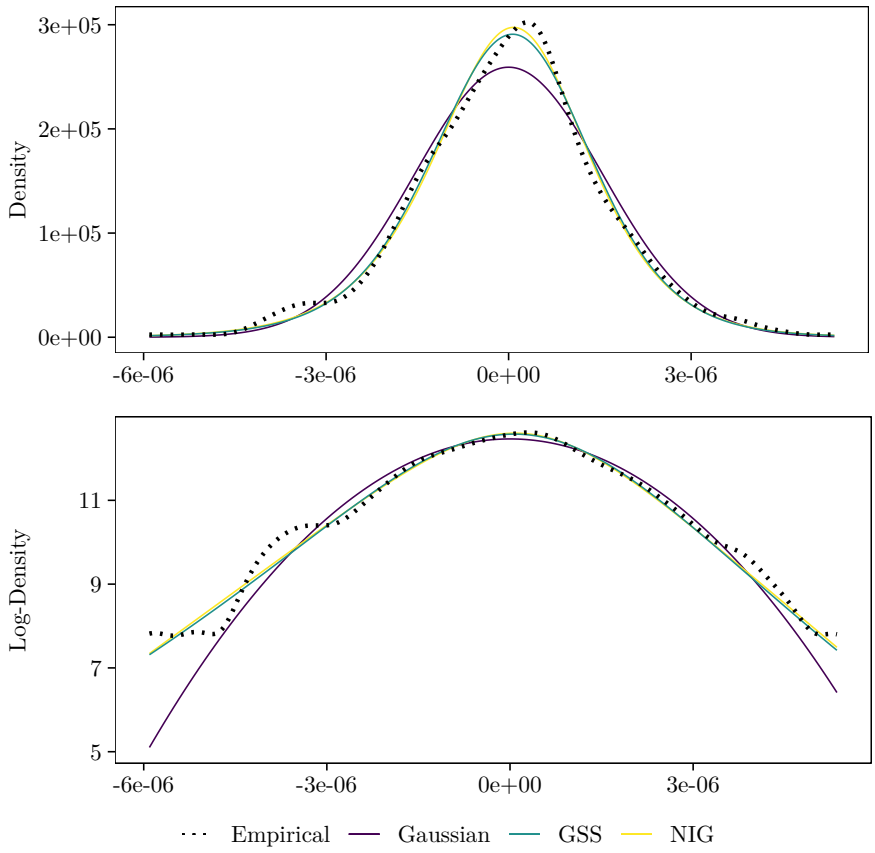

Figure 7.1: Density (top) and log-density (bottom) of observed and fitted increments of the TH driving process, for term structure models generated by TH Gaussian, NIG, and GSS distributions.

are presented in Figure 7.1. The NIG and GSS distributions are more flexible than the Gaussian distribution, and they better approximate the leptokurtic shape of the empirical increment distribution. The Gaussian distribution appears to underestimate the risk in both tails.

The empirical density of log-returns on one-year, five-year, and ten-year zero-coupon bonds and the corresponding densities of the fitted TH and TIH models are given in Figure 7.2. Equivalent to Figure 7.1, the models generated by NIG and GSS distributions approximate the empirical return distribution quite well in both the tails and the mass centre, while the models generated by Gaussian distributions generally underestimate the tail risk.

For high-maturity bonds, the TH and TIH models admit approximately the same return distributions. For one- to three-year bonds, however, the assumption of equal

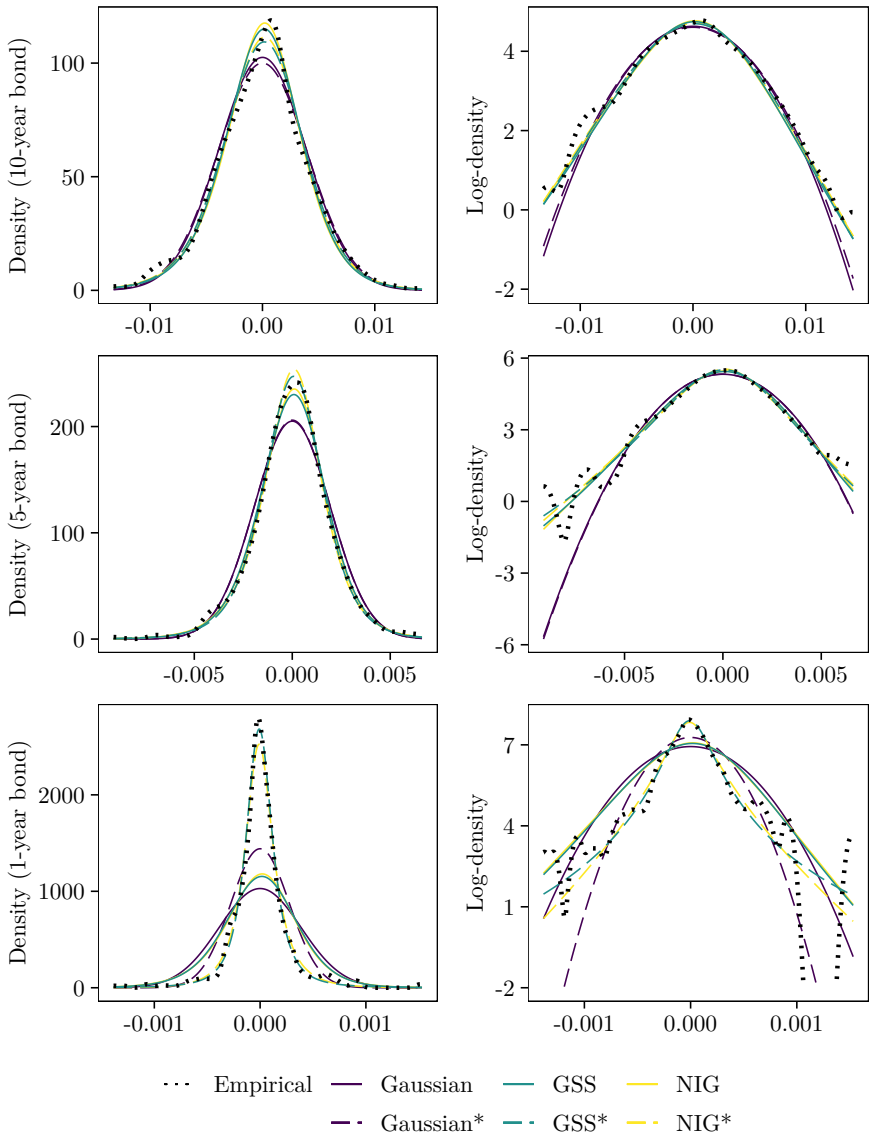

Figure 7.2: Density and log-density of observed and fitted (centred) daily log-returns on zero-coupon ten-year bonds (top row), five-year bonds (middle row), and one-year bonds (bottom row). NIG*, GSS*, and Gaussian* denote term structure models generated by TIH distributions.

return distributions for all bonds breaks down. The time-homogeneous NIG and GSS processes predict a far too wide return distribution for low-maturity bonds, while the time-inhomogeneous NIG and GSS processes fit the empirical return distributions quite well. On the contrary, the poor fit of the TIH Gaussian process causes its TH counterpart to better approximate the tail risk for one-year bonds.

We lastly study the behaviour of the different term structure models in the long run. Figure B.1 in Appendix B presents the 95 % confidence bounds for the discounted price of one-year, three-year, and five-year bonds during the next year. In the long run, the sums of increments from the GSS and NIG distribution converge to a normal distribution, and all TH models admit equal price distributions. Moreover, for maturities greater than three years, all term structure models admit the same price distributions. For one-year bonds, the TIH Gaussian and NIG models admit thinner bounds than the TH models. The time-inhomogeneous GSS model predicts a comparable lower bound, but the model too prices in considerably greater risks in the upper bound.

To better assess the in-sample tail fit, we calibrate the univariate TH and TIH term structure models using zero-coupon bond quotes from 6 July 2011 to 14 January 2019. The empirical and fitted one-day value-at-risk and expected shortfall on one-year, five-year, and ten-year zero-coupon bond log-returns are presented in Figures 7.3 and 7.4.

Similar to the observations in Figure 7.2, the TH and TIH models admit equal tail risk predictions for high-maturity bonds. The models generated by NIG and GSS distributions fit the empirical risk measures quite well, while the models generated by Gaussian distributions consistently underestimate the tail risks. The quality of the Gaussian models declines as we consider more distant tail quantiles.

For one-year bonds, the time-homogeneous NIG and GSS models overestimate the tail risks, but the models improve as we consider more extreme quantiles of the return distribution. The time-inhomogeneous NIG and GSS models approximate the empirical return distribution of low-maturity bonds better than their TH counterparts, but their in-sample fit decline in the distant tails. The poor fit is possibly a result of convergences issues in the EM calibration algorithm.

7.2 Backtests of Zero-Coupon Bonds

Having studied the flexibility of the different term structure models in approximating the empirical return distributions for zero-coupon bonds, we now wish to investigate whether the more precise in-sample fit of models generated by NIG and GSS distributions translates to a better out-of-sample prediction of tail risk measures. Following the discussion of the deficiencies of value-at-risk in Section 5.2.1, our primary attention resides with the expected shortfall statistic. For completeness, we include backtests of value-at-risk, but our focus therein is mostly related to the statistic's relation to backtests of expected shortfall.

We perform an out-of-sample backtest of the one-day value-at-risk and one-day expected shortfall of log-returns for all bonds using trading data from 6 July 2011

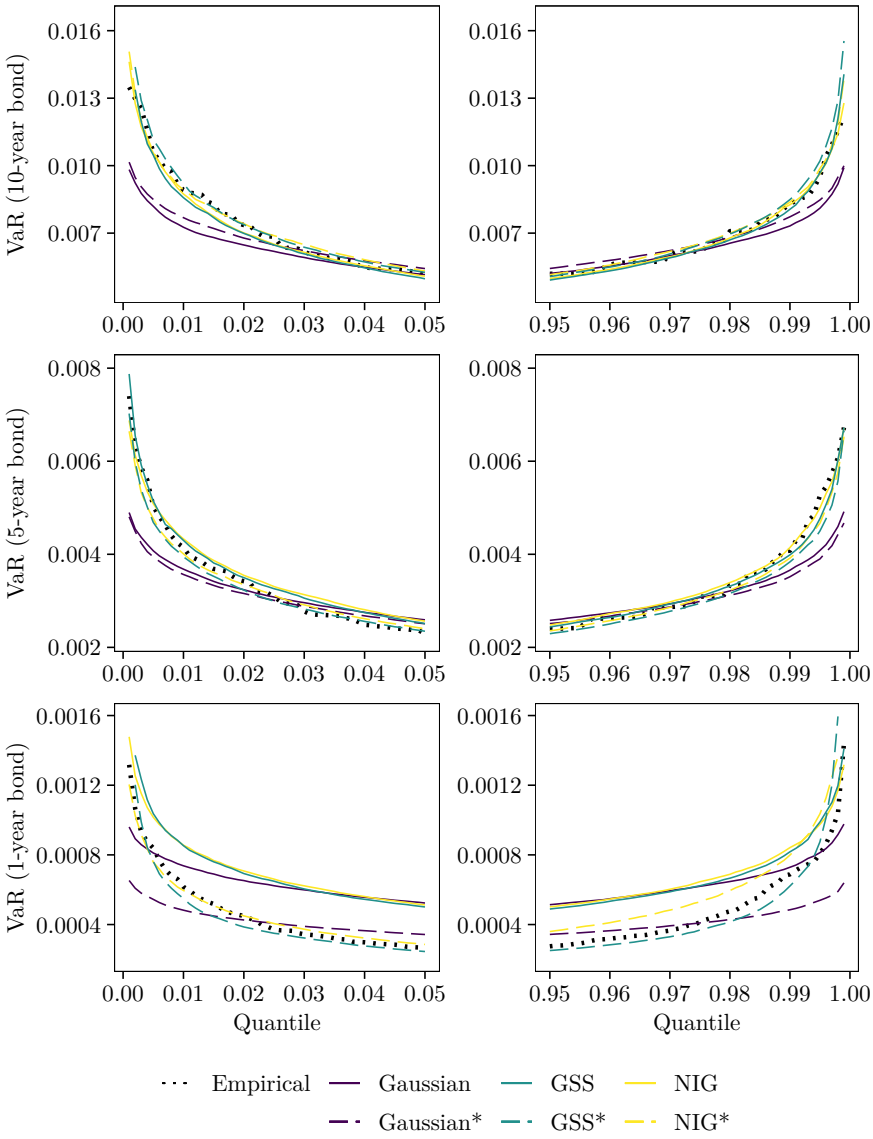

Figure 7.3: One-day value-at-risk of observed and fitted daily log-returns on zero-coupon ten-year bonds (top row), five-year bonds (middle row), and one-year bonds (bottom row) in both tails. NIG*, GSS*, and Gaussian* denote term structure models generated by TIH distributions.

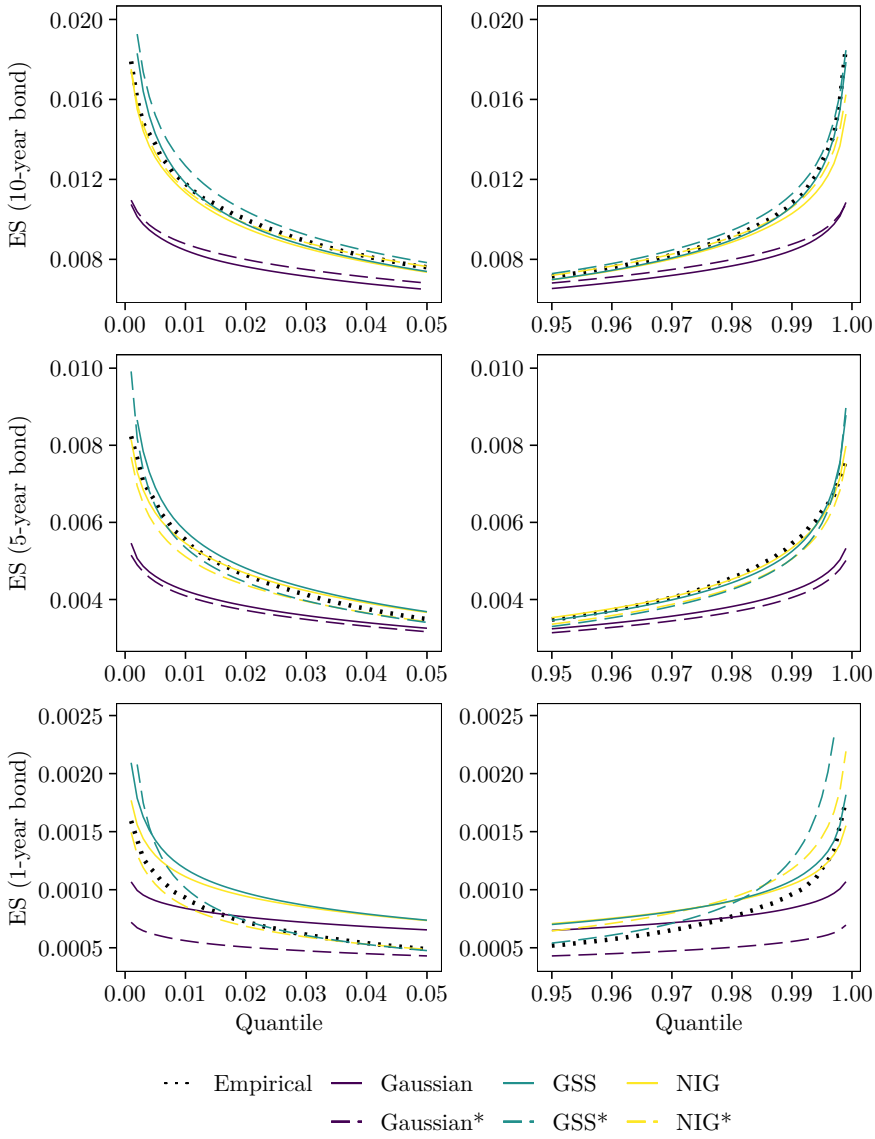

Figure 7.4: One-day expected shortfall of observed and fitted daily log-returns on zero-coupon ten-year bonds (top row), five-year bonds (middle row), and one-year bonds (bottom row) in both tails. NIG*, GSS*, and Gaussian* denote term structure models generated by TIH distributions.

Table 7.1: Results from a one-day value-at-risk backtest of one-year bonds using the previous 250 trading days in the calibration of the term structure models. Reported is the violation percentage and in parenthesis the p-value from the unconditional coverage Kupiec test. NIG*, GSS*, and Gaussian* denote term structure models generated by TIH distributions.

Distribution	**0.5 %**	**1.0 %**	**2.5 %**	**97.5 %**	**99.0 %**	**99.5 %**
Gaussian	0.37	0.41	0.73	1.05	0.64	0.46
	(0.35)	(*0*)	(*0*)	(*0*)	(0.07)	(0.77)
NIG	0.14	0.32	0.68	0.91	0.5	0.32
	(*0*)	(*0*)	(*0*)	(*0*)	(*0.01*)	(0.2)
GSS	0.18	0.32	0.73	0.96	0.59	0.27
	(*0.02*)	(*0*)	(*0*)	(*0*)	(*0.04*)	(0.1)
Gaussian*	1.51	1.96	2.74	2.79	2.05	1.69
	(*0*)	(*0*)	(0.48)	(0.4)	(*0*)	(*0*)
NIG*	0.87	1.55	2.97	2.83	1.64	0.82
	(*0.03*)	(*0.02*)	(0.17)	(0.33)	(*0.01*)	(0.05)
GSS*	0.96	1.87	3.47	3.15	1.96	1
	(*0.01*)	(*0*)	(*0.01*)	(0.06)	(*0*)	(*0*)

to 11 March 2019. The TH and TIH term structure models generated by univariate Gaussian, NIG, and GSS distributions are at each date calibrated to the previous 250 trading days.

The backtests of value-at-risk for one-year, five-year, and ten-year zero-coupon bonds, using the unconditional coverage Kupiec test, are presented in Tables 7.1 to 7.3. For the one-year bonds, all models perform poorly, and the unconditional coverage is rejected at most quantiles for all models. The TH models generally overestimate the risk, while the TIH models generally underestimate the risk. While the time-inhomogeneous NIG and GSS models appear to well-approximate the VaR in-sample in Figure 7.3, the closer in-sample fit does not translate to a better out-of-sample fit.

For the five- and ten-year bonds, all models perform better. The unconditional coverage of time-homogeneous and time-inhomogeneous NIG models is not rejected at any quantile. The unconditional coverage of time-homogeneous GSS models is only rejected at the 97.5 % quantile for five-year bonds. The Gaussian models, however, perform rather poorly, and their unconditional coverage is rejected at several quantiles.

Due to the somewhat unstable predictions of value-at-risk, it is apparent that we should utilise a backtest of expected shortfall which penalises unsatisfactory value-at-risk predictions. The backtests of one-day expected shortfall for one-year, five-year, and ten-year bonds, using the backtest proposed by Embrechts et al. (2005), are presented in Table 7.4. The p-values of significance tests of score differences between the different term structure models at all maturities and quantiles are presented in Table 7.5.

Table 7.2: Results from a one-day value-at-risk backtest of five-year bonds using the previous 250 trading days in the calibration of the term structure models. Reported is the violation percentage and in parenthesis the p-value from the unconditional coverage Kupiec test. NIG*, GSS*, and Gaussian* denote term structure models generated by TIH distributions.

Distribution	**0.5 %**	**1.0 %**	**2.5 %**	**97.5 %**	**99.0 %**	**99.5 %**
Gaussian	0.73	1.14	2.6	2.37	1.46	0.96
	(0.15)	(0.52)	(0.76)	(0.7)	(*0.04*)	(*0.01*)
NIG	0.64	0.73	1.96	2.28	1.32	0.87
	(0.38)	(0.18)	(0.09)	(0.51)	(0.15)	(*0.03*)
GSS	0.59	0.73	1.96	2.37	1.28	0.87
	(0.55)	(0.18)	(0.09)	(0.7)	(0.21)	(*0.03*)
Gaussian*	0.87	1.37	3.01	2.47	1.51	1.14
	(*0.03*)	(0.1)	(0.14)	(0.92)	(*0.03*)	(*0*)
NIG*	0.59	0.87	2.42	2.37	1.37	0.78
	(0.55)	(0.52)	(0.81)	(0.7)	(0.1)	(0.09)
GSS*	0.59	0.96	2.56	2.47	1.28	0.78
	(0.55)	(0.85)	(0.86)	(0.92)	(0.21)	(0.09)

Table 7.3: Results from a one-day value-at-risk backtest of ten-year bonds using the previous 250 trading days in the calibration of the term structure models. Reported is the violation percentage and in parenthesis the p-value from the unconditional coverage Kupiec test. NIG*, GSS*, and Gaussian* denote term structure models generated by TIH distributions.

Distribution	**0.5 %**	**1.0 %**	**2.5 %**	**97.5 %**	**99.0 %**	**99.5 %**
Gaussian	1.19	2.01	3.56	2.69	1.55	1.1
	(*0*)	(*0*)	(*0*)	(0.57)	(*0.02*)	(*0*)
NIG	0.64	1.28	2.83	3.06	1.23	0.78
	(0.38)	(0.21)	(0.33)	(0.11)	(0.29)	(0.09)
GSS	0.64	1.23	3.06	3.24	1.42	0.78
	(0.38)	(0.29)	(0.11)	(*0.03*)	(0.07)	(0.09)
Gaussian*	0.96	1.6	2.97	2.28	1.28	0.82
	(*0.01*)	(*0.01*)	(0.17)	(0.51)	(0.21)	(0.05)
NIG*	0.55	0.96	2.51	2.79	1.23	0.68
	(0.75)	(0.85)	(0.97)	(0.4)	(0.29)	(0.25)
GSS*	0.59	1	2.51	3.01	1.23	0.68
	(0.55)	(0.98)	(0.97)	(0.14)	(0.29)	(0.25)

Table 7.4: Results from a one-day expected shortfall backtest of (a) one-year bonds, (b) five-year bonds, and (c) ten-year bonds, using the previous 250 trading days in the calibration of the term structure models. Reported is the test score from the Embrechts' test. NIG*, GSS*, and Gaussian* denote term structure models generated by TIH distributions.

Distribution	**0.5 %**	**1.0 %**	**2.5 %**	**97.5 %**	**99.0 %**	**99.5 %**
Gaussian	0.00013	0.00012	0.00014	0.00010	0.00006	0.00009
NIG	0.00024	0.00017	0.00015	0.00010	0.00007	0.00003
GSS	0.00018	0.00016	0.00013	0.00010	0.00005	0.00004
Gaussian*	0.00028	0.00020	0.00013	0.00017	0.00023	0.00029
NIG*	0.00017	0.00012	0.00008	0.00007	0.00009	0.00006
GSS*	0.00018	0.00011	0.00008	0.00008	0.00012	0.00007

(a) One-year bonds

Distribution	**0.5 %**	**1.0 %**	**2.5 %**	**97.5 %**	**99.0 %**	**99.5 %**
Gaussian	0.00167	0.00107	0.00047	0.00052	0.00081	0.00106
NIG	0.00082	0.00075	0.00014	0.00036	0.00044	0.00045
GSS	0.00063	0.00060	0.00010	0.00032	0.00041	0.00038
Gaussian*	0.00162	0.00108	0.00052	0.00063	0.00096	0.00114
NIG*	0.00095	0.00072	0.00016	0.00038	0.00040	0.00052
GSS*	0.00065	0.00046	0.00013	0.00032	0.00037	0.00038

(b) Five-year bonds

Distribution	**0.5 %**	**1.0 %**	**2.5 %**	**97.5 %**	**99.0 %**	**99.5 %**
Gaussian	0.00347	0.00232	0.00142	0.00102	0.00147	0.00204
NIG	0.00227	0.00121	0.00070	0.00048	0.00092	0.00124
GSS	0.00154	0.00096	0.00051	0.00039	0.00059	0.00103
Gaussian*	0.00343	0.00223	0.00131	0.00089	0.00133	0.00192
NIG*	0.00208	0.00115	0.00048	0.00036	0.00077	0.00124
GSS*	0.00138	0.00085	0.00044	0.00030	0.00067	0.00109

(c) Ten-year bonds

Table 7.5: p-values for permutation tests of differences between Embrechts' scores reported in Table 7.4. The null and alternative hypotheses are $H_0 : X = Y$ versus $H_1 : X < Y$ for term structure models generated by univariate Gaussian (herein abbreviated as N), NIG, and GSS distributions. NIG* and GSS* denote term structure models generated by TIH distributions.

$\mathbf{H_1}$	**Mat.**	**0.5 %**	**1.0 %**	**2.5 %**	**97.5 %**	**99.0 %**	**99.5 %**
	1Y	0.18	0.20	*0*	0.09	0.29	0.72
NIG*<NIG	5Y	0.87	0.22	0.82	0.88	0.34	0.85
	10Y	0.42	0.08	*0.03*	*0*	0.28	0.61
	1Y	0.53	0.17	*0.02*	*0*	0.89	0.69
GSS*<GSS	5Y	0.37	0.08	0.53	0.40	0.42	0.18
	10Y	0.34	0.32	0.12	0.27	0.88	0.31
	1Y	0.32	0.51	0.39	0.27	0.09	0.87
GSS<NIG	5Y	*0.01*	*0.02*	*0*	0.51	*0.03*	0.32
	10Y	*0.01*	*0*	*0*	*0.03*	*0*	0.18
	1Y	0.95	0.87	0.63	0.57	0.79	0.18
NIG<N	5Y	*0*	0.11	*0*	*0*	*0.01*	*0*
	10Y	*0.01*	*0*	*0*	*0*	*0*	*0.01*
	1Y	0.78	0.86	0.36	0.43	0.32	0.30
GSS<N	5Y	*0*	*0.01*	*0*	*0*	*0*	*0*
	10Y	*0*	*0*	*0*	*0*	*0*	*0.01*

For one-year bonds, all models but the TIH Gaussian perform rather equally. The TH Gaussian is slightly better than the time-homogeneous NIG and GSS models in the left tail, while the time-homogeneous NIG and GSS are slightly better than the TH Gaussian in the right tail. These differences are, however, not significant. The time-inhomogeneous NIG and GSS models are not significantly better than their TH counterparts except at the 2.5 % and 97.5 % quantiles.

For five-year and ten-year bonds, the Gaussian models are consistently and significantly outperformed by the NIG and GSS models, and the GSS models consistently admit a significantly lower Embrechts' scores than the NIG models. The time-inhomogeneous GSS model is not significantly better than its TH counterpart at any quantile, while the time-inhomogeneous NIG is only significantly better than its TH counterpart at the 2.5 % and 97.5 % quantiles for ten-year bonds.

7.3 Backtests of More Complex Portfolios

In Section 7.2, we observed that term structure models generated by NIG and GSS distributions consistently predicted the one-day expected shortfall on zero-coupon bonds better than term structure models generated by Gaussian distributions. We now wish to investigate if this improved out-of-sample predictive power persists for more complex portfolios consisting of interest rate derivatives such as swaps and

caps. Since TIH models did not perform significantly different from their respective TH counterparts – and since it is not directly apparent how to include correlations across different risk factors in TIH models – we henceforth restrict our analysis to TH models.

Using the same backtesting period as in Section 7.2, we backtest one-day value-at-risk and expected shortfall on a selection of portfolios consisting of interest rates derivatives: a portfolio consisting of a single ten-year receiver swap with annual settlements, a portfolio consisting of one- to ten-year receiver swaps with annual settlements, and a portfolio consisting of one- to ten-year caps and receiver swaps with annual settlements. For simplicity, we initialise all swaps to a zero initial value, and we assign to each cap a strike rate identical to the swap rate of the swap with the same maturity.

We will not backtest directly against trading data of swaps and caps, but swap and cap prices derived from our modelled risk factors. The risk-neutral prices of swaps and caps are given by (2.7) and (2.8). The risk-neutral prices of swaps are easily computed from the initial yield curve.

Although the joint density necessary in computing the expectation in (2.8) can be found analytically (see Eberlein and Raible, 1999), the numerical evaluation is extremely time-consuming. Cap prices may instead be estimated by a Monte Carlo simulation (e.g. Glasserman, 2013) or through a bilateral Laplace transform and a fast Fourier algorithm (see Raible, 2000; Eberlein and Kluge, 2006). This approach implies a model-dependent pricing of instruments. However, since our three time-homogeneous models behave approximately similar in the long-run, cf. Figure B.1, the term structure models will asymptotically admit identical cap prices for any initial discount factor and yield curve.

The backtests of value-at-risk and expected shortfall for the three portfolios are given in Tables 7.6 and 7.7, respectively.

For the single ten-year swap, the unconditional VaR coverage of the Gaussian model is rejected at all but one quantile. The unconditional coverage of NIG and GSS models is not rejected at any quantile, though the models appear to consistently underestimate the risk. As reported for zero-coupon bonds, the Gaussian term structure models are consistently outperformed by the NIG and GSS term structure models in predicting one-day expected shortfall, and the NIG models are consistently outperformed by the GSS models.

For the portfolio of one- to ten-year swaps, the unconditional VaR coverage of the Gaussian model is only rejected at one quantile, and we do not reject the unconditional coverage of the NIG and GSS models at any quantile. The Gaussian model is again outperformed by NIG and GSS models in predicting one-day expected shortfall.

For the swap and cap combination, we reject the unconditional VaR coverage of the Gaussian model at all but the 2.5 and 97.5 % quantiles. The unconditional coverage of the NIG model is not rejected at any quantile, and the unconditional coverage of the GSS model is only rejected at the 99.0 % quantile. Lastly, the Gaussian model admits the greatest Embrechts' score at each quantile, while the GSS model consistently scores slightly lower than the NIG model.

Table 7.6: Results from backtests of one-day value-at-risk in portfolios consisting of (a) a ten-year receiver swap with annual settlements, (b) one- to ten-year receiver swaps with annual settlements, and (c) one- to ten-year caps and receiver swaps with annual settlements, using the previous 250 trading days in the calibration of the term structure models. Reported is the violation percentage and in parenthesis the p-value from the unconditional coverage Kupiec test.

Distribution	**0.5 %**	**1.0 %**	**2.5 %**	**97.5 %**	**99.0 %**	**99.5 %**
Gaussian	1.19	1.74	3.38	2.6	1.51	0.96
	(0)	*(0)*	*(0.01)*	(0.76)	*(0.03)*	*(0.01)*
NIG	0.64	1.23	2.79	2.92	1.23	0.78
	(0.38)	(0.29)	(0.40)	(0.22)	(0.29)	(0.09)
GSS	0.64	1.23	2.92	3.2	1.32	0.78
	(0.38)	(0.29)	(0.22)	(0.05)	(0.15)	(0.09)

(a) Ten-year swap

Distribution	**0.5 %**	**1.0 %**	**2.5 %**	**97.5 %**	**99.0 %**	**99.5 %**
Gaussian	0.78	1.23	2.37	2.24	1.46	0.82
	(0.09)	(0.29)	(0.7)	(0.42)	*(0.04)*	(0.05)
NIG	0.5	0.82	1.87	2.28	1.23	0.64
	(0.99)	(0.39)	(0.05)	(0.51)	(0.29)	(0.38)
GSS	0.55	0.87	1.87	2.33	1.23	0.68
	(0.75)	(0.52)	(0.05)	(0.6)	(0.29)	(0.25)

(b) One- to ten-year swaps

Distribution	**0.5 %**	**1.0 %**	**2.5 %**	**97.5 %**	**99.0 %**	**99.5 %**
Gaussian	0.91	1.55	3.01	2.42	1.55	0.91
	(0.01)	*(0.01)*	(0.14)	(0.81)	*(0.02)*	*(0.01)*
NIG	0.59	0.96	2.51	2.47	1.34	0.68
	(0.55)	(0.85)	(0.97)	(0.92)	(0.10)	(0.25)
GSS	0.55	0.91	2.37	2.65	1.46	0.78
	(0.75)	(0.68)	(0.70)	(0.66)	*(0.04)*	(0.09)

(c) One- to ten-year swaps and caps

Table 7.7: Results from backtests of one-day expected shortfall in portfolios consisting of (a) a ten-year receiver swap with annual settlements, (b) one- to ten-year receiver swaps with annual settlements, and (c) one- to ten-year caps and receiver swaps with annual settlements, using the previous 250 trading days in the calibration of the term structure models. Reported is the test score from the Embrechts' test.

Distribution	**0.5 %**	**1.0 %**	**2.5 %**	**97.5 %**	**99.0 %**	**99.5 %**
Gaussian	0.00287	0.00204	0.00119	0.00087	0.00126	0.00180
NIG	0.00178	0.00095	0.00048	0.00037	0.00070	0.00091
GSS	0.00116	0.00065	0.00037	0.00029	0.00053	0.00077

(a) Ten-year swap

Distribution	**0.5 %**	**1.0 %**	**2.5 %**	**97.5 %**	**99.0 %**	**99.5 %**
Gaussian	0.01463	0.00941	0.00482	0.00412	0.00575	0.00851
NIG	0.00794	0.00461	0.00140	0.00196	0.00230	0.00371
GSS	0.00497	0.00283	0.00133	0.00151	0.00174	0.00240

(b) One- to ten-year swaps

Distribution	**0.5 %**	**1.0 %**	**2.5 %**	**97.5 %**	**99.0 %**	**99.5 %**
Gaussian	0.02373	0.01515	0.00809	0.00690	0.00942	0.01356
NIG	0.01341	0.00880	0.00265	0.00388	0.00442	0.00672
GSS	0.01070	0.00651	0.00233	0.00307	0.00391	0.00600

(c) One- to ten-year swaps and caps

Chapter 8

Case Study: Norwegian Rates From February to April 2020

In Chapter 7, we observed that term structure models generated by generalised hyperbolic distributions performed better than traditional Gaussian HJM models in predicting one-day expected shortfall on a series of interest rate derivatives. This was, however, performed during normal market situations. To assess the resilience of financial institutions the Basel's stress testing principles (Basel Committee on Banking Supervision, 2018) specify how financial institutions should perform stress tests of unfavourable economic scenarios to determine whether the institutions have enough capital to withstand the impact of adverse economic developments.

Using the two stressed periods described in Section 6.2, we, therefore, wish to examine whether the Lévy term structure models are better equipped than Gaussian HJM models to describe periods of deep financial stress. We are herein not interested in the models' out-of-sample predictive power, and we concentrate on whether the different models manage to mimic the observed market movements. For simplicity, we restrict our analysis to time-homogeneous term structure models generated by univariate return distributions. Lastly, in light of the discussed term structure models, we highlight some differences between the two financial crises of 2008–2009 and February–April 2020.

8.1 Expected Shortfall Bounds During a Developing Crisis

The Minimum capital requirements for market risk (Basel Committee on Banking Supervision, 2016) states how banks should use expected shortfall as a measure of risks under stress, to ensure a sensible capture of tail risks and capital adequacy during periods of significant financial market stress. The risk measure is usually calculated to the most severe 12-month period of stress available over the observation horizon, which usually implies a subset of the global financial crisis.

We first observe a time series of log-returns of zero-coupon bonds during 2019–2020, to examine how the expected shortfall predictions of our term structure models react to stressed market movements. Using a standard calibration window of the previous 250 trading days, Figure 8.1 presents the observed daily log-returns on one-year, five-year, and ten-year zero-coupon bonds from January 2019 to April

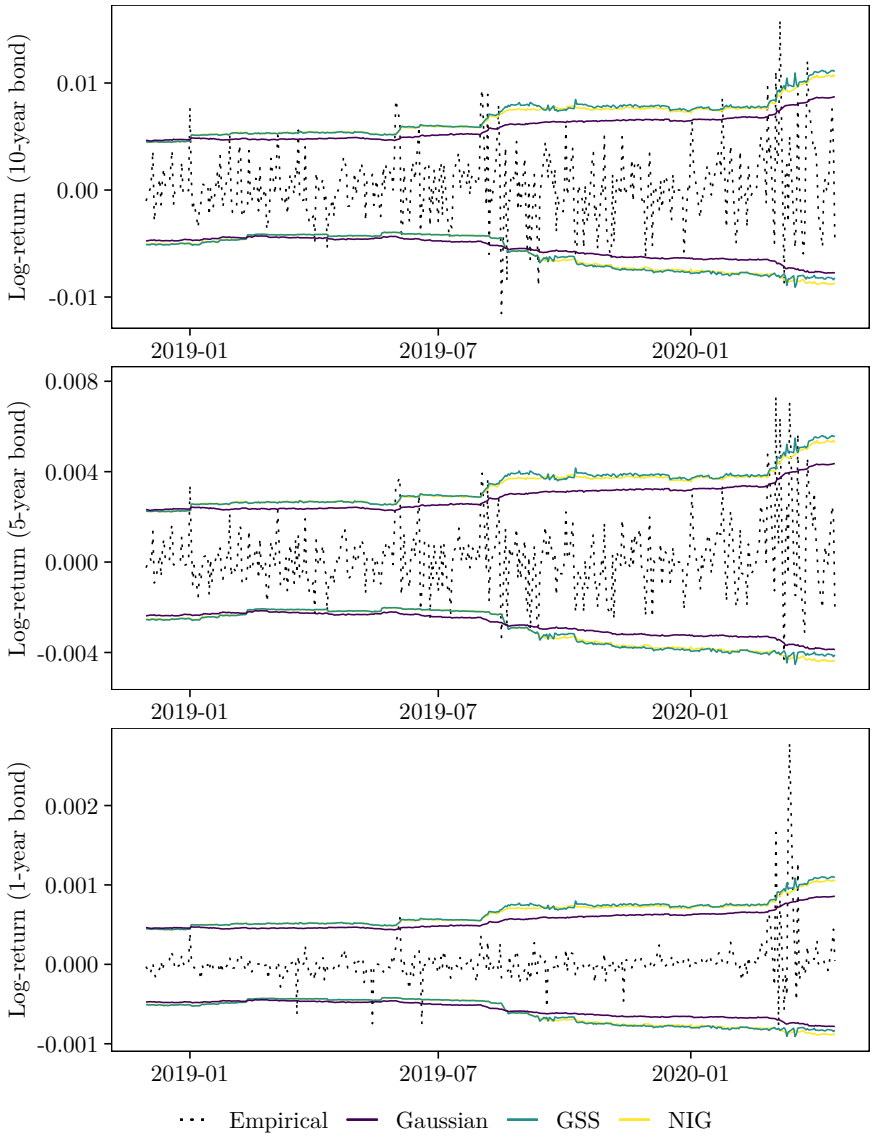

Figure 8.1: Observed daily log-returns on (top) ten-year, (middle) five-year, and (bottom) one-year zero-coupon bonds together with predicted one-day 97.5 % expected shortfall bounds for time-homogeneous term structure models generated by univariate Gaussian, NIG, and GSS distributions.

2020, alongside the predicted lower and upper one-day expected shortfall bounds at the 97.5 % quantiles.

As the crisis begins to unfold during March 2020, the expected shortfall bounds for all models begin to adjust. The adjustment is, however, slow, as our models do not differentiate between distant and close observations. This property underlines the limitations of the studied term structure models in predicting future risk measures when regime changes occur, compared to, e.g., a GARCH model (see Sharma, 2012). That is, when regime changes occur, tail event arrivals are not independent, and our models do not satisfy the conditions of a proper VaR model outlined in Christoffersen (2012).

Moreover, the Gaussian models do not manage to capture the skewness in the observed log-returns. As a result, the discrepancy of expected shortfall bounds between the Gaussian and NIG/GSS models decline in the lower tail but increases in the upper tail during March–April 2020. Since the NIG and GSS models manage to model skewness, they appear to better react to the stressed market movements. The model coverage (i.e., the extent to which the risk bounds contain the observed movements) during March–April 2020 is, nevertheless, abysmal due to the aforementioned uniform treatment of distant and close observations.

8.2 The Global Financial Crisis

Figures 8.2 and 8.3 present the observed and fitted one-day value-at-risk and expected shortfall for one-year, five-year, and ten-year zero-coupon bonds from January 2008 to December 2009. Except for low-maturity bonds, the term structure models provide decent approximations of the observed value-at-risk. For five- and ten-year bonds, the inability of model skewness causes the Gaussian model to underestimate the risk in the lower tail consistently, while the NIG and GSS models fit the tail well. All models admit approximately similar fits in the upper tail, and all models fail to capture the risk beyond the 99 % quantile.

The return distribution for one-year bonds is skewed, and the assumption of equal return distributions for all maturities severely breaks down for one-year bonds. Neither term structure model provides a good risk coverage, and especially in the upper tail, none of the term structure models provide reasonable representations of the observed return distribution.

The in-sample expected shortfall fit is more difficult to assess since the risk measure is sensitive to observations in the distant tail. Moreover, since the return distributions are somewhat irregular and unobserved, cf. the humped shape for five-year bonds in Figure 8.2, the visual expected shortfall fit is irregular for five- and ten-year bonds. That said, in the lower tail, the NIG and GSS models provide reasonable coverages, while the Gaussian models consistently underestimate the expected shortfall. All models underestimate the expected shortfall in the upper tail due to their inability to capture the weight in the distant tail. Nevetheless, the NIG and GSS models admit slightly better predictions than the Gaussian models herein. The fit to one-year bonds is, unsurprisingly, terrible.

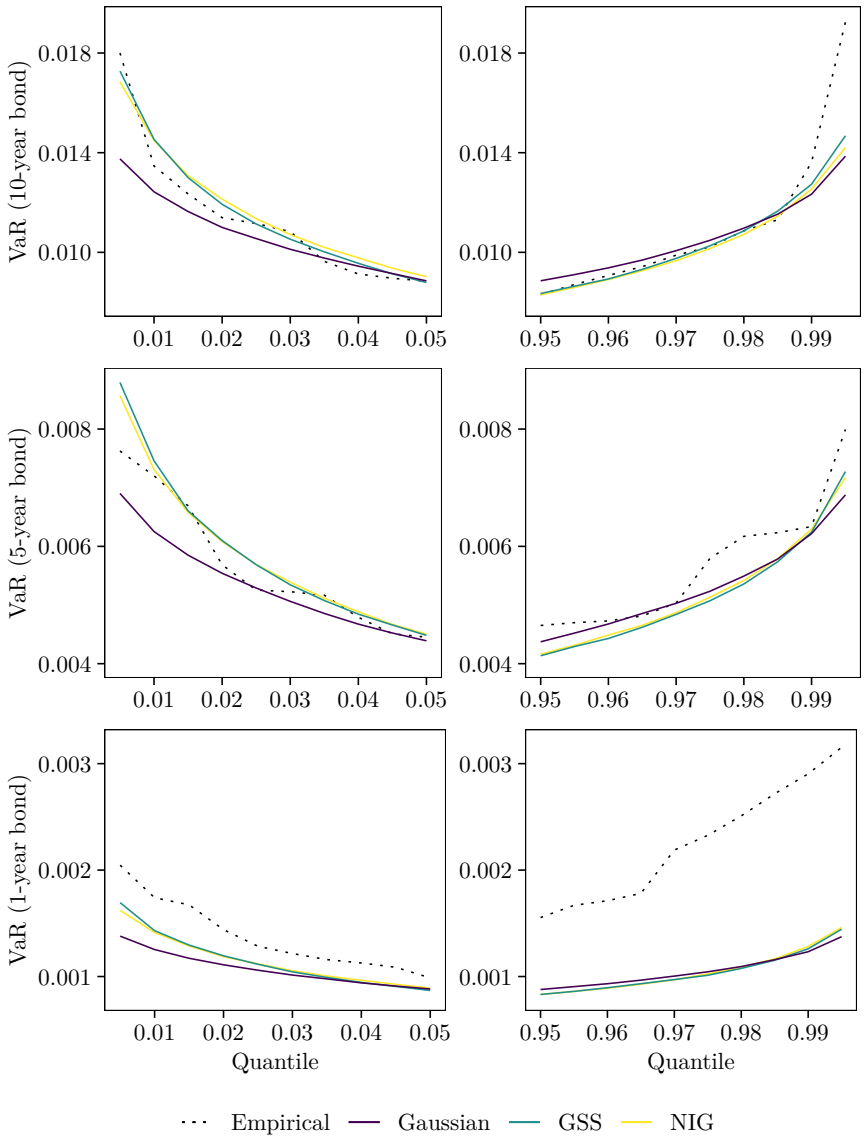

Figure 8.2: Observed and fitted one-day value-at-risk on (top) ten-year, (middle) five-year, and (bottom) one-year zero-coupon bonds during January 2008 to December 2009.

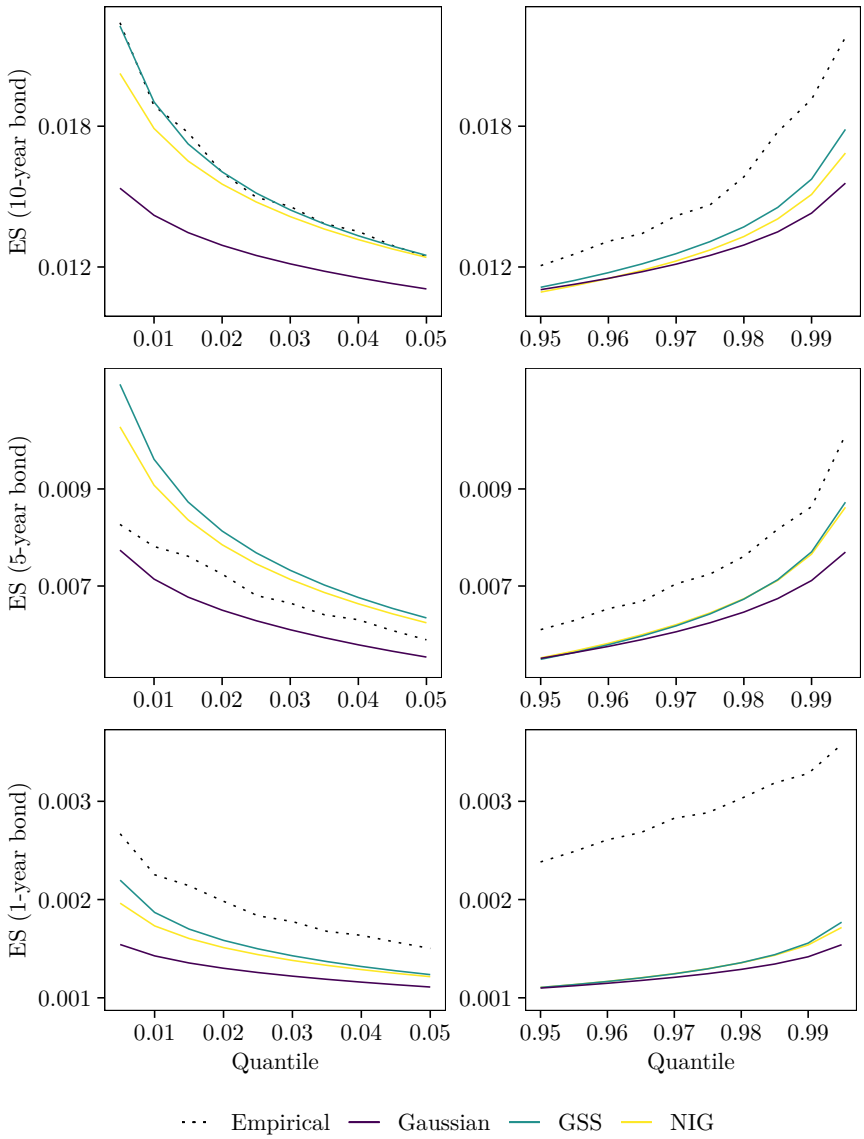

Figure 8.3: Observed and fitted one-day expected shortfall on (top) ten-year, (middle) five-year, and (bottom) one-year zero-coupon bonds during January 2008 to December 2009.

8.3 The Coronavirus Financial Crisis

Figures 8.4 and 8.5 present the observed and fitted one-day value-at-risk and one-day expected shortfall for one-year, five-year, and ten-year zero-coupon bonds from November 2019 to April 2020. Herein, we have also included the risk measures derived from the 2008–2009 data in Figures 8.2 and 8.3.

For the ten-year bonds, the NIG and GSS models provide adequate in-sample approximations of both tails. That is, the models do not accurately approximate the irregular shape in the upper tail, but they fit the distant tail well. The Gaussian model approximates the lower tail well, but the model's inability to model skewness causes it to severely underestimate the risk in the upper tail.

For the five-year bonds, none of the considered models manage to approximate the observed return distribution adequately. Due to its inability to capture skewness, the Gaussian model overestimates the risk in the lower tail and underestimates the risk in the upper tail. The NIG and GSS models are also too conservative in the lower tail, but the two models manage to capture the weight and decay of the upper tail reasonably well.

For the one-year bonds, all models overestimate the risk in the lower tail. The considered models provide, however, a surprisingly admissable approximation of the upper tail. That is, while none of the models manages to capture the weight and decay in the distant upper tail, all models provide a closer approximation of the value-at-risk and expected shortfall measures than in Figures 8.2 and 8.3. For the 2008–2009 data, the time-homogeneous term structure models generated by univariate distributions severely underestimate the risk in one-year bonds in both tails. For the 2019–2020 data, the assumption of equal return distributions is more justified. (The assumption appears, however, to be weaker than during a normal market situation.) That is, during the crash of spring 2020, the risk factors unique to low-maturity bonds are rather correlated and equi-sized with the risk factors generating the movements of intermediate- and high-maturity bonds.

We lastly note that the 2008–2009 data generally admit larger log-returns, and, consequently, the derived risk measure bounds provide good coverages of the observed risks during the spring of 2020. Necessarily, the bounds are way too conservative in the lower tail, and the coverage of one-year bonds is somewhat lacking in the upper tail.

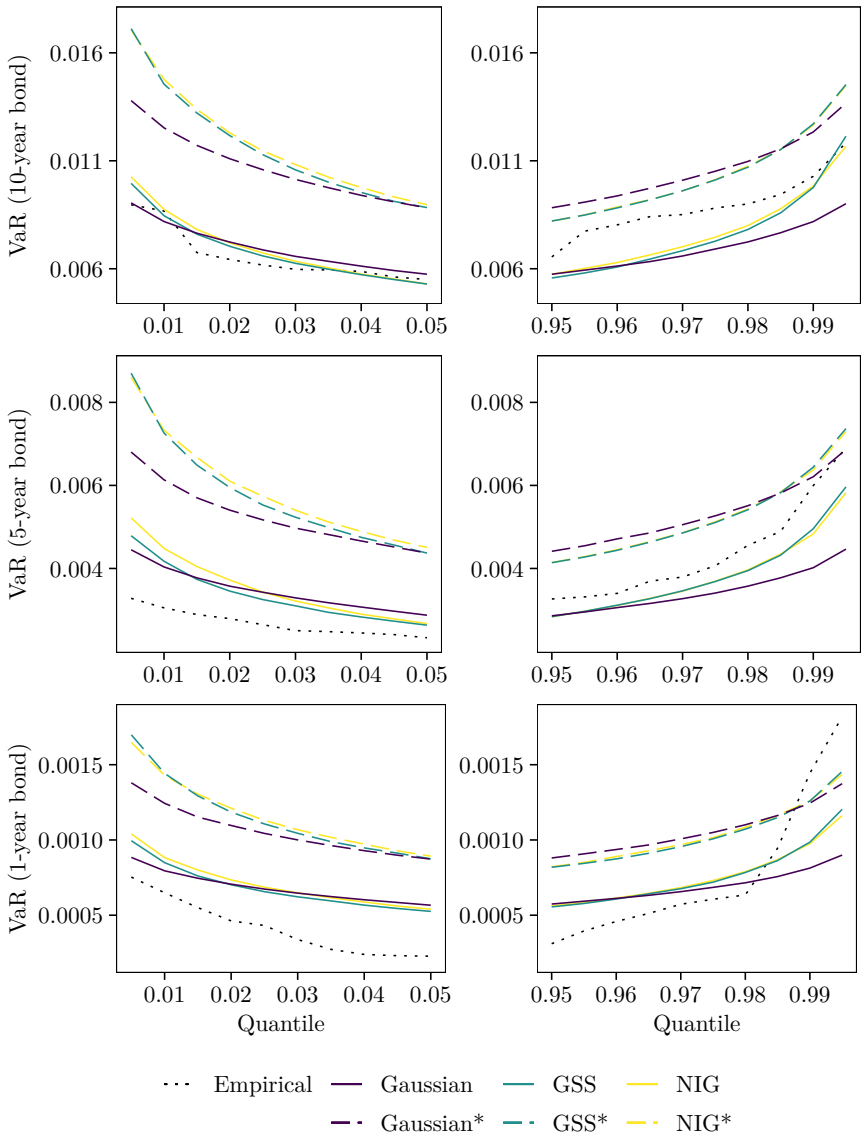

Figure 8.4: Observed and fitted one-day value-at-risk on (top) ten-year, (middle) five-year, and (bottom) one-year zero-coupon bonds during November 2019 to April 2020. Gaussian*, GSS*, and NIG* denote risk measures derived from the 2008–2009 data in Figure 8.2.

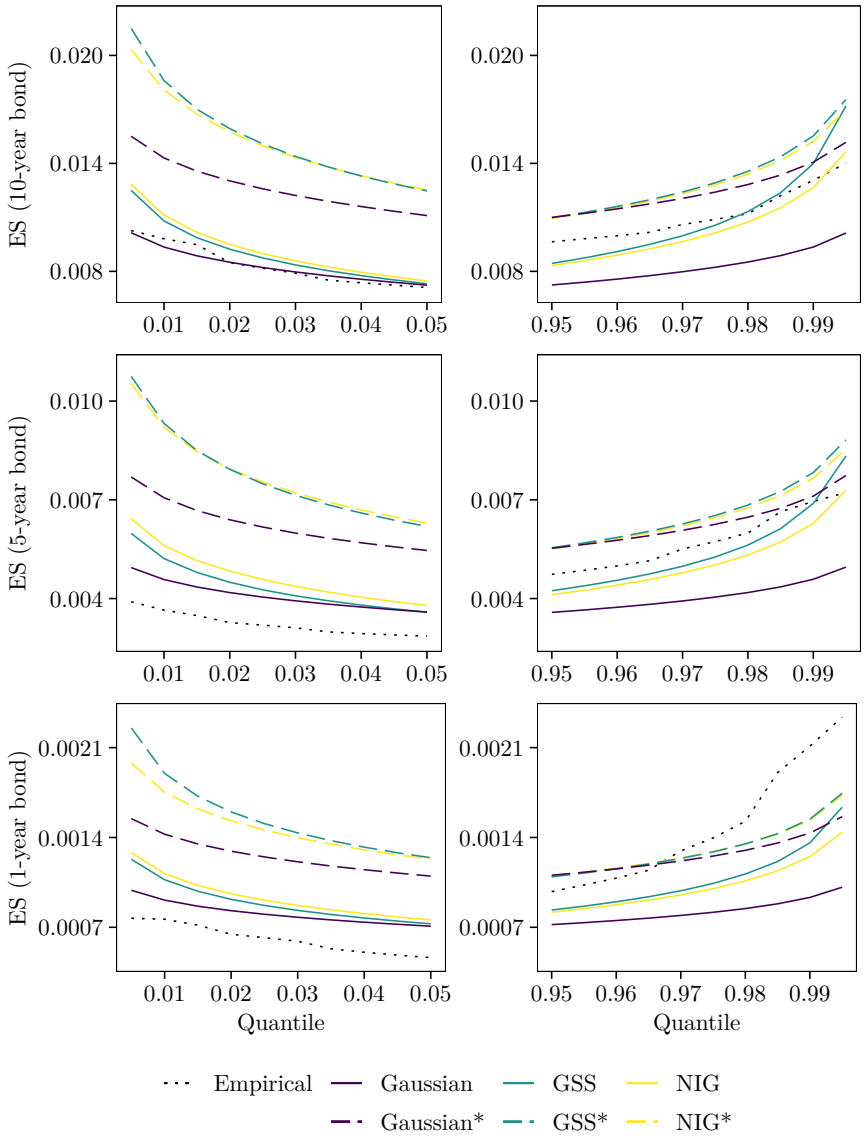

Figure 8.5: Observed and fitted one-day expected shortfall on (top) ten-year, (middle) five-year, and (bottom) one-year zero-coupon bonds during November 2019 to April 2020. Gaussian*, GSS*, and NIG* denote risk measures derived from the 2008–2009 data in Figure 8.3.

Chapter 9

Discussion

As discussed in the introduction of this thesis, empirical analysis (e.g. Eberlein, 2001; Raible, 2000; Das, 2002) demonstrates that term structure models driven by Brownian motions fail to reproduce the empirical return distributions of financial instruments adequately. The Gaussian QQ-plots for daily log-returns on Norwegian zero-coupon bonds from 2009 to 2019 in Figure 6.2 reveal that the empirical return distribution is leptokurtic, heavy-tailed, and possibly skewed. The deviation from a Gaussian distribution appears to increase for shorter maturities. Consequently, we observe in Figures 7.1 and 7.2 that a traditional HJM term structure model generated by a Gaussian distribution provides a poor in-sample fit to daily bond log-return data. The Gaussian model consistently underestimates the tail risks, and as a result, the Gaussian model underestimates the (in-sample) one-day value-at-risk and expected shortfall; see Figures 7.3 and 7.4. The approximation of risk measures further deteriorates as we consider more remote levels of the tails.

To reduce model risk and provide a more accurate description of observed market features, we introduce term structure models generated by generalised hyperbolic distributions. The models incorporate jump dynamics and semi-heavy tails. Specifically, we study models generated by the normal–inverse Gaussian (NIG) distribution and the generalised hyperbolic skew Student's (GSS) t-distribution. As previously demonstrated in, e.g., Raible (2000), the flexibility of generalised hyperbolic distributions constitutes more sophisticated term structure models which closer approximate observed market features. Whereas the Gaussian HJM models failed to capture the heavy-tailed nature of daily zero-coupon bond log-returns, the NIG and GSS term structure models provide accurate in-sample approximations. As a result, the NIG and GSS models closely model the observed one-day value-at-risk and expected shortfall in Figures 7.3 and 7.4.

Using an out-of-sample backtest of zero-coupon bonds from 2009 to 2019, we observe that the improved in-sample fit of NIG and GSS models translate to better out-of-sample predictions. Except for low-maturity bonds, the NIG and GSS models are significantly better than the Gaussian models at predicting one-day expected shortfall. The performance difference in value-at-risk predictions is not equally clear-cut, though the NIG and GSS models appear to provide the better approximation of value-at-risk beyond the 99 % quantiles. From a regulatory standpoint, we too observe that the NIG and GSS models to a lesser extent underestimate tail risks; the Gaussian models have a dubious tendency to underestimate the value-at-risk in the entire tail.

This performance difference furthermore holds for more complex portfolios consisting of swaps and caps, where the NIG and GSS models appear to be better than the Gaussian models at predicting both one-day value-at-risk and expected shortfall in the entire tail. We further note that the GSS models consistently admit better expected shortfall backtesting results than the NIG models. The NIG model has two semi-heavy tails which decay exponentially, while the GSS model has one tail which decays exponentially and one tail which decays as a polynomial. While both models can model skewness, we expect the GSS model to be better at modelling distributions with sufficiently asymmetric tail behaviours.

In the aforementioned analysis, we have focused on time-homogeneous (TH) term structure models generated by univariate return distributions. It is somewhat misleading to classify a model generated by a one-dimensional Lévy process as one-dimensional since the generating Lévy process itself is a high-dimensional object (Eberlein & Kluge, 2006). Nevertheless, each model is generated by *one* risk factor which determines the return distribution for the entire fixed-income market. For the NIG and GSS models, this simple market structure approximates the return distribution for intermediate- and high-maturity bonds well.

That is, the distant future is highly uncertain, and market forces which affect the term structure will not differentiate much between, e.g., five-year and ten-year bonds. We do, however, observe that TH term structure models generated by univariate return distributions fail to capture the return distributions of low-maturity bonds sufficiently, cf. Figure 7.2. For the studied period, this simple market structure leads to a too conservative prediction of risk measures for low-maturity bonds. The observed behaviour likens a weaker form of the *market segmentation theory*, which states that investors hold preferences for specific yields and maturities when they invest in fixed-income securities. These preferences lead to individual smaller markets subject to supply and demand forces unique to each market. The theory suggests that the behaviour of short-term rates is unrelated to the behaviour of long-term rates and that a movement in one is not indicative of an immediate movement in the other. The conclusion herein is that bonds with different maturities are not interchangeable and must be analysed independently.

In order to remedy the unsatisfactory in-sample approximation of low-maturity bonds, we a calibrate time-inhomogeneous (TIH) term structure models generated by univariate return distributions to each bond maturity. (This approach is, in fact, an applied version of the market segmentation theory, where we assume that each bond maturity constitutes a single market generated by unique risk factors.) While the implied assumption of zero correlation between the different maturities is terrible, and while it will lead to an inadequate assessment of risks on term structure-dependent securities, this approach might shed light on where our univariate TH term structure models might be improved.

In Figure 7.2, we observe that the calibrated return distributions of TH and TIH term structure models are approximately equal for intermediate- and high-maturity bonds. For the GSS models, the TIH models are not significantly better than their TH counterparts in an out-of-sample backtest of one-day expected shortfall at any level. For the NIG models, the TIH models are only significantly better than their

TH counterparts at the 2.5 and 97.5 % quantiles for ten-year bonds; see Table 7.5.

For one-year bonds, however, we observe in Figure 7.2 that the TIH models provide a superior in-sample fit to the observed return distribution. While the simple univariate TH market structure cannot reproduce the movement of one-year bonds accurately, the segmented TIH market structure can. This improved in-sample fit does, however, not translate to a significantly better out-of-sample risk measure prediction. While the TH models generally overestimate the tail risks on low-maturity bonds, they provide a rather good fit to the distant tails of the empirical return distribution. The TIH models, however, admit unstable approximations of the distant tails, cf. Figures 7.3 and 7.4, where the in-sample fit of TIH models deteriorates beyond the 97.5 % quantiles. As a result, the time-inhomogeneous NIG and GSS models are only sporadically significantly better than their TH counterparts at the 2.5 and 97.5 % quantiles.

The unstable approximations of the distant tail for TIH models are a result of convergence issues in the EM algorithm when calibrating TIH term structure models on one-year bonds. The reason for these convergence problems have not been thoroughly investigated, though we note the following: In the calibration, we, at time t, attempt to estimate the future return distribution F_{t+1} using observed returns $x_t, x_{t-1}, \ldots, x_{t-n}$. We assume that the returns are independent and identically distributed. Firstly, the assumption of independence is weak for financial data. Secondly, if a regime change has occurred during the observational period, the observed returns are not identically distributed.

If these assumption failures are sufficiently severe, the model contains more parameters than can be estimated from the data, and the likelihood surface may take the shape of a flat ridge with no maximum. An approximative E-step in the EM algorithm may contribute to the problem, and this may affect the stability of the parameter estimates. Moreover, the GSS models, which previously admitted the best predictions of expected shortfall, need to estimate the index parameter λ. This parameter admits a very flat likelihood function difficult to optimise even for sufficiently large data sets (see Prause et al., 1999).

Central banks typically implement monetary policy to guide the market-determined short-rates. Large movements in monetary policy induce temporary or permanent movements in the short-rates, while the impact on long-term rates is less apparent (e.g. Gerlach, 1996). A market where short-term rates are more affected by regime changes than long-term rates could explain the problems recognised in the calibration of the TIH models. Moreover, in the case of regime changes during the calibration window, a closer fit to the observations is not necessarily an advantage, and we would fancy a model which assigns more weight to recent observations (see Sharma, 2012).

An alternative modelling approach, which we have not pursued in this thesis, is time-homogeneous term structure models generated by multivariate distributions. These models combine the time-homogeneous property and the more flexible fit of the TIH models. The modelled market will then naturally exhibit non-linear dependence, which mirrors the fact that extreme market movements usually co-occur for several risk factors.

In this approach, we must calibrate several multidimensional parameters. The calibration requires the optimisation of more complex likelihood functions, where it is possible that the EM algorithm is arbitrarily poor in high dimensions and there can exist an exponential number of local maxima. If we are not careful, this may lead to an inferior description of the tail behaviours of the return distributions. The multivariate approach further leads to a second problem: Multivariate term structure models generated by Lévy processes are, in general, not complete. Theoretically, it is then not possible to define an arbitrage price, as there might exist infinitely many risk-neutral prices (see Pascucci, 2011).

Nevertheless, while the univariate TH models provide adequate descriptions of the distant tails, they frequently fail to provide satisfactory descriptions at the 2.5 and 97.5 % quantiles. As the capital charge for market risks based on expected shortfall in the Basel Accords is derived from the 2.5 and 97.5 % quantiles, we should pursue a more intricate term structure model. Time-homogeneous term structure models generated by multivariate Lévy processes provide reasonable extensions. A feasible complexity is two- or three-dimensional models, which separates the market into short-, intermediate-, and high-maturity bonds.

Having observed that the more general term structure models which exhibit jump dynamics, better approximate the observed market features, we turn our attention to periods of high financial stress. Specifically, we ask whether the different term structure models are suited to describe the observed market behaviour during the financial crisis of 2007–2009 and the coronavirus crisis of spring 2020.

As previously observed for normal market situations, the Gaussian models consistently underestimate the tail risks during the global financial crisis; see Figures 8.2 and 8.3. The Gaussian QQ-plots of observed daily log-returns in Figure 6.6 reveal that the return distributions are heavy-tailed, but compared to the behaviour during 2009–2019, the return distributions on intermediate- and high-maturity bonds are much more "conventional" and well-represented by a Gaussian distribution. The NIG and GSS models, nevertheless, better fit the observed risk measure behaviour on intermediate- and high-maturity bonds, and they manage to capture the moderate skewness in observed returns. The models, however, struggle in capturing the weight in the distant tails, which leads to somewhat inconsistent approximations of the observed expected shortfall. While the added flexibility of semi-heavy tails, jump dynamics, and skewness lead to a better in-sample approximation, the improvement is smaller than it was for the period 2009–2019.

Secondly, we observe that none of the considered term structure models are equipped to describe the behaviour of short-term bonds. The models do not capture the observed skewness, and all models severely underestimate the risk levels. While the assumption of equal return distributions for all maturities was weak during the previously discussed normal market situations, it is much weaker during the global financial crisis. That is, the inadequate fit to low-maturity bonds highlights the need for a more flexible term structure model, e.g. a multivariate model, to capture the dynamics of the entire fixed-income market during this stressed market situation.

The market crash during spring 2020 admits a different market behaviour with extremely skewed return distributions. From the Gaussian QQ-plots in Figure 6.7, we

observe that the upper tail, which is related to movements due to falling interest rates, is substantially heavy, while the lower tail is more well-behaved. The phenomenon is illustrated in Figure 6.5: The financial crisis data admit far greater returns in the lower tail, but the coronavirus crisis data admit an equally heavy upper tail. Furthermore, on 7 May 2020 Norges Bank's policy rate was lowered to 0 %, and the possibility of negative Norwegian interest rates became a highly probable prospect. Unlike, e.g., the popular LIBOR market models, the term structure models studied in this thesis allow for negative interest rates. In fact, the modelled forward rates are unbounded below.

The model property of negative interest rates has historically been considered a drawback (Wilmott, 2006), where the rationale from macroeconomic theory is that interest rates cannot turn negative as this causes a liquidity trap (Bodie, Kane, & Marcus, 2013). Black (1995), moreover, argues that nominal short-rates cannot turn negative as people still can hold currency at this rate. This rationale is, however, contradicted by observed negative interest rates on short-dated Japanese government debt, negative rates on US Treasuries were observed in November 2009, June 2011, and August 2011, and as of May 2020, several European countries, as well as Japan, still maintain benchmark interest rates below zero. Jarrow (2013), moreover, argues that Black's argument is a fallacy, and shows that a negative risk-free spot rate is consistent with an arbitrage-free term structure evolution in a competitive and nearly frictionless economy which can hold cash if cash has a convenience yield for its use in transactions.

Nevertheless, interest rates unbounded below is unreasonable: While one would accept a modest negative rate on a spot account, the cost would outweigh the benefits for an arbitrarily large negative rate. It is, therefore, possible that the term structure model is exaggerating both the probability and the magnitude of the negative rates. A simple, possible solution to deal with unbounded interest rates is to implement a floor, possibly somewhere around -1 to -3 %. It is, nonetheless, difficult to accurately pinpoint the exact effective lower bound.

If we return to the discussion of generating distributions, we again note that the Gaussian term structure models are not able to model skewness, and as a result, they overestimate the risk in the lower tail and underestimate the risk in the upper tail; see Figures 8.4 and 8.5. The NIG and GSS models are generally too conservative in the lower tail, as they do not adequately manage to capture the skewed market situation, but the models do fit the upper tail reasonably well. We also note that compared to the 2008–2009 situation, all models provide surprisingly passable descriptions of the movement of one-year bonds. That is, neither model manages to accurately capture the decay of the upper tail nor the frequent occurrences of extreme returns, but all models to some degree grasp the overall level of the risk measures.

During the global financial crisis, the market movements were dramatic, but they affected the different market structures differently; the behaviour on short-term bonds is quite different from the behaviour on intermediate- and long-maturity bonds. During the coronavirus crisis, the assumption of a univariate return distribution is more justified: The market pessimism almost equally affected the entire market, and short-term and long-term interest rates appear to tumble down together with rather

linear dependencies. To capture the observed market movement herein, it is not that important to consider multivariate models. Nonetheless, we cannot accurately assess the market risks on interest rate securities without considering term structure models which encompass heavy tails, skewness, and jump dynamics.

The incorporation of jump dynamics is especially critical for interest rate derivatives which depend heavily on the tails of the return distribution, cf. (out-of-the-money) caps and floors. We recall that the NIG and GSS models were far better than the Gaussian models at predicting one-day value-at-risk and one-day expected shortfalls on portfolios which included caps during the backtesting period 2009–2019. The observed log-returns on one-year bonds during March–April 2020, see Figure 8.1, are too wild for our simple univariate term structure models, but it is apparent that the risk in caps and floors during a stressed period similar to Match–April 2020, cannot be soundly measured by a Gaussian term structure model.

Despite quite different market behaviours, we note that a term structure model calibrated to the 2008–2009 data provide a good coverage of the 2020 data since the 2008–2009 data generally admit larger log-returns. The coverage on low-maturity bonds is not equally sound, but this can be remedied by considering multivariate return distributions. The model is, obviously, way too conservative in the lower tail of the return distribution. However, when performing a stress test of unfavourable economic scenarios, we are generally more interested in adverse economic developments which occur as a result of falling interest rates. A model too conservative in the tail related to rising interest rates is not all too alarming.

Chapter 10

Conclusion

In this thesis, we follow the papers by Eberlein et al. (2005) and Kluge (2005) to develop term structure models driven by general Lévy processes. Specifically, we consider Lévy processes generated by NIG and GSS distributions, which exhibit jump dynamics, semi-heavy tails, and skewness. Using NIBOR and swap rates from 2009 to 2019, we document that NIG and GSS models are better equipped than classical Gaussian HJM models to describe the observed one-day market risks on interest rate derivatives. The Gaussian models fail to describe the observed heavy-tailed return distribution of interest rate derivatives, while the NIG and GSS models approximate the observed market behaviour well. The GSS model is less tractable than the NIG model, but in the implemented out-of-sample backtests, the GSS model provides significantly better predictions of one-day expected shortfall for the considered instruments.

During the global financial crisis from 2008 to 2009, the inability to capture skewness and semi-heavy tails cause the Gaussian models to underestimate the tail risks consistently. During the recent financial crisis from February to April 2020, the Gaussian assumption aggravates. The highly skewed and heavy-tailed market behaviour is incompatible with a Gaussian generating distribution, while the NIG and GSS models, though too conservative in the lower tail of the return distribution, approximate the risk of falling interest rates well. Consequently, it does not appear that term structure models can accurately assess the market risks of fixed-income markets during times of normal or high financial stress without taking into account jump dynamics, semi-heavy tails, and possible skewness.

We lastly note that the studied time-homogeneous term structure models generated by univariate return distributions are insufficient in fully describing the entire fixed-income market. Further research on the model includes the employment of multivariate return distributions. We have, furthermore, only performed backtests over one-day horizons on stylised portfolios. Capital charges of market risks are usually based on longer time horizons, and it would be interesting to examine how the incorporation of jump features affect the risk pricing of actual market positions during relevant horizons.

References

Aas, K. & Haff, I. H. (2006). The generalized hyperbolic skew Student's t-distribution. *Journal of financial econometrics*, *4*(2), 275–309. https://doi.org/10.1093/jjfinec/nbj006

Abramowitz, M., Stegun, I. A., & Romer, R. H. (1988). *Handbook of mathematical functions with formulas, graphs, and mathematical tables*. American Association of Physics Teachers.

Acerbi, C., Nordio, C., & Sirtori, C. (2001). Expected shortfall as a tool for financial risk management. *arXiv preprint cond-mat/0102304*.

Acerbi, C. & Szekely, B. (2014). Back-testing expected shortfall. *Risk*, *27*(11), 76–81.

Acerbi, C. & Tasche, D. (2002a). Expected shortfall: A natural coherent alternative to value at risk. *Economic notes*, *31*(2), 379–388. https://doi.org/10.1111/1468-0300.00091

Acerbi, C. & Tasche, D. (2002b). On the coherence of expected shortfall. *Journal of Banking & Finance*, *26*(7), 1487–1503. https://doi.org/10.1016/S0378-4266(02)00283-2

Ahn, C. M. (1992). Option pricing when jump risk is systematic 1. *Mathematical Finance*, *2*(4), 299–308. https://doi.org/10.1111/j.1467-9965.1992.tb00034.x

Ahn, C. M. & Thompson, H. E. (1988). Jump-diffusion processes and the term structure of interest rates. *The journal of finance*, *43*(1), 155–174. https://doi.org/10.1111/j.1540-6261.1988.tb02595.x

Amin, K. I. (1993). Jump diffusion option valuation in discrete time. *The journal of finance*, *48*(5), 1833–1863. https://doi.org/10.1111/j.1540-6261.1993.tb05130.x

Andersson, J. (2001). On the normal inverse Gaussian stochastic volatility model. *Journal of Business & Economic Statistics*, *19*(1), 44–54. https://doi.org/10.1198/07350010152472607

Arshanapalli, B., Fabozzi, F. J., & Nelson, W. (2013). The role of jump dynamics in the risk–return relationship. *International Review of Financial Analysis*, *29*, 212–218. https://doi.org/10.1016/j.irfa.2012.11.004

Artzner, P., Delbaen, F., Eber, J.-M., & Heath, D. (1999). Coherent measures of risk. *Mathematical finance*, *9*(3), 203–228. https://doi.org/10.1111/1467-9965.00068

Babbs, S. H. & Webber, N. (1994). A theory of the term structure with an official short rate. *Financial Options Research Centre Working Paper*, (94/49).

Bank for International Settlements. (2020). OTC derivatives outstanding. https://www.bis.org/statistics/derstats.htm

Barndorff-Nielsen, O. E. (1997). Processes of normal inverse Gaussian type. *Finance and stochastics*, *2*(1), 41–68. https://doi.org/10.1007/s007800050032

Barndorff-Nielsen, O. E. & Blaesild, P. (1981). Hyperbolic distributions and ramifications: Contributions to theory and application. In *Statistical distributions*

in scientific work (pp. 19–44). Springer. https://doi.org/10.1007/978-94-009-8549-0_2

Barndorff-Nielsen, O. E. & Halgreen, C. (1977). Infinite divisibility of the hyperbolic and generalized inverse Gaussian distributions. *Zeitschrift für Wahrscheinlichkeitstheorie und verwandte Gebiete*, *38*(4), 309–311. https://doi.org/10.1007/BF00533162

Barndorff-Nielsen, O. E. & Shephard, N. (2002). Normal modified stable processes. *Theory of probability and Mathematical Statistics*, *65*, 1–20.

Basel Committee on Banking Supervision. (1996). *Supervisory framework for the use of back-testing in conjunction with the internal models approach to market risk capital requirements*. Bank for International Settlements. https://www.bis.org/publ/bcbs22.htm

Basel Committee on Banking Supervision. (2013). *Fundamental review of the trading book: A revised market risk framework*. Bank for International Settlements. https://www.bis.org/publ/bcbs265.pdf

Basel Committee on Banking Supervision. (2016). *Minimum capital requirements for market risk*. Bank for International Settlements. https://www.bis.org/bcbs/publ/d352.pdf

Basel Committee on Banking Supervision. (2018). *Stress testing principles*. Bank for International Settlements. https://www.bis.org/bcbs/publ/d450.pdf

Bates, D. S. (1991). The crash of '87: Was it expected? The evidence from options markets. *The journal of finance*, *46*(3), 1009–1044. https://doi.org/10.1111/j.1540-6261.1991.tb03775.x

Björk, T. (1995). On the term structure of discontinuous interest rates. *Surveys in Industrial and Applied Mathematics*, *2*(4), 626–657.

Björk, T. (2004). *Arbitrage theory in continuous time*. Oxford university press.

Björk, T., Di Masi, G., Kabanov, Y., & Runggaldier, W. (1997). Towards a general theory of bond markets. *Finance and Stochastics*, *1*(2), 141–174. https://doi.org/10.1007/s007800050020

Black, F. (1995). Interest rates as options. *the Journal of Finance*, *50*(5), 1371–1376. https://doi.org/10.1111/j.1540-6261.1995.tb05182.x

Black, F. & Scholes, M. (1973). The pricing of options and corporate liabilities. *Journal of political economy*, *81*(3), 637–654. https://doi.org/10.1086/260062

Bodie, Z., Kane, A., & Marcus, A. J. (2013). *Investments and portfolio management*. McGraw Hill Education (India) Private Limited.

Bølviken, E. & Benth, F. E. (2000). Quantification of risk in Norwegian stocks via the normal inverse Gaussian distribution. In *Proceedings of the AFIR 2000 Colloquium, Tromsø, Norway* (Vol. 8798). AFIR.

Brace, A., Gÿatarek, D., & Musiela, M. (1997). The market model of interest rate dynamics. *Mathematical finance*, *7*(2), 127–155. https://doi.org/10.1111/1467-9965.00028

Breymann, W. & Lüthi, D. (2013). ghyp: A package on generalized hyperbolic distributions. *Manual for R Package ghyp*.

Brigo, D. & Mercurio, F. (2007). *Interest rate models-theory and practice: With smile, inflation and credit*. Springer Science & Business Media. https://doi.org/10.1007/978-3-540-34604-3

Broadie, M. & Jain, A. (2008). The effect of jumps and discrete sampling on volatility and variance swaps. *International Journal of Theoretical and Applied Finance*, *11*(08), 761–797. https://doi.org/10.1142/S0219024908005032

Chen, Y., Härdle, W., & Jeong, S.-O. (2008). Nonparametric risk management with generalized hyperbolic distributions. *Journal of the American Statistical Association*, *103*(483), 910–923. https://doi.org/10.1198/016214507000001003

Christoffersen, P. F. (1998). Evaluating interval forecasts. *International economic review*, 841–862.

Christoffersen, P. F. (2012). *Elements of financial risk management*. Academic Press.

Clift, S., Costanzino, N., & Curran, M. (2016). Empirical performance of backtesting methods for expected shortfall. *SSRN*. https://doi.org/10.2139/ssrn.2618345

Costanzino, N. & Curran, M. (2015). Backtesting general spectral risk measures with application to expected shortfall. *SSRN*. https://doi.org/10.2139/ssrn.2514403

Costanzino, N. & Curran, M. (2018). A simple traffic light approach to backtesting expected shortfall. *Risks*, *6*(1), 2. https://doi.org/10.3390/risks6010002

Cox, J. C., Ingersoll Jr, J. E., & Ross, S. A. (1985). A theory of the term structure of interest rates. *Econometrica*, *53*, 385–407.

Danelsson, J., Jorgensen, B. N., Samorodnitsky, G., Sarma, M., & de Vries, C. G. (2013). Fat tails, VaR and subadditivity. *Journal of econometrics*, *172*(2), 283–291. https://doi.org/10.1016/j.jeconom.2012.08.011

Das, S. R. (2002). The surprise element: Jumps in interest rates. *Journal of Econometrics*, *106*(1), 27–65. https://doi.org/10.1016/S0304-4076(01)00085-9

Dempster, A. P., Laird, N. M., & Rubin, D. B. (1977). Maximum likelihood from incomplete data via the EM algorithm. *Journal of the Royal Statistical Society: Series B (Methodological)*, *39*(1), 1–22. https://doi.org/10.1111/j.2517-6161.1977.tb01600.x

Dothan, L. U. (1978). On the term structure of interest rates. *Journal of Financial Economics*, *6*(1), 59–69. https://doi.org/10.1016/0304-405X(78)90020-X

Du, Z. & Escanciano, J. C. (2017). Backtesting expected shortfall: Accounting for tail risk. *Management Science*, *63*(4), 940–958. https://doi.org/10.1287/mnsc.2015.2342

Eberlein, E. (2001). Application of generalized hyperbolic Lévy motions to finance. In *Lévy processes* (pp. 319–336). Springer. https://doi.org/10.1007/978-1-4612-0197-7_14

Eberlein, E., Jacod, J., & Raible, S. (2005). Lévy term structure models: No-arbitrage and completeness. *Finance and Stochastics*, *9*(1), 67–88. https://doi.org/10.1007/s00780-004-0138-3

Eberlein, E., Keller, U. et al. (1995). Hyperbolic distributions in finance. *Bernoulli*, *1*(3), 281–299.

Eberlein, E. & Kluge, W. (2006). Exact pricing formulae for caps and swaptions in a Lévy term structure model. *Journal of Computational Finance*, *9*(2).

Eberlein, E. & Kluge, W. (2007). Calibration of Lévy term structure models. In *Advances in mathematical finance* (pp. 147–172). Springer. https://doi.org/10.1007/978-0-8176-4545-8_9

Eberlein, E. & Özkan, F. (2003). Time consistency of Lévy models. *Quantitative Finance*, *3*(1), 40–50. https://doi.org/10.1088/1469-7688/3/1/304

Eberlein, E. & Raible, S. (1999). Term structure models driven by general Lévy processes. *Mathematical Finance*, *9*(1), 31–53. https://doi.org/10.1111/1467-9965.00062

Einhorn, D. & Brown, A. (2008). Private profits and socialized risk. *Global Association of Risk Professionals*, *42*, 10–26.

Embrechts, P., Kaufmann, R., & Patie, P. (2005). Strategic long-term financial risks: Single risk factors. *Computational optimization and applications*, *32*(1-2), 61–90. https://doi.org/10.1007/s10589-005-2054-7

Engle, R. F. & Manganelli, S. (2004). Caviar: Conditional autoregressive value at risk by regression quantiles. *Journal of Business & Economic Statistics*, *22*(4), 367–381.

Feinstone, L. J. (1987). Minute by minute: Efficiency, normality, and randomness in intra-daily asset prices. *Journal of Applied Econometrics*, *2*(3), 193–214.

Fergusson, K. & Platen, E. (2006). On the distributional characterization of daily log-returns of a world stock index. *Applied Mathematical Finance*, *13*(01), 19–38. https://doi.org/10.1080/13504860500394052

Filipovi, D. & Tappe, S. (2008). Existence of Lévy term structure models. *Finance and Stochastics*, *12*(1), 83–115. https://doi.org/10.1007/s00780-007-0054-4

Forsberg, L. & Bollerslev, T. (2002). Bridging the gap between the distribution of realized (ECU) volatility and ARCH modelling (of the Euro): The GARCH-NIG model. *Journal of Applied Econometrics*, *17*(5), 535–548. https://doi.org/10.1002/jae.685

Gerlach, S. (1996). Monetary policy and the behaviour of interest rates: Are long rates excessively volatile?

Glasserman, P. (2013). *Monte Carlo methods in financial engineering*. Springer Science & Business Media. https://doi.org/10.10071978-0-387-21617-1

Glasserman, P. & Kou, S. G. (2003). The term structure of simple forward rates with jump risk. *Mathematical Finance: An International Journal of Mathematics, Statistics and Financial Economics*, *13*(3), 383–410. https://doi.org/10.1111/1467-9965.00021

Good, P. (2013). *Permutation tests: A practical guide to resampling methods for testing hypotheses*. Springer Science & Business Media. https://doi.org/10.1007/978-1-4757-3235-1

Gürkaynak, R. S., Sack, B., & Swanson, E. (2005). The sensitivity of long-term interest rates to economic news: Evidence and implications for macroeconomic models. *American economic review*, *95*(1), 425–436. https://doi.org/10.2139/ssrn.1633934

Gürkaynak, R. S., Sack, B., & Wright, J. H. (2007). The US Treasury yield curve: 1961 to the present. *Journal of monetary Economics*, *54*(8), 2291–2304. https://doi.org/10.1016/j.jmoneco.2007.06.029

Heath, D., Jarrow, R., & Morton, A. (1992). Bond pricing and the term structure of interest rates: A new methodology for contingent claims valuation. *Econometrica: Journal of the Econometric Society*, 77–105. https://doi.org/10.2307/2951677

Ho, T. S. & Lee, S.-B. (1986). Term structure movements and pricing interest rate contingent claims. *the Journal of Finance*, *41*(5), 1011–1029. https://doi.org/10.1111/j.1540-6261.1986.tb02528.x

Hu, W. (2005). Calibration of multivariate generalized hyperbolic distributions using the EM algorithm, with applications in risk management, portfolio optimization and portfolio credit risk.

Hull, J. & White, A. (1990). Valuing derivative securities using the explicit finite difference method. *Journal of Financial and Quantitative Analysis*, *25*(1), 87–100. https://doi.org/10.2307/2330889

Jacod, J. & Protter, P. (2012). *Probability essentials*. Springer Science & Business Media. https://doi.org/10.1007/978-3-642-55682-1

Jacod, J. & Shiryaev, A. N. (2003). *Limit theorems for stochastic processes*. Springer. https://doi.org/10.1007/978-3-662-05265-5

El-Jahel, L., Lindberg, H., Perraudin, W., et al. (1996). *Yield curves with jump short rates*. Sveriges Riksbank.

James, G., Witten, D., Hastie, T., & Tibshirani, R. (2013). *An introduction to statistical learning*. Springer. https://doi.org/10.1007/978-1-4614-7138-7

Jamshidian, F. (1997). LIBOR and swap market models and measures. *Finance and Stochastics*, *1*(4), 293–330. https://doi.org/10.1007/s007800050026

Jarrow, R. (2013). The zero-lower bound on interest rates: Myth or reality? *Finance Research Letters*, *10*(4), 151–156.

Jarrow, R. (2018). *Continuous-time asset pricing theory*. Springer. https://doi.org/10.1007/978-3-319-77821-1

Jarrow, R. & Madan, D. (1995). Option pricing using the term structure of interest rates to hedge systematic discontinuities in asset returns. *Mathematical Finance*, *5*(4), 311–336. https://doi.org/10.1111/j.1467-9965.1995.tb00070.x

Jarrow, R. & Rosenfeld, E. R. (1984). Jump risks and the intertemporal capital asset pricing model. *Journal of Business*, 337–351.

Jensen, M. B. & Lunde, A. (2001). The NIG-S&ARCH model: A fat-tailed, stochastic, and autoregressive conditional heteroskedastic volatility model. *The Econometrics Journal*, *4*(2), 319–342. https://doi.org/10.1111/1368-423X.00070

Johannes, M. (2004). The statistical and economic role of jumps in continuous-time interest rate models. *The Journal of Finance*, *59*(1), 227–260. https://doi.org/10.1111/j.1540-6321.2004.00632.x

Joulin, A., Lefevre, A., Grunberg, D., & Bouchaud, J.-P. (2008). Stock price jumps: News and volume play a minor role. *arXiv preprint arXiv:0803.1769*.

Karlis, D. (2002). An EM type algorithm for maximum likelihood estimation of the normal–inverse Gaussian distribution. *Statistics & probability letters*, *57*(1), 43–52. https://doi.org/10.1016/S0167-7152(02)00040-8

Kassberger, S. (2009). Efficient portfolio optimization in the multivariate generalized hyperbolic framework. *Available at SSRN 1018241*.

Kassberger, S. & Kiesel, R. (2006). A fully parametric approach to return modelling and risk management of hedge funds. *Financial markets and portfolio management*, *20*(4), 472–491. https://doi.org/10.1007/s11408-006-0035-1

Kletskin, I., Lee, S. Y., Li, H., Li, M., Liu, R., Tolmasky, C., & Wu, Y. (2004). Correlation structures corresponding to forward rates. *Canadian Applied Mathematics Quarterly*, *12*(1), 125–135.

Kluge, W. (2005). *Time-inhomogeneous Lévy processes in interest rate and credit risk models* (Doctoral dissertation, Verlag nicht ermittelbar).

Koch-Medina, P. & Munari, C. (2016). Unexpected shortfalls of expected shortfall: Extreme default profiles and regulatory arbitrage. *Journal of Banking & Finance*, *62*, 141–151. https://doi.org/10.1016/j.jbankfin.2015.11.006

Kupiec, P. (1995). Techniques for verifying the accuracy of risk measurement models. *The J. of Derivatives*, *3*(2).

Kyprianou, A. E. (2006). *Introductory lectures on fluctuations of Lévy processes with applications*. Springer Science & Business Media. https://doi.org/10.1007/978-3-540-31343-4

Lahaye, J., Laurent, S., & Neely, C. J. (2011). Jumps, cojumps and macro announcements. *Journal of Applied Econometrics*, *26*(6), 893–921. https://doi.org/10.1002/jae.1149

Lee, S. S. (2012). Jumps and information flow in financial markets. *The Review of Financial Studies*, *25*(2), 439–479. https://doi.org/10.1093/rfs/hhr084

Lekkos, I. (2000). A critique of factor analysis of interest rates. *The Journal of Derivatives*, *8*(1), 72–83. https://doi.org/10.3905/jod.2000.319111

Litterman, R. & Scheinkman, J. (1991). Common factors affecting bond returns. *Journal of fixed income*, *1*(1), 54–61.

Longin, F. M. (2001). Beyond the var. *The Journal of Derivatives*, *8*(4), 36–48. https://doi.org/10.3905/jod.2001.319161

McNeil, A. J. & Frey, R. (2000). Estimation of tail-related risk measures for heteroscedastic financial time series: An extreme value approach. *Journal of empirical finance*, *7*(3-4), 271–300. https://doi.org/10.1016/S0927-5398(00)00012-8

McNeil, A. J., Frey, R., & Embrechts, P. (2005). Quantitative risk management: Concepts, techniques, and tools. *Princeton Series in Finance*.

Medvegyev, P. (2007). *Stochastic integration theory*. Oxford University Press.

Mencía, J. & Sentana, E. (2005). Estimation and testing of dynamic models with generalized hyperbolic innovations.

Meng, X.-L. & Rubin, D. B. (1993). Maximum likelihood estimation via the ECM algorithm: A general framework. *Biometrika*, *80*(2), 267–278. https://doi.org/10.1093/biomet/80.2.267

Merton, R. C. (1975). Option pricing when underlying stock returns are discontinuous.

Miltersen, K. R., Sandmann, K., & Sondermann, D. (1997). Closed form solutions for term structure derivatives with log-normal interest rates. *The Journal of Finance*, *52*(1), 409–430. https://doi.org/10.1111/j.1540-6261.1997.tb03823.x

Möller, A., Lenkoski, A., & Thorarinsdottir, T. L. (2013). Multivariate probabilistic forecasting using ensemble Bayesian model averaging and copulas. *Quarterly*

Journal of the Royal Meteorological Society, *139*(673), 982–991. https://doi.org/10.1002/qj.2009

Musiela, M. & Rutkowski, M. (1997). Continuous-time term structure models: Forward measure approach. *Finance and Stochastics*, *1*(4), 261–291. https://doi.org/10.1007/s007800050025

Naik, V. & Lee, M. (1990). General equilibrium pricing of options on the market portfolio with discontinuous returns. *The Review of Financial Studies*, *3*(4), 493–521. https://doi.org/10.1093/rfs/3.4.493

Norges Bank. (2009, July 17). *Key policy rate reduced by 0.25 percentage point to 1.25 per cent* [Press release]. https://www.norges-bank.no/en/news-events/news-publications/Press-releases/2009/Press-release-17-June-2009/

Norges Bank. (2011, December 14). *Key policy rate reduced by 0.50 percentage point to 1.75 percent* [Press release]. https://www.norges-bank.no/en/news-events/news-publications/Press-releases/2011/Press-release-14-December-2011/

Norges Bank. (2015, December 17). *Key policy rate unchanged at 0.75 percent* [Press release]. https://www.norges-bank.no/en/news-events/news-publications/Press-releases/2015/Press-release-17122015/

Norges Bank. (2020, May 7). *Policy rate reduced to zero percent* [Press release]. https://www.norges-bank.no/en/topics/Monetary-policy/Monetary-policy-meetings/2020/may-2020/

Pascucci, A. (2011). *PDE and martingale methods in option pricing*. Springer Science & Business Media. https://doi.org/10.1007/978-88-470-1781-8

Piazzesi, M. (2005). Bond yields and the Federal Reserve. *Journal of Political Economy*, *113*(2), 311–344.

Prause, K. (1997). Modelling financial data using generalized hyperbolic distributions. *fDM Preprint*, *48*.

Prause, K. et al. (1999). *The generalized hyperbolic model: Estimation, financial derivatives and risk measures* (Doctoral dissertation).

Protassov, R. S. (2004). EM-based maximum likelihood parameter estimation for multivariate generalized hyperbolic distributions with fixed λ. *Statistics and Computing*, *14*(1), 67–77. https://doi.org/10.1023/B:STCO.0000009419.12588.da

Protter, P. E. (2005). *Stochastic integration and differential equations*. Springer. https://doi.org/10.1007/978-3-662-10061-5

Raible, S. (2000). *Lévy processes in finance: Theory, numerics, and empirical facts* (Doctoral dissertation, Verlag nicht ermittelbar).

Rydberg, T. H. (1997). The normal inverse Gaussian Lévy process: Simulation and approximation. *Communications in statistics. Stochastic models*, *13*(4), 887–910. https://doi.org/10.1080/15326349708807456

Samuelson, P. A. (1965). Rational theory of warrant prices. *Industrial Management Review*, *6*, 13–32.

Sharma, M. (2012). Evaluation of basel iii revision of quantitative standards for implementation of internal models for market risk. *IIMB Management Review*, *24*(4), 234–244. https://doi.org/10.1016/j.iimb.2012.09.001

Shirakawa, H. (1991). Interest rate option pricing with Poisson-Gaussian forward rate curve processes. *Mathematical Finance*, *1*(4), 77–94. https://doi.org/10.1111/j.1467-9965.1991.tb00020.x

The World Bank. (2020). Market capitalization of listed domestic companies. https://data.worldbank.org/indicator/cm.mkt.lcap.cd

Vasicek, O. (1977). An equilibrium characterization of the term structure. *Journal of financial economics*, *5*(2), 177–188. https://doi.org/10.1016/0304-405X(77)90016-2

Wilmott, P. (2006). *Paul Wilmott on quantitative finance-3 volume set*. John Wiley & Sons.

Wilmott, P., Howson, S., Howison, S., Dewynne, J., et al. (1995). *The mathematics of financial derivatives: A student introduction*. Cambridge university press.

Wong, W. K. (2008). Backtesting trading risk of commercial banks using expected shortfall. *Journal of Banking & Finance*, *32*(7), 1404–1415. https://doi.org/10.1016/j.jbankfin.2007.11.012

Xia, F. (2014). *The term structure of interest rates, monetary policy, and macroeconomy* (Doctoral dissertation, UC San Diego).

Appendix A

Parameter Estimation Using the EM Algorithm

The generalised hyperbolic distribution can be represented as a normal variance–mean mixture with the generalised inverse Gaussian (GIG) distribution as a mixing distribution (Barndorff-Nielsen & Blaesild, 1981). Hence, a generalised hyperbolic variable $X \sim \mathrm{GH}(\lambda, \alpha, \beta, \delta, \mu)$ can be represented as

$$X \stackrel{d}{=} \mu + \beta Z + \sqrt{Z} Y, \tag{A.1}$$

where $Y \sim N(0,1)$ and $Z \sim \mathrm{GIG}(\lambda, \delta, \gamma)$, with Y and Z independent and $\gamma := \sqrt{\alpha^2 - \beta^2}$. The GIG distribution admits the density (Barndorff-Nielsen & Halgreen, 1977)

$$f_{\mathrm{GIG}}(x; \lambda, \delta, \gamma) = \left(\frac{\gamma}{\delta}\right)^{\lambda} \frac{x^{\lambda-1}}{2K_\lambda(\gamma\delta)} \exp\left(-\frac{1}{2}(\delta^2 x^{-1} + \gamma^2 x)\right), \tag{A.2}$$

where $\lambda \in \mathbb{R}$ and $\gamma, \delta \in \mathbb{R}_+$.

The problem of Section 4.6 is to maximise the log-likelihood

$$\log L(\lambda, \alpha, \beta, \delta, \mu; X_1, \ldots, X_n) = \sum_{i=1}^{n} \log f_{\mathrm{GH}}(x_i; \lambda, \alpha, \beta, \delta, \mu). \tag{A.3}$$

The optimisation is simplified if we exploit the normal variance–mean mixture of the GH distribution. We may then apply the expectation–maximization (EM) algorithm (Dempster et al., 1977), which performs a maximum likelihood estimation on data containing missing or latent values. This approach is convenient in our problem since a mixing distribution produces unobserved variables, in (A.1) the quantities Z.

At each step in the EM algorithm, we compute the expectation of the sufficient statistic for the mixing distribution, conditional on the current maximum likelihood estimators. Next, updated maximum likelihood estimators are derived using the recently computed expectation of the sufficient statistic for the mixing distribution. The iterative cycle is continued until some convergence criterion is satisfied. The algorithm needs good initial values for the maximum likelihood estimators to avoid local maxima; we will use the moment estimators.

A.1 The NIG Distribution

A.1.1 Maximisation Step

We assume that we have independent and identically distributed observations $X = (x_1, \ldots, x_n)$ and unobserved latent mixing variables $Z = (z_1, \ldots, z_n)$. The joint density of X and Z from (A.1) is $f_{x,z}(x, z) = f_{x|z}(x|z)f_z(z)$. We restrict our analysis to the univariate NIG distribution ($\lambda = -1/2$), which admits the augmented log-likelihood function

$$\begin{aligned}\log L(\alpha, \beta, \delta, \mu; X, Z) &= \sum_{i=1}^{n} \log f_{x|z}(x_i|z_i; \mu, \beta) + \sum_{i=1}^{n} \log f_z(z_i; \delta, \gamma) \\ &= \log L_1(\mu, \beta) + \log L_2(\delta, \gamma).\end{aligned}$$

From (A.1), it follows that $(X|Z = z) \sim N(\mu + \beta z, z)$, such that

$$\log L_1(\mu, \beta) = -\frac{n}{2}\log(2\pi) - \frac{1}{2}\sum_{i=1}^{n} \log z_i - \frac{1}{2}\sum_{i=1}^{n} \frac{(x_i - \mu - \beta z_i)^2}{z_i}.$$

Maximising the log-likelihood with respect to β and μ, the maximum likelihood estimators at the kth iteration of the EM algorithm are

$$\beta^{(k+1)} = \frac{\sum_{i=1}^{n} \frac{x_i}{z_i} - \bar{x}\sum_{i=1}^{n} \frac{1}{z_i}}{n - \bar{z}\sum_{i=1}^{n} \frac{1}{z_i}} \quad \text{and} \quad \mu^{(k+1)} = \bar{x} - \beta^{(k+1)}\bar{z}, \tag{A.4}$$

where $\bar{x} = \sum_{i=1}^{n} x_i/n$ and $\bar{z} = \sum_{i=1}^{n} z_i/n$. Likewise, $Z \sim \text{GIG}(-\frac{1}{2}, \delta, \gamma) = \text{IG}(\delta, \gamma)$ for the NIG distribution, where $\text{IG}(\cdot)$ denotes the inverse Gaussian distribution with density (Karlis, 2002)

$$f_{\text{IG}}(z; \delta, \gamma) = \frac{\delta}{\sqrt{2\pi}} \exp(\delta\gamma) z^{-3/2} \exp\left(-\frac{1}{2}\left(\frac{\delta^2}{z} + \gamma^2 z\right)\right).$$

This gives the log-likelihood

$$\log L_2(\delta, \gamma) = n \log \frac{\delta}{\sqrt{2\pi}} + n\delta\gamma - \frac{3}{2}\sum_{i=1}^{n} \log z_i - \frac{\delta^2}{2}\sum_{i=1}^{n} \frac{1}{z_i} - \frac{\gamma^2}{2}\sum_{i=1}^{n} z_i.$$

Maximising the log-likelihood with respect to δ and γ, the maximum likelihood estimators at the kth iteration of the EM algorithm are

$$\delta^{(k+1)} = \sqrt{\frac{n}{\sum_{i=1}^{n} \frac{1}{z_i} - \frac{n}{\bar{z}}}} \quad \text{and} \quad \alpha^{(k+1)} = \sqrt{(\delta^{(k+1)}/\bar{z})^2 + (\beta^{(k+1)})^2}. \tag{A.5}$$

A.1.2 Expectation Step

We observe in (A.4) and (A.5) that we need to estimate the pseudovalues $\mathbb{E}(Z_i|X_i = x_i)$ and $\mathbb{E}(Z_i^{-1}|X_i = x_i)$. For the NIG distribution, $(Z|X = x) \sim \text{GIG}(-1, q(x), \alpha)$ for $q(x) = \sqrt{\delta^2 + (x-\mu)^2}$, such that (Karlis, 2002)

$$\mathbb{E}(Z_i|X_i = x_i) = \frac{q(x_i)}{\alpha}\frac{K_0(\alpha q(x_i))}{K_1(\alpha q(x_i))} \quad \text{and} \quad \mathbb{E}(Z_i^{-1}|X_i = x_i) = \frac{\alpha}{q(x_i)}\frac{K_2(\alpha q(x_i))}{K_1(\alpha q(x_i))}.$$

A.1.3 Initialisation

The algorithm is initialised by the parameters' moment estimators, given that these exist. That is, let $\tilde{m}_1$, $\tilde{m}_2$, $\tilde{m}_3$, and $\tilde{m}_4$ denote the sample mean, standard deviation, skewness, and kurtosis, respectively. Then, equating the theoretical moments with their sample counterparts, the moment estimators are given by

$$\begin{aligned}
\hat{\beta} &= (\tilde{m}_3 \tilde{m}_2 \tilde{\gamma}^2)/3, \\
\hat{\delta} &= \tilde{m}_2^2 \tilde{\gamma}^3/(\tilde{\beta}^2 + \tilde{\gamma}^2), \\
\hat{\alpha} &= (\tilde{\gamma}^2 + \tilde{\beta}^2)^{1/2}, \\
\hat{\mu} &= \tilde{m}_1 - \tilde{\beta}\tilde{\delta}/\tilde{\gamma},
\end{aligned}$$

where

$$\hat{\gamma} := \frac{3}{\tilde{m}_2\sqrt{3\tilde{m}_4 - 5\tilde{m}_3^2}}.$$

We note that the moment estimators do not exist if $\tilde{m}_3 > \sqrt{\frac{3}{5}\tilde{m}_4}$.

A.2 The Generalised Hyperbolic Skew Student's t-Distribution

We now restrict our analysis to the univariate generalised hyperbolic skew Student's t-distribution ($\alpha \to |\beta|$ and $\lambda = -\nu/2$ for $\nu > 0$) and present the EM algorithm presented in Aas and Haff (2006).

In the numerical analysis of this thesis we, however, fit the distribution using the calibration algorithm implemented in the R package `ghyp` (Breymann & Lüthi, 2013), which uses a different parametrisation that makes the fitting procedure faster. The package too uses a modified EM scheme, called the multi-cycle, expectation, conditional estimation (MCECM) algorithm (Meng & Rubin, 1993; McNeil et al., 2005), which replaces several complicated maximisation steps with computationally simpler conditional maximisation steps.

A.2.1 Maximisation Step

We again assume that we have independent and identically distributed observations $X = (x_1, \ldots, x_n)$ and unobserved latent mixing variables $Z = (z_1, \ldots, z_n)$. The joint density $f_{x,z}(x, z) = f_{x|z}(x|z)f_z(z)$ admits the augmented log-likelihood function

$$\begin{aligned}\log L(\nu, \beta, \delta, \mu; X, Z) &= \sum_{i=1}^{n} \log f_{x|z}(x_i|z_i; \mu, \beta) + \sum_{i=1}^{n} \log f_z(z_i; \nu, \delta) \\ &= \log L_1(\mu, \beta) + \log L_2(\nu, \delta),\end{aligned}$$

where $\log L_1(\mu, \beta)$ is the same as in Section A.1, such that the maximum likelihood estimators for β and μ are given by (A.4). The mixing distribution for the GSS distribution is $Z \sim \text{GIG}(-\nu/2, \delta, 0)$. If we use the properties of the modified Bessel function (4.20), the density of Z can be written as

$$f_z(z; \nu, \delta) = \frac{\delta^\nu z^{-\nu/2-1}}{\Gamma\left(\frac{\nu}{2}\right) 2^{\nu/2}} \exp\left(-\frac{\delta^2}{2} z^{-1}\right),$$

which can be recognised as the density of the inverse gamma distribution with parameters $\nu/2$ and $\delta^2/2$. Hence,

$$\log L_2(\nu, \delta, \gamma) = -n \log \Gamma\left(\frac{\nu}{2}\right) - \frac{n \log 2}{2}\nu + n\nu \log \delta - \frac{\nu + 2}{2} \sum_{i=1}^{n} \sum_{i=1}^{n} \log z_i - \frac{\delta^2}{2} \sum_{i=1}^{n} \frac{1}{z_i}.$$

Differentiating $\log L_2(\nu, \delta, \gamma)$ with respect to δ gives

$$\delta^{(k+1)} = \sqrt{\frac{n\nu^{(k+1)}}{\sum_{i=1}^{n} z_i^{-1}}}. \tag{A.6}$$

Differentiating $\log L_2(\nu, \delta, \gamma)$ with respect to ν gives an equation that needs to be solved numerically for ν,

$$\log \frac{n}{2} - \log \sum_{i=1}^{n} \frac{1}{z_i} - \frac{1}{n} \sum_{i=1}^{n} \log z_i = \Psi\left(\frac{\nu^{(k+1)}}{2}\right) - \log \nu^{(k+1)}, \tag{A.7}$$

where $\Psi(\cdot)$ is the Digamma function.

A.2.2 Expectation Step

We observe in (A.6) and (A.7) that we need to estimate the pseudovalues $\mathbb{E}(Z_i|X_i = x_i)$, $\mathbb{E}(Z_i^{-1}|X_i = x_i)$, and $\mathbb{E}(\log Z_i|X_i = x_i)$. For the GSS distribution, $(Z|X = x) \sim \text{GIG}(-(\nu + 1)/2, q(x), |\beta|)$, for $q(x) = \sqrt{\delta^2 + (x - \mu)^2}$. Thus (Aas & Haff, 2006),

$$\mathbb{E}(Z_i|X_i = x_i) = \frac{q(x_i)}{|\beta|} \frac{K_{\frac{1-\nu}{2}}(|\beta| q(x_i))}{K_{\frac{1+\nu}{2}}(|\beta| q(x_i))},$$

$$\mathbb{E}(Z_i^{-1}|X_i = x_i) = \frac{|\beta|}{q(x_i)} \frac{K_{\frac{\nu+3}{2}}(|\beta|q(x_i))}{K_{\frac{\nu+1}{2}}(|\beta|q(x_i))},$$

$$\mathbb{E}(\log Z_i|X_i = x_i) = \log\left(\frac{q(x_i)}{|\beta|}\right) + \frac{1}{K_{\frac{\nu+1}{2}}(|\beta|q(x_i))} \frac{\partial K_{\frac{\nu+1}{2}}(|\beta|q(x_i))}{\partial\left(\frac{\nu+1}{2}\right)}.$$

A.2.3 Initialisation

The algorithm is initialised by the parameters' moment estimators. That is, let $\tilde{m}_1$, $\tilde{m}_2$, $\tilde{m}_3$, and $\tilde{m}_4$ denote the sample mean, standard deviation, skewness, and kurtosis, respectively. Then, equating the theoretical moments with their sample counterparts, the moment estimators are given by (Aas & Haff, 2006)

$$\begin{aligned}
\hat{\mu} &= \tilde{m}_1 - \frac{\hat{\beta}\hat{\delta}^2}{\hat{\nu}-2}, \\
\hat{\beta} &= \text{sign}(\tilde{m}_3)\frac{\sqrt{(\hat{\nu}-2)(\hat{\nu}-4)(\tilde{m}_2(\hat{\nu}-2)-\hat{\delta}^2)}}{\sqrt{2}\hat{\delta}^2}, \\
\hat{\delta}^2 &= 6(\hat{\nu}-2)^2(\hat{\nu}-4)\tilde{m}_2\kappa,
\end{aligned}$$

where κ is given by

$$\kappa = \left(1 - \sqrt{1 - \frac{(3\hat{\nu}^2 - 2\hat{\nu} - 32)(12(5\hat{\nu}-22) - (\hat{\nu}-6)(\hat{\nu}-8)\tilde{m}_4)}{216(\hat{\nu}-2)^2(\hat{\nu}-4)}}\right),$$

and the moment estimator for ν is the solution of the equation

$$(4 - 6(\hat{\nu}+2)(\hat{\nu}-2)\kappa)\sqrt{2}\sqrt{\hat{\nu}-4}\sqrt{1-6(\hat{\nu}-2)(\hat{\nu}-4)\kappa} - \tilde{m}_3(\hat{\nu}-6) = 0.$$

The search for ν is conducted within a limited area, see Aas and Haff (2006).

Appendix B

Additional Results

B.1 Calibration to Zero-Coupon Bond Quotes

Table B.1: Parameter estimates for the fitted time-inhomogeneous Gaussian processes using one- to ten-year zero-coupon bond quotes from 24 June 2011 to 19 June 2013.

Time-to-maturity	$\hat{\boldsymbol{\delta}}$	$\hat{\boldsymbol{\mu}}$
1 year	$1.10 \cdot 10^{-6}$	$8.32 \cdot 10^{-24}$
2 years	$1.36 \cdot 10^{-6}$	$-7.00 \cdot 10^{-24}$
3 years	$1.46 \cdot 10^{-6}$	$-1.73 \cdot 10^{-23}$
4 years	$1.51 \cdot 10^{-6}$	$-4.10 \cdot 10^{-24}$
5 years	$1.53 \cdot 10^{-6}$	$-1.74 \cdot 10^{-23}$
6 years	$1.55 \cdot 10^{-6}$	$-2.80 \cdot 10^{-23}$
7 years	$1.56 \cdot 10^{-6}$	$-1.09 \cdot 10^{-24}$
8 years	$1.57 \cdot 10^{-6}$	$1.02 \cdot 10^{-23}$
9 years	$1.57 \cdot 10^{-6}$	$-1.54 \cdot 10^{-23}$
10 years	$1.58 \cdot 10^{-6}$	$-1.02 \cdot 10^{-23}$

Table B.2: Parameter estimates for the fitted time-inhomogeneous NIG processes using one- to ten-year zero-coupon bond quotes from 24 June 2011 to 19 June 2013.

Time-to-maturity	$\hat{\boldsymbol{\alpha}}$	$\hat{\boldsymbol{\beta}}$	$\hat{\boldsymbol{\delta}}$	$\hat{\boldsymbol{\mu}}$
1 year	733594	49435.6	$6.80 \cdot 10^{-7}$	$-4.90 \cdot 10^{-8}$
2 years	535202	12519.4	$9.80 \cdot 10^{-7}$	$-2.29 \cdot 10^{-8}$
3 years	708379	−12208.4	$1.40 \cdot 10^{-6}$	$2.38 \cdot 10^{-8}$
4 years	664582	−34206.8	$1.49 \cdot 10^{-6}$	$7.80 \cdot 10^{-8}$
5 years	762927	−51295.7	$1.79 \cdot 10^{-6}$	$1.21 \cdot 10^{-7}$
6 years	867777	−69162.9	$2.08 \cdot 10^{-6}$	$1.66 \cdot 10^{-7}$
7 years	942164	−81975.8	$2.30 \cdot 10^{-6}$	$2.02 \cdot 10^{-7}$
8 years	995568	−73420.3	$2.45 \cdot 10^{-6}$	$1.82 \cdot 10^{-7}$
9 years	1040271	−84167.9	$2.57 \cdot 10^{-6}$	$2.08 \cdot 10^{-7}$
10 years	1093163	−87307.3	$2.71 \cdot 10^{-6}$	$2.17 \cdot 10^{-7}$

Table B.3: Parameter estimates for the fitted time-inhomogeneous GSS processes using one- to ten-year zero-coupon bond quotes from 24 June 2011 to 19 June 2013.

Time-to-maturity	$\hat{\boldsymbol{\nu}}$	$\hat{\boldsymbol{\beta}}$	$\hat{\boldsymbol{\delta}}$	$\hat{\boldsymbol{\mu}}$
1 year	2.23	26492.52	$7.90 \cdot 10^{-7}$	$-3.89 \cdot 10^{-8}$
2 years	2.89	11166.68	$1.44 \cdot 10^{-6}$	$-2.14 \cdot 10^{-8}$
3 years	3.43	− 7510.35	$1.83 \cdot 10^{-6}$	$1.68 \cdot 10^{-8}$
4 years	4.97	−33930.58	$2.56 \cdot 10^{-6}$	$7.58 \cdot 10^{-8}$
5 years	5.23	−48235.10	$2.78 \cdot 10^{-6}$	$1.15 \cdot 10^{-7}$
6 years	6.34	−66766.83	$3.24 \cdot 10^{-6}$	$1.62 \cdot 10^{-7}$
7 years	7.43	−83273.58	$3.65 \cdot 10^{-6}$	$2.04 \cdot 10^{-7}$
8 years	8.19	−77028.06	$3.91 \cdot 10^{-6}$	$1.90 \cdot 10^{-7}$
9 years	8.89	−85466.94	$4.13 \cdot 10^{-6}$	$2.12 \cdot 10^{-7}$
10 years	9.56	−88549.44	$4.34 \cdot 10^{-6}$	$2.21 \cdot 10^{-7}$

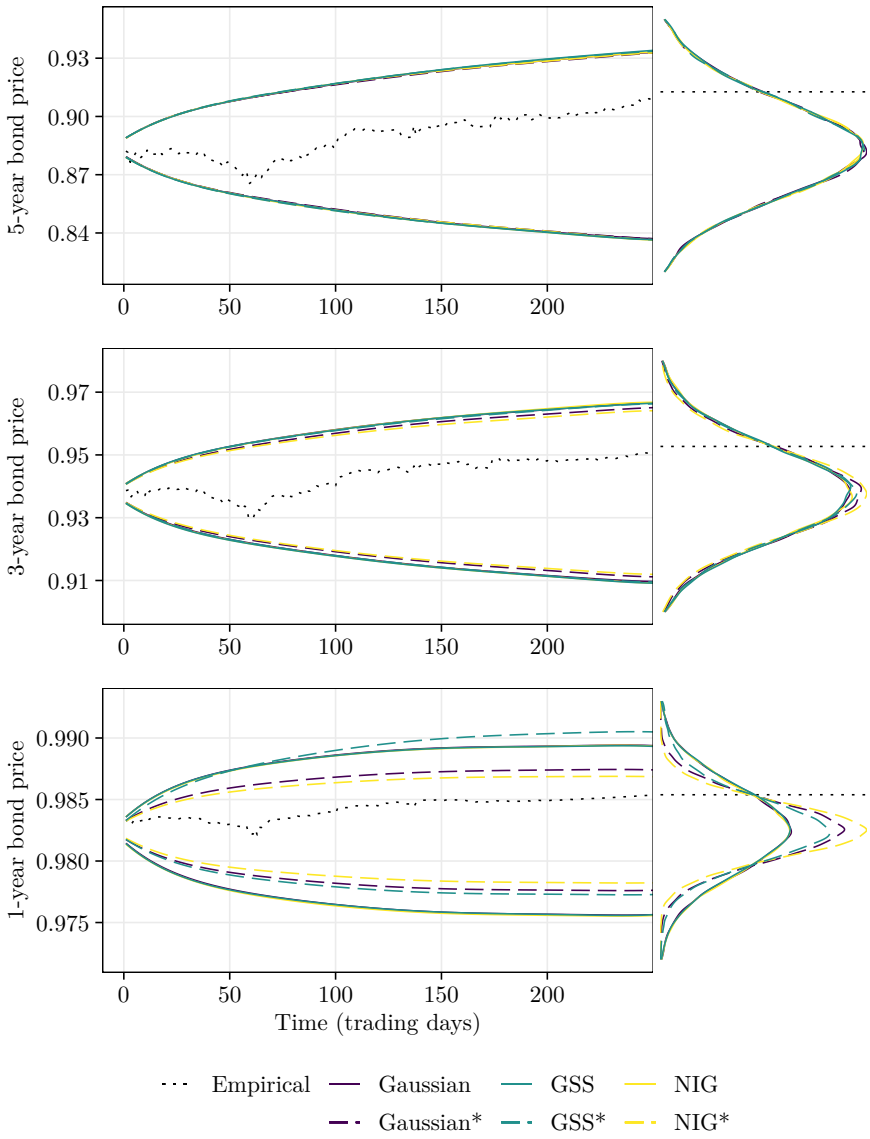

Figure B.1: Estimated 95 % confidence bounds for the discounted value of a (top) five-year, (middle) three-year, and (bottom) one-year zero-coupon bond, initialised at 19 June 2013, during the next 250 trading days. NIG*, GSS*, and Gaussian* denote term structure models generated by time-inhomogeneous distributions. The density curves of discounted bond prices at the final date are scaled and not comparable between the three panels.

B.2 Backtests of Zero-Coupon Bonds

Table B.4: Results from (a) one-day value-at-risk and (b) one-day expected shortfall backtests of two-year bonds, using the previous 250 trading days in the calibration of the term structure models. Reported in the value-at-risk backtest is the violation percentage and in parenthesis the p-value from the unconditional coverage Kupiec test. Reported in the expected shortfall backtest is the test score from the Embrechts' test. NIG*, GSS*, and Gaussian* denote term structure models generated by time-inhomogeneous distributions.

Distribution	**0.5 %**	**1.0 %**	**2.5 %**	**97.5 %**	**99.0 %**	**99.5 %**
Gaussian	0.41	0.73	1.10	1.32	1.14	0.96
	(0.54)	(0.18)	(*0*)	(*0*)	(0.52)	(*0.01*)
NIG	0.23	0.55	1.05	1.46	0.91	0.55
	(*0.04*)	(*0.02*)	(*0*)	(*0*)	(0.68)	(0.75)
GSS	0.23	0.5	1.10	1.55	0.91	0.59
	(*0.04*)	(*0.01*)	(*0*)	(*0*)	(0.68)	(0.55)
Gaussian*	1.28	1.60	2.56	2.83	2.10	1.55
	(*0*)	(*0.01*)	(0.86)	(0.33)	(*0*)	(*0*)
NIG*	0.78	1.14	2.47	2.69	1.37	0.91
	(0.09)	(0.52)	(0.92)	(0.57)	(0.10)	(*0.01*)
GSS*	0.82	1.23	2.74	2.74	1.64	0.91
	(0.05)	(0.29)	(0.48)	(0.48)	(*0.01*)	(*0.01*)

(a) Value-at-risk

Distribution	**0.5 %**	**1.0 %**	**2.5 %**	**97.5 %**	**99.0 %**	**99.5 %**
Gaussian	0.00032	0.00016	0.00018	0.00021	0.00028	0.00031
NIG	0.00025	0.00013	0.00020	0.00011	0.00004	0.00003
GSS	0.00023	0.00016	0.00019	0.00009	0.00001	0.00009
Gaussian*	0.00045	0.00036	0.00023	0.00035	0.00051	0.00062
NIG*	0.00024	0.00020	0.00012	0.00018	0.00025	0.00025
GSS*	0.00019	0.00018	0.00009	0.00017	0.00012	0.00017

(b) Expected shortfall

Table B.5: Results from (a) one-day value-at-risk and (b) one-day expected shortfall backtests of three-year bonds, using the previous 250 trading days in the calibration of the term structure models. Reported in the value-at-risk backtest is the violation percentage and in parenthesis the p-value from the unconditional coverage Kupiec test. Reported in the expected shortfall backtest is the test score from the Embrechts' test. NIG*, GSS*, and Gaussian* denote term structure models generated by time-inhomogeneous distributions.

Distribution	**0.5 %**	**1.0 %**	**2.5 %**	**97.5 %**	**99.0 %**	**99.5 %**
Gaussian	0.59	0.78	1.64	1.69	1.37	1.00
	(0.55)	(0.27)	(*0.01*)	(*0.01*)	(0.10)	(*0*)
NIG	0.41	0.59	1.28	1.92	1.23	0.78
	(0.54)	(*0.04*)	(*0*)	(0.07)	(0.29)	(0.09)
GSS	0.41	0.59	1.42	1.96	1.19	0.78
	(0.54)	(*0.04*)	(*0*)	(0.09)	(0.39)	(0.09)
Gaussian*	1.23	1.55	2.79	2.83	1.92	1.46
	(*0*)	(*0.02*)	(0.40)	(0.33)	(*0*)	(*0*)
NIG*	0.64	1.05	2.47	2.60	1.32	1.05
	(0.38)	(0.81)	(0.92)	(0.76)	(0.15)	(*0*)
GSS*	0.73	1.14	2.51	2.83	1.28	0.96
	(0.15)	(0.52)	(0.97)	(0.33)	(0.21)	(*0.01*)

(a) Value-at-risk

Distribution	**0.5 %**	**1.0 %**	**2.5 %**	**97.5 %**	**99.0 %**	**99.5 %**
Gaussian	0.00063	0.00043	0.00016	0.00039	0.00052	0.00057
NIG	0.00017	0.00021	0.00023	0.00019	0.00018	0.00015
GSS	0.00008	0.00018	0.00019	0.00017	0.00014	0.00011
Gaussian*	0.00071	0.00053	0.00031	0.00051	0.00073	0.00086
NIG*	0.00041	0.00026	0.00012	0.00026	0.00031	0.00024
GSS*	0.00038	0.00028	0.00015	0.00020	0.00025	0.00023

(b) Expected shortfall

Table B.6: Results from (a) one-day value-at-risk and (b) one-day expected shortfall backtests of four-year bonds, using the previous 250 trading days in the calibration of the term structure models. Reported in the value-at-risk backtest is the violation percentage and in parenthesis the p-value from the unconditional coverage Kupiec test. Reported in the expected shortfall backtest is the test score from the Embrechts' test. NIG*, GSS*, and Gaussian* denote term structure models generated by time-inhomogeneous distributions.

Distribution	**0.5 %**	**1.0 %**	**2.5 %**	**97.5 %**	**99.0 %**	**99.5 %**
Gaussian	0.64	1.00	1.96	2.10	1.37	1.10
	(0.38)	(0.98)	(0.09)	(0.22)	(0.10)	(*0*)
NIG	0.55	0.68	1.74	2.24	1.14	0.91
	(0.75)	(0.12)	(*0.02*)	(0.42)	(0.52)	(*0.01*)
GSS	0.50	0.68	1.69	2.37	1.19	0.96
	(0.99)	(0.12)	(*0.01*)	(0.70)	(0.39)	(*0.01*)
Gaussian*	1.00	1.46	2.83	2.97	1.83	1.42
	(*0*)	(*0.04*)	(0.33)	(0.17)	(*0*)	(*0*)
NIG*	0.55	0.87	2.47	2.79	1.32	0.82
	(0.75)	(0.52)	(0.92)	(0.40)	(0.15)	(0.05)
GSS*	0.59	0.96	2.60	2.92	1.32	0.87
	(0.55)	(0.85)	(0.76)	(0.22)	(0.15)	(*0.03*)

(a) Value-at-risk

Distribution	**0.5 %**	**1.0 %**	**2.5 %**	**97.5 %**	**99.0 %**	**99.5 %**
Gaussian	0.00115	0.00070	0.00035	0.00046	0.00068	0.00071
NIG	0.00043	0.00038	0.00016	0.00025	0.00033	0.00020
GSS	0.00020	0.00028	0.00017	0.00021	0.00027	0.00024
Gaussian*	0.00113	0.00078	0.00042	0.00055	0.00083	0.00092
NIG*	0.00067	0.00048	0.00014	0.00026	0.00032	0.00039
GSS*	0.00043	0.00037	0.00013	0.00020	0.00023	0.00029

(b) Expected shortfall

Table B.7: Results from (a) one-day value-at-risk and (b) one-day expected shortfall backtests of six-year bonds, using the previous 250 trading days in the calibration of the term structure models. Reported in the value-at-risk backtest is the violation percentage and in parenthesis the p-value from the unconditional coverage Kupiec test. Reported in the expected shortfall backtest is the test score from the Embrechts' test. NIG*, GSS*, and Gaussian* denote term structure models generated by time-inhomogeneous distributions.

Distribution	**0.5 %**	**1.0 %**	**2.5 %**	**97.5 %**	**99.0 %**	**99.5 %**
Gaussian	0.82	1.32	3.01	2.47	1.46	1.00
	(0.05)	(0.15)	(0.14)	(0.92)	(*0.04*)	(*0*)
NIG	0.59	0.87	2.42	2.56	1.28	0.96
	(0.55)	(0.52)	(0.81)	(0.86)	(0.21)	(*0.01*)
GSS	0.59	0.87	2.6	2.69	1.37	0.82
	(0.55)	(0.52)	(0.76)	(0.57)	(0.1)	(0.05)
Gaussian*	0.82	1.42	3.15	2.42	1.51	1.00
	(0.05)	(0.07)	(0.06)	(0.81)	(*0.03*)	(*0*)
NIG*	0.59	0.87	2.42	2.42	1.28	0.78
	(0.55)	(0.52)	(0.81)	(0.81)	(0.21)	(0.09)
GSS*	0.59	0.91	2.69	2.51	1.28	0.68
	(0.55)	(0.68)	(0.57)	(0.97)	(0.21)	(0.25)

(a) Value-at-risk

Distribution	**0.5 %**	**1.0 %**	**2.5 %**	**97.5 %**	**99.0 %**	**99.5 %**
Gaussian	0.00203	0.00134	0.00067	0.00065	0.00099	0.00123
NIG	0.00116	0.00077	0.00021	0.00038	0.00057	0.00053
GSS	0.00080	0.00058	0.00011	0.00034	0.00046	0.00057
Gaussian*	0.00202	0.00130	0.00065	0.00067	0.00100	0.00129
NIG*	0.00100	0.00073	0.00019	0.00036	0.00048	0.00053
GSS*	0.00072	0.00057	0.00010	0.00033	0.00044	0.00063

(b) Expected shortfall

Table B.8: Results from (a) one-day value-at-risk and (b) one-day expected shortfall backtests of seven-year bonds, using the previous 250 trading days in the calibration of the term structure models. Reported in the value-at-risk backtest is the violation percentage and in parenthesis the p-value from the unconditional coverage Kupiec test. Reported in the expected shortfall backtest is the test score from the Embrechts' test. NIG*, GSS*, and Gaussian* denote term structure models generated by time-inhomogeneous distributions.

Distribution	**0.5 %**	**1.0 %**	**2.5 %**	**97.5 %**	**99.0 %**	**99.5 %**
Gaussian	0.87	1.64	3.52	2.60	1.55	1.10
	(*0.03*)	(*0.01*)	(*0*)	(0.76)	(*0.02*)	(*0*)
NIG	0.59	0.91	2.65	2.69	1.28	0.82
	(0.55)	(0.68)	(0.66)	(0.57)	(0.21)	(0.05)
GSS	0.59	0.87	2.88	2.88	1.37	0.82
	(0.55)	(0.52)	(0.27)	(0.27)	(0.10)	(0.05)
Gaussian*	0.82	1.60	3.20	2.51	1.37	1.10
	(0.05)	(*0.01*)	(0.05)	(0.97)	(0.10)	(*0*)
NIG*	0.55	0.87	2.56	2.56	1.23	0.68
	(0.75)	(0.52)	(0.86)	(0.86)	(0.29)	(0.25)
GSS*	0.64	0.87	2.74	2.60	1.28	0.73
	(0.38)	(0.52)	(0.48)	(0.76)	(0.21)	(0.15)

(a) Value-at-risk

Distribution	**0.5 %**	**1.0 %**	**2.5 %**	**97.5 %**	**99.0 %**	**99.5 %**
Gaussian	0.00236	0.00146	0.00079	0.00073	0.00108	0.00138
NIG	0.00136	0.00091	0.00030	0.00040	0.00064	0.00081
GSS	0.00089	0.00074	0.00019	0.00035	0.00051	0.00074
Gaussian*	0.00232	0.00139	0.00077	0.00066	0.00105	0.00127
NIG*	0.00113	0.00078	0.00021	0.00033	0.00051	0.00071
GSS*	0.00063	0.00065	0.00012	0.00028	0.00041	0.00060

(b) Expected shortfall

Table B.9: Results from (a) one-day value-at-risk and (b) one-day expected shortfall backtests of eight-year bonds, using the previous 250 trading days in the calibration of the term structure models. Reported in the value-at-risk backtest is the violation percentage and in parenthesis the p-value from the unconditional coverage Kupiec test. Reported in the expected shortfall backtest is the test score from the Embrechts' test. NIG*, GSS*, and Gaussian* denote term structure models generated by time-inhomogeneous distributions.

Distribution	**0.5 %**	**1.0 %**	**2.5 %**	**97.5 %**	**99.0 %**	**99.5 %**
Gaussian	1.10	1.92	3.47	2.74	1.60	1.05
	(*0*)	(*0*)	(*0.01*)	(0.48)	(*0.01*)	(*0*)
NIG	0.59	1.05	2.79	2.83	1.32	0.82
	(0.55)	(0.81)	(0.40)	(0.33)	(0.15)	(0.05)
GSS	0.59	1.05	2.92	3.06	1.37	0.68
	(0.55)	(0.81)	(0.22)	(0.11)	(0.10)	(0.25)
Gaussian*	0.91	1.60	3.20	2.42	1.55	1.00
	(*0.01*)	(*0.01*)	(0.05)	(0.81)	(*0.02*)	(*0*)
NIG*	0.59	0.96	2.56	2.69	1.28	0.55
	(0.55)	(0.85)	(0.86)	(0.57)	(0.21)	(0.75)
GSS*	0.59	0.96	2.69	2.83	1.23	0.59
	(0.55)	(0.85)	(0.57)	(0.33)	(0.29)	(0.55)

(a) Value-at-risk

Distribution	**0.5 %**	**1.0 %**	**2.5 %**	**97.5 %**	**99.0 %**	**99.5 %**
Gaussian	0.00249	0.00162	0.00100	0.00075	0.00111	0.00150
NIG	0.00161	0.00092	0.00036	0.00038	0.00056	0.00080
GSS	0.00098	0.00065	0.00027	0.00032	0.00043	0.00093
Gaussian*	0.00258	0.00164	0.00093	0.00072	0.00097	0.00134
NIG*	0.00156	0.00097	0.00033	0.00028	0.00041	0.00087
GSS*	0.00130	0.00084	0.00026	0.00018	0.00042	0.00068

(b) Expected shortfall

Table B.10: Results from (a) one-day value-at-risk and (b) one-day expected shortfall backtests of nine-year bonds, using the previous 250 trading days in the calibration of the term structure models. Reported in the value-at-risk backtest is the violation percentage and in parenthesis the p-value from the unconditional coverage Kupiec test. Reported in the expected shortfall backtest is the test score from the Embrechts' test. NIG*, GSS*, and Gaussian* denote term structure models generated by time-inhomogeneous distributions.

Distribution	**0.5 %**	**1.0 %**	**2.5 %**	**97.5 %**	**99.0 %**	**99.5 %**
Gaussian	1.19	1.92	3.38	2.74	1.60	1.00
	(*0*)	(*0*)	(*0.01*)	(0.48)	(*0.01*)	(*0*)
NIG	0.64	1.05	2.83	2.97	1.19	0.73
	(0.38)	(0.81)	(0.33)	(0.17)	(0.39)	(0.15)
GSS	0.59	1.14	3.06	3.15	1.37	0.73
	(0.55)	(0.52)	(0.11)	(0.06)	(0.10)	(0.15)
Gaussian*	0.91	1.55	3.06	2.51	1.37	0.82
	(*0.01*)	(*0.02*)	(0.11)	(0.97)	(0.10)	(0.05)
NIG*	0.64	0.87	2.60	2.74	1.14	0.59
	(0.38)	(0.52)	(0.76)	(0.48)	(0.52)	(0.55)
GSS*	0.59	0.91	2.74	2.79	1.19	0.55
	(0.55)	(0.68)	(0.48)	(0.40)	(0.39)	(0.75)

(a) Value-at-risk

Distribution	**0.5 %**	**1.0 %**	**2.5 %**	**97.5 %**	**99.0 %**	**99.5 %**
Gaussian	0.00289	0.00197	0.00124	0.00084	0.00122	0.00175
NIG	0.00183	0.00118	0.00051	0.00037	0.00066	0.00098
GSS	0.00124	0.00073	0.00036	0.00032	0.00044	0.00085
Gaussian*	0.00304	0.00196	0.00112	0.00071	0.00109	0.00163
NIG*	0.00149	0.00116	0.00037	0.00029	0.00056	0.00103
GSS*	0.00090	0.00066	0.00026	0.00025	0.00046	0.00128

(b) Expected shortfall